SHORT DISTANCE AND AVERAGE ABSOLUTE DISTANCE WITH WAVELET TRANSFORM FOR THE HIGH IMPEDANCE FAULT LOCATION IN THE 11KV DISTRIBUTION UNDERGROUND SYSTEM

MOHD SYUKRI BIN ALI

DISSERTATION SUBMITTED IN FULFILMENT OF THE REQUIREMENTS FOR THE DEGREE OF MASTER OF PHILOSOPHY

INSTITUTE OF GRADUATE STUDIES
UNIVERSITY OF MALAYA
KUALA LUMPUR

2013

ORIGINAL LITERARY WORK DECLARATION

Name of Candidate : **Mohd Syukri Bin Ali**

IC. No

Registration/Matric No : **KGA 100068**

Name of Degree : **Master of Engineering Science (MEngSc)**

Title of Project Paper/Research Report/Dissertation/Thesis ("this Work'**) :**

Short Distance and Average Absolute Distance with Wavelet Transform for the High Impedance Fault Location in the 11KV Distribution Underground System

Field of Study : **Power System**

I do solemnly and sincerely declare that :

(1) I am the sole author/writer of this work;
(2) This work is original;
(3) Any use of any work in which copyright exists was done by way of fair dealing and for permitted purposes and any except or extract from, or reference to or reproduction of any copyright work has been disclosed expressly and sufficiently and the title of the work and its authorship have been acknowledged in this work;
(4) I do not have any actual knowledge nor do I ought reasonably to know that the making of this work constitutes an infringement of any copyright work;
(5) I hereby assign all and every right in the copyright to this work and that any reproduction or use in any form or by any means whatsoever is prohibited without the written consent of UM having been first had and obtained;
(6) I am fully aware that if in the course of making this work I have infringed any copyright whether intentionally or otherwise. I may be subject to legal action or any other action as may be determined by UM.

Candidate's Signature Date

_____ _____

ABSTRAK

Secara amnya, kesalahan rintangan tinggi (HIF) adalah kerosakan apabila sentuhan yang tidak diingini berlaku antara elemen konduktor bagi rangkaian dengan objek atau permukaan bukan konduktor yang menyebabkan arus kerosakan yang sangat kecil terhasil. Kejadian HIF boleh menyebabkan pencetusan yang membawa bahaya kepada kehidupan manusia dan alam sekitar. Selain itu, risiko kebakaran yang ketara sebagai akibat daripada fenomena pencetusan boleh menimbulkan kemungkinan merosakkan kepada peralatan sistem kuasa. Pada jangka masa yang panjang, jika HIFs tidak dirawat, ianya akan menjejaskan kualiti sistem kuasa dari segi kesinambungan perkhidmatan dan kehilangan tenaga.

Dalam usaha untuk mengatasi masalah tersebut, syarikat utiliti kuasa perlu mencari dan mengasingkan HIF secepat yang mungkin supaya kerja-kerja pembaikan dan proses pemulihan rangkaian boleh dilakukan dengan segera. Malangnya, mencari bahagian yang rosak adalah sangat mencabar terutamanya bagi rangkaian pengedaran. Ini adalah disebabkan oleh kerumitan rangkaian seperti kehadiran talian bukan homogen, cawangan dan perubahan beban. Walaupun beberapa teknik untuk mengenalpasti lokasi HIF telah dicadangkan, namun teknik tersebut tidak mudah diguna pakai disebabkan oleh kos pemasangan dan penyelenggaraan yang tinggi, keperluan peranti penghantaran data yang berkesan dan boleh dipercayai dan juga data yang banyak diperlukan untuk dianalysis.

Memandangkan pentingnya mengenal pasti lokasi HIF dalam sistem pengagihan, teknik dengan kos yang rendah, penggunaan data yang minimum dan melibatkan hanya satu titik pengukuran telah dicadangkan dalam kajian ini. Kaedah ini menggunakan ciri-ciri

yang diekstrak daripada tiga fasa voltan isyarat dan dipadankan dengan set ciri-ciri yang disimpan. Dua pendekatan yang berbeza iaitu teknik Jarak Terpendek dan teknik Purata Perbezaan Mutlak telah dicadangkan untuk mengenal pasti bahagian yang rosak. Satu analisis kedudukan diperkenalkan untuk mengenal pasti keutamaan pemeriksaan bagi bahagian-bahagian yang mungkin rosak.

Simulasi telah dijalankan menggunakan perisian PSCAD / EMTDC untuk mendapatkan isyarat kerosakan voltan semasa acara HIF. Keputusan simulasi menunjukkan bahawa kaedah yang dicadangkan mampu untuk mengenal pasti lokasi kesalahan dengan nilai kesalahan impedans yang pelbagai. Juga, kaedah yang dicadangkan dianggap berkesan dan ekonomi kerana kaedah tersebut hanya memerlukan satu ukuran isyarat voltan untuk menentukan bahagian rosak yang sebenar semasa acara HIF.

ABSTRACT

In general, high impedance fault (HIF) is a fault when an undesirable contact occurs between a conducting element of a network and a non-conducting object or surface resulting in a very small fault current leaking out. The occurrence of HIF may result an arcing which leads to potential hazards to human life and the environment. Moreover, a significant risk of fire as a consequence of the arcing phenomenon may pose damaging possibility to the power system equipment. On the long run, if HIFs are left untreated, they will affect power system quality in terms of service continuity and energy loss.

In order to overcome the problems, power utilities need to locate and isolate the HIF as quickly as possible so that repair works and restoration process of the network can be done in a short period of time. Unfortunately, locating the fault is very challenging especially for a distribution network. This is due to the complexity of the network such as the presence of non-homogeneous line, branches and load variations. Although some HIF location techniques had been proposed, the technique may not be easily adopted due to the high cost of installation and maintenance, the requirement of an effective and reliable data transmitting devices and also a large amount of data that needed to be analysed.

Considering the importance of identifying the HIF location in the distribution system, a low cost technique, utilizing minimum data and involving a single measurement point is proposed in this study. The method uses extracted features of three-phase voltage signal and matched with sets of stored features. Two different approaches which are the Shortest Distance and Average of Absolute Difference techniques have been proposed

to identify the faulty section. A ranking analysis is introduced to priorities the inspection of the multiple possible faulty sections.

The simulation was carried out using the PSCAD/EMTDC software to obtain the fault voltage signal during HIF event. The simulation results show that the proposed method is able to identify the fault location with various fault impedance values. Also, the proposed method is considered effective and economical since the method requires only a single measurement of voltage signal to determine the actual faulty section during the HIF event.

ACKNOWLEDGEMENTS

In this opportunity, I would like to express my appreciation and thankfulness to this following person whose have support and contribute directly or indirectly towards the completion of my research.

First and foremost, I would like to express my greatest appreciation to my supervisor, Dr Ab. Halim Bin Abu Bakar and co-supervisor, Dr Hazlie Bin Mokhlis for their precious teaching and guidance, which is main contribution to the completion of this research. My gratitude to Dr Hamzah Bin Arof and Dr Hazlee Azil Bin Illias whose indirectly assist and support me along the research. Secondly, my highest thankfulness to all my friends in Power System Laboratory for their support and encouragement until the accomplishment of this research.

Last but not least, I would like to extend my acknowledgement to my beloved parent and family whose continuously support me until completion of my research. Also, to all my friends those being supportive and encouraging me towards the successes of my research. May ALLAH give reward and blessing to all of those people for their kindness and true friendship.

TABLE OF CONTENTS

LIST OF FIGURES

LIST OF TABLES

LIST OF ABBREVIATIONS AND SYMBOLS

SLGF	Single Line to Ground Fault
LLLF	Three Phase Fault
LLGF	Double Line to Ground Fault
LLF	Line to Line Fault
HIF	High Impedance Fault
LIF	Low Impedance Fault
RFI	Radio Frequency Interference
PSCAD/EMTDC	Power System Computer Aided Design/Electromagnetic Transient Including DC
GPS	Global Positioning System
CWT	Continuous Wavelet Transform
DWT	Discrete Wavelet Transform
MRA-DWT	Multi-Resolution Analysis-Discrete Wavelet Transform
ST-DWT	Spanning Tree-Discrete Wavelet Transform
Daub/Db	Daubechies Mother Wavelet
Ψ (t)	Mother Wavelet
a	Dilation value of the mother wavelet
b	Translation value of the mother wavelet
cA	Approximation coefficients
cD	Detail coefficients
$\sum a$	Summation of approximation coefficients
$\sum d$	Summation of detail coefficients
SD	Shortest Distance technique
d_k	Shortest distance
AAD	Average of Absolute Difference technique
A_v	Average of the summation of detail coefficients
AAD_m	Difference value between measured and database data
AR	Approximation ratio

LIST OF APPENDICES

CHAPTER 1

INTRODUCTION

1.1. Overview of High Impedance Fault

A fault on a distribution network is an abnormal circuit condition caused by ageing of equipment, animal contact, accident or weather condition which results in energy being dissipated in a manner other than serving the intended load. Typically, there are two fault types which are low impedance fault and high impedance fault. In a low impedance fault, it causes a substantial increase in current flow towards the fault point. However, in a high impedance fault (HIF), no substantial increase in current will be observed. The high impedance object restricts the flow of fault current. As a result, it is difficult to detect fault events in high impedance fault than in low impedance fault.

The Power System Relay Committee working group of HIF Detection Technology has defined HIF as those which do not produce enough fault current to be detectable by the conventional overcurrent protection relays or fuses (John Tengdin et al., 1996). It happens due to undesirable contact made between conductive and non-conducting object or surface. Usually, it is caused by a physical damage to the conductor which causes the conductor to break and touch a high impedance surface. HIF can also occur without a path to ground, such as when a tree limb bridge two phase conductors. For an underground cable, HIF is normally caused by an insulation defect that expose the conductor to making contact with non-conducting element such as partial discharge. Common causes of insulation defects include cable cut, flash fault and insulation degradation due to moisture and corrosive contamination.

The occurrence of HIF may result in an arc which leads to potential hazards to human and the environment. Moreover, a significant risk of fire as a consequence of the arcing phenomenon associated with the HIF may cause damage to the power system equipment. In the long run, if the HIF is left untreated, it will affect power system quality in terms of service continuity, disturbance propagation and energy losses. Thus, the occurrence of HIF must be detected immediately before the system encounters complete failure, which may cause power outages that leads to loss of productivity.

1.2. Research Motivations

Due to the severe impact of the HIF towards the reliability and security of power system components, it is crucial to detect HIF immediately. For this purpose, two categories of HIF detection are commonly utilised; mechanical HIF and electrical HIF detections (Mark Adamiak et al.). Mechanical detection of HIF is a technique comprises of devices that forces contact with a solid ground in order to allow conventional overcurrent protection relay to operate. During the HIF event, fault current produced is not sufficient to be detected by the overcurrent protection relay. Thus mechanical detection is developed to produce a low impedance ground fault when a conductor physically breaks and falls towards the ground to activate the overcurrent protection relay. The mechanical HIF detection technique is very reliable, however, it requires to apply these devices at each pole. This increases the cost of the mechanical HIF technique which makes it uneconomical to be used in the distribution network.

In order to overcome the drawbacks of the mechanical HIF detection, the electrical HIF detection has been developed. In general, the technique utilizes the voltage and current signal obtained from measurement devices. The voltage and current signal are analysed

using the digital based technique to extract the signal features. The occurrence of a HIF event in the distribution network can be determined from the extracted features.

Once HIF has been successfully detected, the power system protection engineer needs to identify the exact location of HIF. This is a very important task because HIF in the distribution system involves residential and industrial customers. The occurrence of HIF event will expose public safety to danger. For example, children or unaware peoples may come close to the HIF location unintentionally. Besides, it is crucial to reduce outage time to avoid possible unsafe conditions such as traffic light malfunction at busy intersections (traffic hazards). Industrial customer may face huge losses due to the shutdown of the production process. Therefore, locating the fault as quickly as possible with reasonable accuracy is necessary to expedite the restoration process.

In the past, various works have been conducted in locating low impedance faults, fault on transmission line and overhead distribution line. However, limited research is carried out on locating the HIF in an underground distribution network. Commonly, HIF is located using a surge generator by thumping high voltage at each cable section. However, if all cables at each section are thumped, especially for a long cable, it could take days to locate the fault. Besides, this will also cause potential damage to aged cable and reduce the life span of new cables. Therefore, estimating the fault location with reasonable accuracy has led to the development of various fault localization techniques. These techniques are crucial for the distribution system to speed up the process of locating the HIF and protect the aged cable.

1.3. Research Objectives

Considering the importance of the HIF detection and localization in the distribution network, the following are the main objectives of this research:

1) To utilise the Discrete Wavelet Transform (DWT) for feature extraction on voltage signal during the high impedance fault occurrence.
2) To propose the SD and AAD techniques for the high impedance fault location using the extracted features of detail coefficients in the database.
3) To compare the performance of SD and AAD techniques in determining accurate location of HIF on the typical 11kV Distribution Network in Malaysia.

The information needed to detect and locate the fault during a HIF event is a voltage signal. This data can be obtained from any type of measurement devices such as Voltage and Current Recorder, at primary substation. The proposed method is expected to be effective and economical since the method considers only a single measurement of voltage signal and does not require communication links to access remote nodes.

1.4. Methodology of the Research

The following tasks will be performed to achieve the outlined objectives:

a) The background of distribution networks and fault location issues will be studied.
b) High impedance fault detection and localization methods for distribution system will be reviewed. The advantages and disadvantages of each method will be studied in order to propose a reliable fault localization method. Since the proposed method will be based on voltage, the related methods using voltage signal to identify the fault location will be studied thoroughly.

c) Application of digital signal processing techniques for extracting information from the voltage sinusoidal will be reviewed. The reliability of each technique in identifying and classifying a high impedance fault event based on voltage signal will be studied.

d) The relationship between faults and extracted voltage characteristics will be studied thoroughly. This task also involves the determination of fault location based on the extracted features of the voltage signal.

e) A typical 11kV distribution network system of Malaysia will be modelled using the PSCAD/EMTDC software. A high impedance fault simulation will be implemented using the developed model to obtain the post-disturbance voltage waveform data for the test.

f) In order to identify the occurrence of high impedance fault and fault location, the discrete wavelet transform multi-resolution analysis program will be developed to implement the proposed method. For this purpose, MATLAB will be chosen for programming the method.

g) Proposed two methods to identify the HIF location in the distribution network. The proposed methods of the Shortest Distance (SD) and Average of Absolute Difference (AAD) are explained briefly and the proposed method program will be developed in MATLAB.

h) Finally, the reliability and effectiveness of the proposed method will be tested using the typical Malaysian distribution network for different type of fault, fault values and locations.

1.5. Dissertation Outline

This thesis is made up of six chapters. **Chapter 1** provides an overview of HIF fault with research motivation. The objectives of the research are presented followed by research methodology. Dissertation outline is given at the end of this chapter.

Chapter 2 presents the previous fault detection and localization methods in the distribution system. The low impedance fault location methods are discussed briefly. In order to detect and locate the high impedance fault location, the overview of feature extraction techniques used to analyse the voltage and current signals are studied. The techniques discussed to identify the high impedance fault location include network topology, travelling wave and knowledge-based techniques. The advantages and limitations of these techniques are reviewed. In **Chapter 3,** the theoretical background for high impedance fault and different type of wavelet transform are presented. The working principles, advantages and disadvantages of each type of wavelet transform will be discussed.

The methodology of the proposed techniques is presented and discussed in **Chapter 4**. Two different methods have been proposed to determine the fault location. A typical 11kV radial distribution system of Malaysia is considered for the validation of the method. This network is modelled using PSCAD/EMTDC software to generate faulted voltage signal data tests.

The performance of the proposed methods considering various types of fault (SLGF, LLLF, LLGF and LLF), fault resistance and fault location are discussed in **Chapter 5**. Finally, **Chapter 6** concludes the study. The main findings of the research and future work to improve the proposed method are discussed.

CHAPTER 2

REVIEW ON FAULT LOCATION FOR DISTRIBUTION SYSTEM

2.1. Introduction

In the previous chapter, a brief introduction about high impedance fault in power system was presented. The significance of detecting and locating the fault, effects of faults and the problems associated with locating the faults in the distribution system was discussed.Considering the necessity for accurate and fast fault location, this research propose a high impedance fault localization technique that is both cost effective and reliable. In order to achieve this objective, the overview of existing high impedance fault detection and localization methods are reviewed in this chapter. The working principle, advantages and drawbacks of the proposed techniques will be studied thoroughly. From this review, a new approach will be proposed to overcome the limitation of previous techniques.

2.2. Fault Analysis Classification

In a fault analysis, it is necessary to differentiate between low impedance fault (LIF) and high impedance fault (HIF) with other transient faults as shown in Figure 2.1. There are several examples of transient phenomena in power system such as capacitor bank switching, inrush current, harmonic load and insulator leakage current (Sarlak et al., 2011). Transient faults are a temporary event whereas LIF and HIF are a permanent event occur in the distribution system.

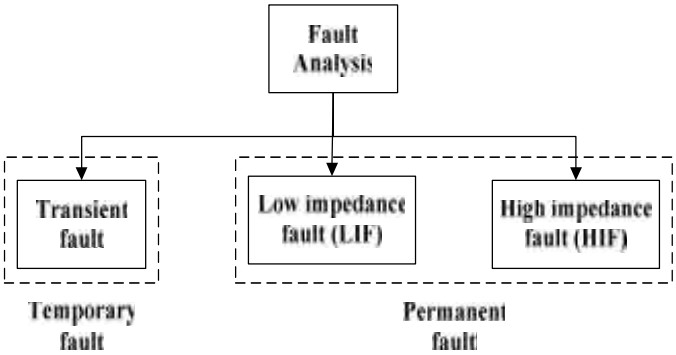

Figure 2.1 : Fault analysis classification

Autoreclosure is a device that has a mechanism to automatically open and close the breaker after a brief interval. During a transient fault, autoreclosure will be opened and closed until the transient is cleared from the system after a few attempts. If the fault still persists in the system after the maximum number of autoreclosure operation, then the autoreclosure will be locked out (opened permanently). Thus, human intervention is required to manually clear the fault and reset the autoreclosure to restore the system.

Aside of transient phenomena in power system, there are two types of permanent faults; LIF and HIF event. During the permanent fault, the autoreclosure will terminate its pre-programmed attempt and remain tripped off until it is manually reset. Basically LIF and HIF are caused by the same reasons such as cable fall to the ground, animal contact, a tree branch bridge across the cable, insulation breakdown caused by aging and adverse weather condition. The difference between LIF and HIF is the impedance of the object which make contact with the cable. LIF is caused by a low impedance object whereas HIF is due to the high impedance object which restrict the flow of fault current. During LIF event, it will generate sufficient fault current magnitude to be detectable by conventional overcurrent protection relay, circuit breaker or fuse. The fault is cleared by isolating the faulted line from healthy lines. However, the problem arises in determining the exact location of the fault in a fast manner. With fast fault detection and location identification, immediate action to restore power can be conducted. There are various

LIF location techniques such as conventional technique, impedance-based technique, travelling wave and high frequency –based techniques and knowledge-based technique.

Unlike LIF, the occurrence of HIF does not produce sufficient fault current magnitude to trigger the conventional overcurrent protection relay, circuit breaker or fuse to operate. Thus, the faulted line is not being isolated from the system which can cause a hazard to the system, human and environment. Due to these risks, it is important to detect the occurrence of HIF event as well as distinguished it from other fault phenomena in power system. Besides that, it is also crucial to identify the fault location to repair or change the faulted cable. Unfortunately, to determine the faulty section during HIF event is difficult due to the small changes in voltage and current signals. This very small anomaly on the signals make it hard to differentiate the faulty section especially for non-homogenous line and branch network system. Due to this reason, many research had been conducted to detect and distinguish HIF event from other fault phenomena in power system. However, only a few research had been done to identify the fault location in power system during the occurrence of HIF. Several approaches were proposed to determine the HIF location such as network topology technique, travelling wave technique and knowledge-based technique.

2.3. Overview of Low Impedance Fault Location Method

In this sub-chapter, the overview methods of locating low impedance faults are presented. The methods were proposed due to the importance of fast and accurate fault location identified in the distribution system. The method presented consider the need of an inexpensive method that gives a reasonably accurate. Different techniques are discussed such as conventional technique, impedance-based technique, travelling wave and high frequency –based techniques and intelligent technique.

2.3.1. Conventional Techniques

In this technique, the fault is located through visual inspection, trial and error switching and fault indicators (""Final report of the CIRED Working Group WG03 Fault Management, 'Fault management in electrical distribution systems',""; "IEEE Guide for Determining Fault Location on AC Transmission and Distribution Lines," 2005; Krajnak, 2000). Visual inspection technique is a technique where engineers have to patrol along the faulty feeder to identify the fault location. Initially, the possible location of the fault was guessed by an experienced engineer before checking the selected location. This technique is inefficient and time consuming since multiple locations need to be checked if the first estimated fault location is incorrect.

For the second technique, trial and error switching approach was employed. In this technique, switch on and off is required at every substation until circuit breaker trip off is identified which indicates the faulty section. This technique is time consuming and also expose the equipments to additional stress due to the switch on and off process.

The last technique used to locate the fault is fault indicators. Fault indicator is a device installed in each section which identify the faulty section via the signal provided by two adjacent indicators. This technique is not quite practical due to the high cost of installation and maintenance of the device. In addition, visual inspection still required to be conducted to identify the functional fault indicator.

2.3.2. Impedance-based Technique

Impedance-based technique is a mathematical technique in which impedance value is calculated from the faulted current and voltage values. There are two types of impedance-based technique: one-ended measurement which faulted current and voltage

values are measured at one end of the line (Aggarwal et al., 1997; Filomena et al., 2009; Girgis et al., 1993; Santoso et al., 2000; Takagi et al., 1982). Whereas two-ended measurement requires faulted current and voltage values to be measured at both ends of the line (Girgis et al., 1992; Novosel et al., 1996; Ying-Hong et al., 2002).

The advantage of this technique is a simplicity to determine the fault location. It only requires a fundamental component of current and voltage signals during the fault. The general equation used to calculate the fault impedance value, Z_f and the distance of the fault, d from the measurement point can be calculated as in (2.1) and (2.2) respectively:

$$Z_f = \frac{V_f}{I_f} \tag{2.1}$$

$$d = \frac{Z_f}{Z_l} \tag{2.2}$$

where

Z_f = calculated faulted impedance value

V_f = faulted voltage value measured from voltage transformer

I_f = faulted current value measured from current transformer

Z_l = line impedance per unit length

d = fault distance from the measurement point

This technique is widely used for fault location identification in transmission line systems but not for distribution systems. This is because of the complexity of the distribution network such as non-homogeneous cable and lateral branches which contribute to inaccurate result.

2.3.3. Travelling Wave and High Frequency-based Techniques

The operating principle of travelling wave technique is based on the injection and reflection of the voltage or current signal that produce travelling waves. This concept is illustrated as shown in Figure 2.2. Likewise, the high frequency-based technique to identify the fault location based on the high frequency transient of voltage or current signal that is generated due to the fault. It applies the same concept as the travelling wave theory. Both techniques have been applied to determine the fault location especially for the overhead transmission line system (Ancell et al., 1994; Bo et al., 1999; Gale et al., 1997; Ibe et al., 1986; Johns et al., 1991; Lee et al., 1996; Magnago et al., 1999; Spoor et al., 2006; Vazquez et al., 2007; Zeng et al., 2004).

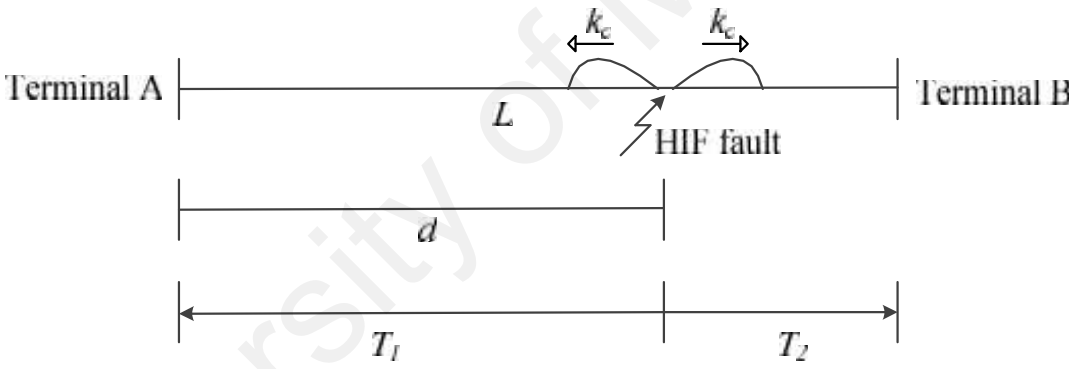

Figure 2.2 : Travelling wave diagram

The fault location is estimated using the equation (2.3):

$$d = \frac{L + k_c(T1 - T2)}{2} \tag{2.3}$$

where

L = length of the line

k_c = propagation speed of the wave

T1 and T2 = time stamp the wave front reaches terminal A and B of the transmission line

Recently, the application of these methods has been adopted to identify the location of the fault in the distribution system (El-Hami et al., 1992; Hizman et al., 2002; Mahmoud et al., 2007). It can be observed that both techniques have the capability to locate the fault accurately. Unfortunately, the implementation of these techniques is complex and costly. These are due to the requirement of the sensors, high speed data acquisition devices and a Global Positioning System (GPS) to capture the transient waveform (Lee, et al., 1996). Besides, these techniques are not applicable for fault location identification for radial distribution system in which the feeder has many laterals.

2.3.4. Intelligent Technique

To overcome the complexity of distribution network in locating faults, an intelligent technique has been explored by many researchers. It is a popular technique due to its capability to analyse a large amount of information in order to achieve a defined goal. Several information such as feeder switch status, atmospheric condition, feeder measurement and signal provided by fault detection devices were used. This technique is highly depending on the amount of information and its accuracy in producing accurate results. There are a few examples of intelligent technique that widely used such as:

a. Expert system (ES)
b. Genetic algorithm (GA)
c. Artificial neural network (ANN)
d. Fuzzy set theory (FST)
e. Matching approach (MA).

a. Expert System (ES)

ES is a technique where human reasoning approach has been adopted in doing diagnosis to get an answer for a given problem. This technique requires pre-defined rules and information about system behaviours such as a breaker and relay status to estimate the fault location. Therefore, reliable and correct information obtained from an experience engineers in this field and genuine data from the SCADA system is necessary for this technique. It can be observed that ES technique had successful in locating the fault in (Kumano et al., 1993; Martinez et al., 1991; Yuan-Yih et al., 1991). However, this technique has its own disadvantages. In order to develop a reliable ES technique, a large amount of data are required to be collected and analysed. Also, to generate a pre-defined rules are difficult in which the rules need to be updated and replaced according to the system changes where expertise and knowledge are required from an expert and experience engineers.

b. Genetic Algorithm (GA)

GA is one of the adaptive heuristic search algorithm that is based on the evolutionary idea. In this algorithm, intelligent exploitation of a random search within a defined search space was utilized to solve a given problem. The basic concept of GA is to simulate a population of randomly generated for evolution. In each evolution, the fitness of the population is evaluated. Population with good fitness will be selected for mutation and recombination process to form a new population. This new population will undergo a same process and it will iterate until a satisfactory fitness level is achieved for that population. The process can be terminated if a maximum number of generations have been produced. In this case satisfactory solution may or may not have been achieved.

In (Wen et al., 1995), GA was utilized to estimate the potentials of faulty section. The faulty section was determined based on the fitness value where section with the higher fitness will be selected as faulty section. However, GA may produce incorrect answers due to its nature of random processes and also force termination due to the maximum number of generation process was achieved. The main drawback of this technique is time consuming. This is because of the repetition process to get a satisfactory fitness level.

c. Artificial Neural Network (ANN)

ANN technique was used to locate faults in the distribution system(Cardoso et al., 2004; Glinkowski et al., 1995) and transmission network system (Mohamed et al., 2003). In order to locate faults, difficult pattern of information undergoes a training process. Through the learning process, the expected target is required for that particular information. Several information such as feeder and circuit breaker status, voltage and current signals can be employed to train ANN.

The disadvantages of this technique are that it is highly dependent on information given to generate a well-trained ANN net. If the information given is inaccurate or limited, it will affect the learning process to identify the fault location correctly. Besides, the ANN net has to be re-trained when there are changes in the system.

d. Fuzzy Set Theory (FST)

In (Jarventausta et al., 1994; Jung et al., 2007; Wen-Hui et al., 2000), the FST was used to determine the fault location. FST has the capability to model the uncertainty and inexactness regarding decision making of fault location. The FST requires the information obtained from the network database, data from the SCADA system such as

relay and circuit breaker status and heuristic knowledge of the control centre operators to estimate the possible fault location.

The main drawback of this technique is the requirement of a large set of data. Thus, the reliability of the supplied data is important to determine the accuracy of the result. Besides, the technique is only applicable for distribution system with the integrated SCADA system.

e. Matching Approach (MA)

MA technique requires a simulated fault to be established at each node and stored the data as references in database. With this approach, measured data during fault is compared with simulated data (reference data stored in database) to determine the faulty section. The faulty section is identified if the measured data fall between two adjacent nodes of simulated data. Usually voltage and current signals are used for this purpose as these signals are easily obtained at the primary substation.

Voltage sags pattern and database approach had been proposed to locate the faulty section in (Li et al., 2005; Mokhlis, Li, & Khalid, 2010; Mokhlis, Li, Mohamad, et al., 2010; Mokhlis, Mohamad, Bakar, et al., 2011; Mokhlis, Mohamad, Li, et al., 2011). The faulty section is identified when the measured magnitude of voltage sags lies between two simulated magnitude of voltage sags that represent two adjacent nodes of a line section. Furthermore, this method had been improved by introducing ranking analysis (Mokhlis, et al., 2011). Ranking analysis is responsible to rank the possible faulty section especially for lateral branches. This ranking priorities the search area, starting from the higher possibility down to the less possibility of faulty section.

2.4. High Impedance Fault Detection Method

High impedance fault is a disturbance event which produces an arcing and may lead to a fire hazard. It may lead to potential hazard for both human being and the environment. If this event is not being treated immediately, it will cause an unnecessary incident to happen as well as the interruption on power system equipment and operations. Therefore, it is crucial to detect the occurrence of HIF and locate the fault immediately.

HIF detection can be categorized into 2 types: mechanical HIF detection and electrical HIF detection. Both techniques are utilized to identify the occurrence of HIF in the distribution network system. Brief reviews on both techniques are explained in the following sections.

2.4.1. Mechanical HIF Detection

Mechanical detection of HIF is a technique that comprises a device that forcing contact with a solid ground in order to allow conventional overcurrent protection relay to operate (Mark Adamiak et al.). During the HIF event, fault current magnitude is not sufficient to be detected by the overcurrent protection relay. Thus, mechanical detection is developed to produce a low impedance ground fault when a conductor physically breaks and falls to the ground.

There are 2 examples of mechanical HIF detection methods. The first method consists of the device mounted to a cross arm or pole. These devices are installed under each phase wire in order to catch the falling conductor to the ground. During the HIF event, the force of the falling conductor produces an internal spring which ejects a bus bar to make contact with the fallen wire. This contact will create a low impedance ground fault which will trigger the conventional overcurrent protection relay to operate.

The second method of mechanical detection involving the pendulum mounted aluminium rod with hooked end. This device is suspended from an under-built neural conductor. When the conductor falls to the ground, it will get caught by the hook and produce a low impedance ground fault. This will cause the conventional overcurrent protection relay to operate.

Both methods are responsible to catch the falling conductor and produce a low impedance ground fault to trigger the overcurrent protection relay. Unfortunately, these mechanical methods can also detect sagging conductor which does not come in contact with grounded object or earth. This will lead to false detection and falsely trip the line. Also, these methods require a high cost of installation and maintenance. Due to this constraint, certain area of distribution network cannot be protected for HIF detection. Besides that, these mechanical methods are only applicable for overhead distribution network and transmission line. In order to detect the occurrence of HIF for underground cable, an electrical HIF detection is needed.

2.4.2. Electrical HIF Detection

This technique utilises the voltage and current signal measured from the measurement devices at primary substation. The voltage and current signal will be analysed using the digital based technique to extract the signal signature. Then, from the extracted signal signature, the occurrence of HIF in the distribution network is determined. This technique gives better HIF detection compared to the previous technique.

Generally, the process of electrical HIF detection comprises of two basic steps; feature extraction and pattern recognition (classification). In the feature extraction process, the significant information from voltage and current signal is extracted using various

feature extractors or digital signal processing. Whereas in the pattern recognition process, the extracted features will be fed to the classifier to be trained to define and determine the characteristics of the distorted voltage and current signal caused by the HIF. Also, the classifier will be trained to discriminate the HIF event from other similar fault phenomena such as inrush current, load switching, line switching, insulator leakage current and harmonic load.

2.4.2 (a) Feature Extraction

There are several techniques that have been employed to extract important information from the voltage and current signals such as:

a. Fourier Transform
b. S-Transform and TT-transform
c. Multi-Resolution Morphological Gradient
d. Wavelet Transform

The output obtained from this feature extractor will be used to detect and discriminate HIF and non-HIF event.

a. Fourier Transform

Fourier Transform, FT is a mathematical operation that transforms a signal from a function of time representation to a function of frequency representation and it can be depicted using the frequency spectrum. Generally, FT can be described as a mathematical tool that decomposes the signal waveform, F(x) into its sinusoidal components that consists of sine and cosine waves as shown in Equation (2.4). The equation can be expressed as a sum of cosine and sine function with a defined variable $a_0, a_1, a_2, \ldots a_n$ and $b_1, b_2, b_3, \ldots b_n$.

$$F(x) = a_0/2 + a_1\cos x + b_1\sin x + a_2\cos 2x + b_2\sin 2x + \ldots + a_n \cos nx + b_n\sin nx \quad (2.4)$$

The variables of a_0, a_1, a_2, … a_n and b_1, b_2, b_3, … b_n are calculated up to the largest possible value of n to achieve more accurate F(x) representation. Some of FT applications are to isolate individual components of a compound waveform and concentrating them for easier detection and/or removal purposes. Besides that, the FT also can be applied to remove unwanted frequency or noise for example in audio recording.

In (Zadeh, 2005) , Discrete Fourier Transform (DFT) is used to extract the second and third harmonic (magnitude and angle) components of the voltage and current signals. The third and fifth harmonic components are extracted using Fast Fourier Transform (FFT) in (Bansal et al., 2007). In these studies, the variation in amplitude of the second, third and fifth order harmonic components is monitored to detect the occurrence of HIF.

The main disadvantage of FT is that it only represents a signal with perfect frequency representation but no time information. FT gives poor performance when it is applied to transform the time domain signal embedded in noise. It will limit the certainty of magnitudes, phases, peak frequencies and widths to be computed by FT because the time domain noise is distributed uniformly throughout the frequency domain during the transformation process. Also, a truncated time domain signal will produce undesirable frequency domain which makes it difficult to observe a small peak in the vicinity of a large peak.

b. S-Transform and TT-Transform

In (Samantaray et al., 2008), S-transform and TT-transform are used to extract energy and standard deviation information from the current signal to classify the HIF from no fault event. S-transform and TT-transform are the time-frequency and time-time transformations of the signal respectively.

Generally, the S-transform is a simplification of the short-time Fourier transform (STFT) and extension to the idea of continuous wavelet transform (CWT) (Stockwell et al., 1996). It is based on a moving (translation) and scalable (dilation) localizing Gaussian window. S-transform overcome some of the disadvantages of the STFT and CWT. It has a window whose width and height vary with frequency unlike STFT which has fixed width and height of the window.

Therefore, the S-transform is capable to give both time and frequency information with proper time and frequency resolutions respectively. The frequency and time information are extracted separately in order to give better frequency and time resolutions. The extracted frequency information provides better frequency resolution to give accurate frequency information but provides poor time resolution. Whereas, the extracted time information delivers a better time resolution to obtain the accurate information of time but delivers poor frequency resolution.

The TT-transform is a two-dimensional time-time representation, which is derived from a one-dimensional time series based on S-transform (Pinnegar et al., 2003). TT-transform represents the time–local view of the time series through the scaled windows. In TT-transform, the horizontal time axis denotes the position of the window and the vertical axis denotes the time axis of the time series. The degree of localization of the

signal component is frequency invariant unlike the S-transform which is frequency dependent. TT-transform provides proper time-local properties of the time series which is necessary to localize the frequency components of the time series.

c. Multi-Resolution Morphological Gradient

Mathematical Morphology (MM) is a technique used in the analysis and processing of geometrical structure, based on set theory, lattice theory, randomness and topology functions. It is usually applied in digital image application but it also can be applied to graph, solids, surface meshes and other spatial structures. The purpose of the MM is to extract image components and provides image descriptions and representation. This method gives a qualitative description of geometrical structure for image analysis. Most MM operators are based on simple shrinking and expanding operations.

In (Sarlak, et al., 2011), MM was utilized to detect the occurrence of HIF and to differentiate it from other similar phenomenon such as load switching, fault on adjacent feeders, capacitor bank switching, harmonic load and insulator leakage current. In this study, the Multi-resolution Morphological Gradient (MMG) is used to extract time-based features from post-disturbance current waveform. This technique will highlight the irregularities of the current signal during disturbances. The large magnitude of MMG's output coefficient indicates that there is a strong irregularity in the current signal. While, a small magnitude shows a weak abnormality in the signal. In this method, the average, standard deviation, minimum and maximum value of MMG's output extracted from the gradient current signal are computed and assigned as the input features for pattern recognition purpose.

The main drawback of MMG is no information available about the moment of event occurrence. It is also hard to differentiate a signal that has very small difference. Thus, providing an inaccurate result.

d. Wavelet Transform

Wavelet signal is a wavelike oscillation with an amplitude that starts from zero, increases and then decreases back to zero within a limited duration that has an average value of zero. It behaves as a mathematical function that satisfies certain mathematical requirement to represent the signal in time domain. Wavelet transform (WT) had overcome the drawback of FT in term of constructing a time-frequency representation of a signal that offers very good time and frequency localization.

In engineering application of signal processing, WT has replaced the conventional Fourier Transform and it is being applied for a variety applications such as signal processing, image processing and speech recognition. Also, in power system application, the WT has been widely used in extracting information for HIF detection (Akorede et al., 2010; Elkalashy et al., 2008c; Etemadi et al., 2008; Haghifam et al., 2006; Lai et al., 2005; Michalik et al., 2007; Michalik et al., 2006).

In (Michalik, et al., 2007; Michalik, et al., 2006), continuous wavelet transform, CWT is used to extract important features from current and voltage signals to determine the occurrence of HIF. The HIF detection algorithm is based on a discrete form of continuous wavelet coefficients, CWCs.

The discrete wavelet transform, DWT had been used to analyse the voltage and current signal during the HIF event (Akorede, et al., 2010; Elkalashy, et al., 2008c; Haghifam, et al., 2006; Lai, et al., 2005). In (Lai, et al., 2005), the DWT output coefficients were converted into RMS values in various frequency ranges to be the input data to the classifier for the pattern recognition process to classify HIF event from other various types of faults.

The multi-resolution analysis-discrete wavelet transforms, MRA-DWT is an extension of the DWT, where the decomposition process is iterated with successive approximation components. It gives better signal representation because its resolution is balanced at any time and frequency. In (Etemadi, et al., 2008), the MRA-DWT was utilized to extract the input features from the nonlinear behaviour of the current waveform for the HIF detection purpose.

The main advantage of wavelet transform is it localization property in both time and frequency domain. It can represent the signal that has tiny discontinuity and sharp peaks. It also gives an indication of the frequency content of the disturbance signal and reveals the important features in the signal by partitioning the signal energy at a different frequency band.

2.4.2 (b) Pattern Recognition (Classification)

The second step to identify and discriminate the HIF after the important features are extracted from voltage and current signals is training the classifiers. This step is important to distinguish the HIF event with other fault types. There are several pattern recognition techniques that can be applied such as:

a. Artificial Neural Network
b. Fuzzy Inference System
c. Nearest Neighbour Rule
d. Moving Window Approach

In order to achieve good performance for HIF identification and discrimination, a sufficient set of data is necessary during the training process.

a. Artificial Neural Network

Artificial neural network (ANN) is an information processing method that is motivated by the idea of the nerve system. The neural network structure deal with the imprecise and large amount of data as an input data to be trained or adjusted for a specific target output. Due to its outstanding ability to extract information or pattern from imprecise or complicated data, ANN had been used widely to detect and classify the HIF event from other type of fault (Bansal, et al., 2007; Michalik, et al., 2006; Samantaray, et al., 2008; Sarlak, et al., 2011; Zadeh, 2005).

Although ANN has the capability to recognize difficult patterns of information, it requires a large set of input data to be trained to be able to differentiate various types of faults in power system. Lack of information or unreliable input data will affect the result accuracy. There are several types of neural network had been used for that purpose such as feedforward neural network, probabilistic neural network and learning vector quantization neural network.

The feedforward neural network (FNN) is one of the simplest type of artificial neural network where the information is moving in only one direction (do not form a directed cycle or loops). The information travels straightforward, from the input nodes through the hidden nodes (if any) and lastly to the output nodes. Thus, the output of any layer does not affect that same layer.

The FNN can be divided into two types; single-layer perceptron neural network (SLPNN) and multi-layer perceptron neural network (MLPNN). In SLPNN, it consists only a single layer of output nodes which means that the inputs are moving directly to the outputs via a series of weights. Whereas in MLPNN, it consists of multiple layers of computational units. Each neuron in one layer has direct connections to the neurons of the subsequent layer. In (Michalik, et al., 2006; Sarlak, et al., 2011; Zadeh, 2005), MLPNN was used to detect the occurrence of HIF. Different number of neurons and hidden layers were chosen for the network. In (Sarlak, et al., 2011), the output from each MLPNN were combined using the average method producing two output neurons (final outcome) which show the two states of HIF and non-HIF condition respectively.

The second type of neural network is a probabilistic neural network (PNN). A PNN is an implementation of a statistical algorithm called Kernel Fisher discriminant analysis. The operations of PNN are organized into a multi-layered feed forward network, which was derived from Bayesian network. Unlike FNN which is constructed by three layers, PNN consists of four layers consists of input layer, hidden layer, pattern layer/summation layer and output layer. PNN model is a supervised learning network with the very fast learning process. It is very suitable to be implemented for fault diagnosis and signal classification problem in real time. The basic principle of PNN is the classification of training data according to their distribution value of probabilistic

density function (PDF). In (Samantaray, et al., 2008), the standard deviation and energy were computed and applied to train and test the performance of PNN for HIF classification.

The third type of neural network is learning vector quantization (LVQ). Similarly to PNN, LVQ is a supervised learning network, supervised version of vector quantization (VQ). VQ is a technique in which the input space is divided into a number of different regions, and for each region a reconstruction vector is defined. When a new input is present, a vector quantizer will determine the input data belong to which region where the vector lies. By LVQ network, the quality of the classifier decision region is improved. In (Bansal, et al., 2007), LVQ is adopted to classify and differentiate the HIF pattern with other fault types patterns.

It can be concluded that the neural network is an interesting technique used mainly for classification and diagnosis purpose. However, this technique requires a lot of input data to achieve a good analysis. Besides, the accuracy of the input data is important to produce an accurate result.

b. Fuzzy Inference System

Fuzzy inference system (FIS) is a process of formulating the mapping for a given input using the fuzzy logic to produce an output. Basically, the modelling of the FIS is to identify the structure and parameters of a fuzzy "IF-THEN" rule base in order to get a desired input/output mapping. From the mapping output, a decision can be made based on the distinguished patterns. In (Haghifam, et al., 2006), the FIS had been implemented for fault classification. It consists of three main parts which are fuzzy set theory, fuzzy 'if-then' rules and fuzzy reasoning.

Since the FIS is a rule base method in which the output of FIS is determined based on the membership function, an effective method is required for tunning the membership function to minimize the output error. In (Etemadi, et al., 2008), the learning capability of the neural network is utilized to tune the membership function. The combination method of fuzzy logic modelling and neural network as the learning algorithm had led to the field of adaptive neural fuzzy inference system (ANFIS).

The approach of ANFIS is to produce only one target output for a several given input. In order to obtain a targeted output, the membership function parameters in the input and output sides are adjusted through a learning process. The learning process uses a combination between least-square estimation and back-propagation techniques as both techniques give very fast convergence and more accurate output target.

c. Moving Window Approach

Moving window (MW) method is a nonparametric approach. The idea of MW is to impose a window centred at the point of interest to estimate the weighted sum of coefficients at the given log-spacing point. It only observes the data within the window which regarded as 'neighbour' to be included in the weighted sum of coefficients. Then, the window is moved again to the next point, where new parameters are estimated using only its neighbouring observations. This procedure is repeated until the moving window visits all the estimation points in the study area.

This appealing method provides a unique pattern from the weighted sum of coefficients. In (Akorede, et al., 2010), this method was used to discriminate different pattern of fault types. One-cycle window is moved continuously by one sample and concurrently

calculate the absolute sum of coefficients for the sample that falls within the respective window.

d. Nearest Neighbour Rule

Nearest neighbour rule (NNR) technique is also a non-parametric approach in supervised learning method. NNR is a typical pattern classification method in which the object is classified based on the closest distance between the input data and the classified data in the feature space.

In (Lai, et al., 2005), NNR method was used to demonstrate the classification result for two sorts of data based on the decision boundaries. The data and boundaries were plotted in two dimensional contour graph to see the distribution pattern of the data. In this study, NNR method was utilized to differentiate HIF cases and normal cases. However, this method has a major problem when the input data falls in overlapping areas of HIF cases and normal cases. In this case, an analysis by an expert and experienced engineers are required.

2.5. High Impedance Fault Location Method

In a previous sub-chapter, fault location techniques for low impedance fault had been discussed. In this sub-chapter, fault locating techniques for a specific type of fault which is the high impedance fault, HIF is presented. Unlike locating low impedance faults, to identify the HIF location, it consists of two steps: feature extraction and fault location classification. The main objective of identifying the HIF location is to limit the extend and duration of service interruption and power outage.

Initially, important features were extracted from the voltage and current signals before a fault location is identified. There were several approaches to determine the HIF location such as:

a. Network Topology Technique
b. Travelling Wave Technique
c. Knowledge-based Technique

2.5.1. Network Topology Technique

Network topology is an arrangement of various elements such as cable, nodes, measurement unit and sensor. This technique requires a sensor or measurement device to be installed on each node. The sensor or measurement devices then will communicate to each other and send data to the primary substation through Global Positioning System (GPS). The received data will be analysed to determine the fault location.

In (Gohokar et al., 2005), current transformer (CT) was installed on each node. The CT will assign symbol digit 0 and 1 as an indicator for the fault occurrence. Symbol digit 0 was assigned when there is no fault indicate a normal load current event. Whereas symbol digit 1 was issued to indicate the occurrence of HIF. The symbol digit 0 and 1 were determined based on the magnitude of the current signal after fault. Therefore, the current signal measured was analysed using the Discrete Fourier Transform (DFT) to get the fundamental component of current signal before symbol digit can be allocated. In DFT analysis, the high frequency component was filtered out from the distorted waveform of current signal due to the HIF. The resulting fundamental component of current signal is converted to root mean square (RMS) value. This RMS value will be used for further decision-making process to assign a symbol digit to CTs. The faulty section is determined based on the combination of symbol digit of two adjacent CTs

which has symbol digit of 1 and 0 respectively. If 0 and 0 or 1 and 1 symbol digits are given out by two adjacent CTs, its indicate a normal section. Otherwise, a faulty section is located. However, for the last line section at the end of the feeder, the fault occurrence in this section is identified based on 1 and 1 symbol digit.

The identification of the faulty section based on the status of voltage sensor installed at each end of the network branch was proposed in (Garcia-Santander et al., 2005). Initially, the condition of the sensor is determined whether above or below the fault. A sensor which is located below the fault will be called as an “active sensor”. To determine the status of “active sensor”, the absolute difference value of voltage magnitude before and after the fault is measured at each voltage sensor. Voltage sensor which has an absolute difference of voltage signal exceeded the threshold value, the voltage sensor will be considered below the fault. Otherwise, the voltage sensor is assumed to be above the fault (“passive sensor”). Then, a route for each “active sensor” until the substation (downstream to upstream) is identified. Finally, the faulty section is determined based on the first common path travelled by all the active sensors.

An application of Discrete Wavelet Transform (DWT) to extract features from the voltage and current signals to trace the fault location was presented in (Elkalashy et al., 2008a, 2008b). The power polarity concept was employed to identify the faulty feeder in (Elkalashy, et al., 2008b) and determine the faulty section in (Elkalashy, et al., 2008a). Initially, the power was calculated by multiplying the DWT detail coefficients of the residual voltage and current signals at each feeder. Based on the calculated power, the polarity of the power will determine the status of the feeder. Feeder with positive power polarity is presumed to be a healthy feeder and negative power polarity indicate a faulty feeder.

The power polarity concept was extended to identify the faulty section in (Elkalashy, et al., 2008a). In order to ensure the success of this approach, wireless sensors are required to be installed at each measuring node. The wireless sensors must have the capability to measure voltage and current signals and also transmit the signal data to the main substation to be analysed. For the first stage, power polarity is used to recognize a faulty feeder. Then, the fault location is narrowed down to classify more specific main faulty section within the faulty feeder. Finally, the actual faulty section is point out among all the possible sections in main faulty section. By utilizing this process, it enables fault route to be traced easily and expedite the process to determine the fault location.

Another approach proposed to identify the faulty section is based on the ratio of the residual current amplitude (Elkalashy et al., 2007). In this approach, the phase currents were measured by the wireless sensor and collected at the main substation to be analysed. The residual current signal was analysed using the recursive Discrete Fourier Transform (DFT) in order to obtain the fundamental component of the current signal. Determination of the faulty section is based on the ratio of the fundamental component of current signal at each section with respect to the parent section. Parent section is the first section (from the upstream) of the feeder. The faulty section was identified through the highest ratio of the residual current amplitude. To increase the efficiency of this approach, the difference value of the fundamental residual current amplitude during and pre-fault is considered.

Lastly, the determination of fault location based on the information given by sectionalizer and recloser devices had been done in (Uriarte et al., 2005). The third and fifth harmonic contents are used to identify the faulty section.

It has been found that utilizing topology technique promising an accurate high impedance fault localization. However, this technique requires a sensor device or measurement unit to be installed on each node. Thus, it is not cost effective technique due to the need of high cost installation and maintenance. Besides, it is compulsory to ensure that all the sensor devices or measurement units are in a good condition and functioning well to measure and transmit voltage and current signals to main substation. Failure to do so will affect the overall performance of locating the fault. It will cause fault location to be wrongly identified thus slow down the system restoration.

2.5.2. Travelling Wave Technique

Travelling wave technique is a method in which travelling wave signal was generated both forward and backward from the point of disturbance, propagating towards the end of both nodes. Time taken for the travelling wave signal pass through both ends is used to estimate the fault location. In previous sub-chapter, application of travelling wave technique which had been widely used in detecting low impedance fault location was discussed. Recently, this technique has come into interest to the researchers to trace the fault location during HIF event (Bernadić et al., 2012; Dutra et al.).

Travelling wave technique is an interesting technique because it has the capability to identify the fault location regardless of the fault type. Also, this technique gives an excellent reliability and high accuracy in identifying fault location which leads to a faster restoration process.

In (Bernadić, et al., 2012), travelling wave technique was applied to find the fault location in transmission system during HIF incident. Initially, the measured three-phase faulty voltage signals were converted to its complex space-phasor by means of vector of

absolute values. A fault travelling wave is represented by the vector of absolute value due to its quoted physical properties. This complex space-phasor has all the characteristics of travelling wave particularly the correct wave speed which leads to fast and accurate fault location identification.

The drawback of this technique is that its requires a Global Positioning System (GPS) to transmit a measured data from both ends to be analysed. Therefore, a reliable communication link is necessary to send the data successfully to the main substation. It was noticed that the travelling wave technique mostly be used to locate faults in the transmission system. Till now, there is no research has been conducted to investigate the fault location for distribution system during the occurrence of HIF. This is due to the topology of the distribution system such as radial and branches which requires a high speed data acquisition device to be installed on each node. Thus, this technique is costly and only suitable to be implemented on transmission system which has long distance between two nodes.

2.5.3. Knowledge-based Technique

Several knowledge-based techniques had been proposed to identify the fault location for HIF in the distribution system. In general, knowledge-based technique requires a training and testing procedure to obtain a reliable '.net' file. A simulated fault was created and the obtained voltage and current signals will be trained and tested. The obtained '.net' file will have the advantage to generalize the output during random fault based on the learning process acquired during the training and testing process.

Two different types of knowledge-based techniques used for determining the fault location are a Feedforward Neural Network (FFNN) (Bretas et al., 2006; Jensen et al., 1998) and Adaptive Neuro Fuzzy Inference System (ANFIS) (Abdel Aziz et al., 2012).

a. Feedforward Neural Network

In (Jensen, et al., 1998), feedforward neural network (FFNN) had been employed to determine the fault location. The input features used for training and testing process of FFNN are based on a grid description of the feeder by impulse response. A set of impulse response cover the feeder in the grid with equal space step using the finite impulse response, FIR filter.

Whereas in (Bretas, et al., 2006), the input features used for net development are extracted from the Discrete Fourier Transform (DFT). From the DFT analysis, fundamental current and voltage signals and also third harmonic current signal were extracted to generate the input patterns that will be used in fault localization process whose the output indicate the fault location. The proposed fault location routine consists of two FFNN which represent phase fault and ground fault. The FFNN consists of five input neurons, seven hidden neurons and one output neuron where the output neuron was employed with a pure linear function.

The proposed technique had successfully located the fault with the percentage error below 5% of the feeder's length with the presence of distributed generation, DG. Unfortunately, the studied distribution system is a radial network, neglecting a lateral network which is a common network topology nowadays. Therefore, the proposed method cannot be justified the capability to identify the fault location for a radial network with lateral.

b. Adaptive Neuro Fuzzy Inference System

Identifying the location of the fault based on an adaptive neuro fuzzy inference system (ANFIS) had been conducted in (Abdel Aziz, et al., 2012). The input features for ANFIS is the third harmonic components of magnitude and angle of three phase current extracted using DFT. ANFIS technique consists of five main components; fuzzy sets, fuzzifiers, fuzzy rules, an interference engine and defuzzifiers.

In can be noticed that ANFIS application is limited to the modelling system with a defined ill system. It also requires the expertise of experienced engineers to develop a rule structure. It found that ANFIS technique is quite complicated and burdensome technique especially during a system changes where the fuzzy rules need to be updated and changed.

2.5.4. Summary

It can be observed that few researchers had studied the fault location during the HIF event in a distribution system. The discussed methods have its own advantages and limitation. The following conclude each of the discussed methods:

- Network topology technique

  This technique is efficient and give high accuracy to identify the faulty section. However, this technique requires a sensor or measurement device to be installed on each node. Therefore, high cost of installation and maintenance are required to provide accurate faulty section detection. The accuracy of the technique can be affected if one of the sensor or measurement device is faulty or not working.

- Travelling wave technique

  This technique gives high accuracy in locating the fault location for transmission line system. For distribution system, this technique is not suitable to be

implemented due to the high cost. Also, a radial distribution system with multiple lateral make it impossible to narrow down all possible faulty sections. The requirement of Global Positioning System (GPS) to transmit a measured data from both ends can affect the accuracy to locate the fault when the communication link is broken and unreliable.

- Knowledge-based technique

  This technique is easy and fast technique to determine the fault location based on the learning vector. However, this technique requires a large number of data to be trained and tested to produce a reliable net in order to identify the fault location accurately. Besides, the accuracy of this technique relies on the reliability and validity of the input data.

All of the above techniques require an input feature which is extracted using a filter or digital signal processing such as DFT and DWT. There is a proposed technique which only requires extracted features to directly determine the fault location. In (Dwivedi et al., 2008), only a sum of third level detail coefficients of current signal is needed. The faulty section is identified by comparing the sharp variation value of the sum of detail coefficients. It is found that all the proposed techniques were able to estimate the location of the fault successfully. Unfortunately , each of the technique is associated with certain drawback which limit its reliability and effectiveness. Therefore, a reliable technique with high accuracy, cost effective, efficient and practical to be applied in a radial distribution system with lateral is needed.

CHAPTER 3

BACKGROUND OF HIGH IMPEDANCE FAULT AND WAVELET TRANSFORM

3.1. High Impedance Fault

3.1.1. Introduction

HIF detection and localization on a distribution system is a challenging problem encountered by power utility companies. Unlike normal type of fault that cause a substantial increase in current flow, HIF does not cause a substantial increase in current flow. As a result, the fault current occurrence does not trigger the overcurrent protection relay. Thus, it is difficult to detect the occurrence of a HIF event by the fault locating devices. The problem is worse for identifying the fault location especially for a radial distribution system with lateral. This chapter presents a brief synopsis of HIF based on the definition, characteristics, causes, effects, reliability and actions to be taken during the HIF.

3.1.2. Definitions and Objectives

Generally, HIF is a phenomenon when undesirable contact is made between a conductor and non-conducting or poor conductivity object or surface. Also, HIF can be defined as those that do not produce enough fault current to be detectable by the conventional overcurrent protection relay to trip the faulty section (John Tengdin, et al., 1996). This is because of the high impedance restricts the flow of fault current causing no substantial increase in current signal can be observed. It can get confused with the

slightly increase in current signal due to the load increase events, thus will lead to malfunction of the protective devices.

The objectives of HIF detection, classification and localization are to reduce the duration of power outages and service interruption. It also to avoid the damaging possibility to the power system equipment and more importantly to prevent hazards to human life.

3.1.3. Characteristics

The main characteristic of HIF is low fault current due to the restrict of high impedance to the flow of fault current. Typically, the magnitude of fault current is ranging between 10 to 100 Amperes. Also, the current signal tends to exhibit a random behaviour with wide fluctuation and unstable waveform (John Tengdin, et al., 1996).

The presence of arcing can be used as an indication of the occurrence of HIF. Arcing is a phenomenon in power system which is a result of the air gap produced between the conductor and ground or a grounded object. This air gap will create a high potential over a short distance where the arcing is generated when the air gap is broken down.

Also, it can be observed that HIF does give very little effect on voltage waveform. As shown in Figure 3.1, there is a very little fluctuation in the voltage waveform which is hardly to be seen and detected by the naked eyes. The HIF also can be characterized by the presence of harmonics and high frequency components. The harmonic components can be classified using the Fourier Transform whereas the high frequency components can be extracted using the Wavelet Transform.

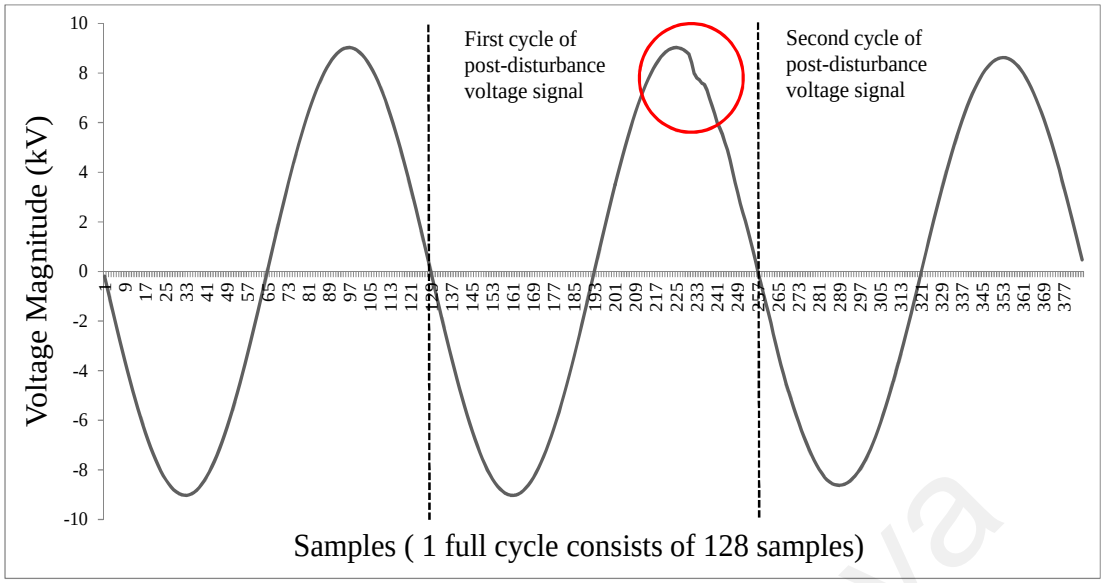

Figure 3.1 : Voltage sinusoidal measured from voltage transformer during HIF event

It can be found that most of the HIF event occurs in the distribution system with distribution voltage of 15kV and below. The problem of HIF event is worse at the lower voltage and less severe for distribution voltage of 25kV and above.

3.1.4. Causes

Technically, HIF can occur at overhead and underground distribution system. Normally, HIF at overhead system occurred when the conductor is physically broken and make undesirable contact with a ground or high impedance surface. A broken pole also might cause a line conductor to touch a ground or high impedance object. It can be observed that, the HIF can also happen without a path to ground, such as when a tree limb bridge two phase conductors. Failure on the conductor mounting system also can contribute to the occurrence of HIF.

Whereas, for an underground cable, HIF is normally caused by insulation defects that exposes the conductor to contact with non-conducting elements. Common causes of insulation defects include cracking, chafing, abrasion, flash fault and insulation degradation due to moisture and corrosive contamination. HIF can also happen due to

the cable cut, causing a contact between conductor with non-conducting element such as cable core and sheath.

3.1.5. Effects

The occurrence of HIF may result an arcing which leads to potential hazards to human life and the environment. The arcing in the underground cable can lead to unexpected explosion due to the very high flashover energy as shown in Figure 3.2. The flashover is an electric discharge over or around the surface of an insulator. Therefore, it is crucial to isolate an energized part immediately to prevent exposing personnel and the public to the explosion, arcing and fire.

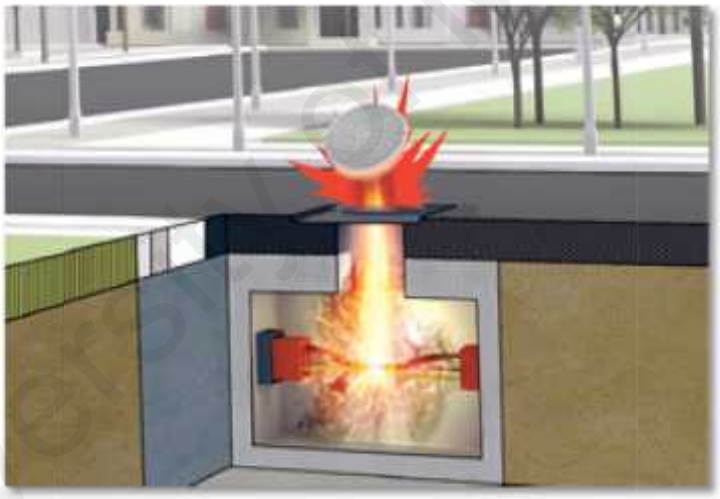

Figure 3.2 : Explosion during HIF event
(http://www.gedigitalenergy.com/multilin/feeder_spotlight.htm)

In Figure 3.3, an electric arcing phenomenon is created when the tree branch bridge across an operating 7,200 volt operating distribution line at the PSAL test facility on the Riverside Campus at Texas A&M.

Figure 3.3 : An electric arcing phenomenon
(**http://phys.org/news/2010-11-faults-vegetation-contact-lines.html#jCp**)

Moreover, a significant risk of fire as a consequence of the arcing phenomenon may pose damaging possibility to the power system equipment. On the long run, if HIFs are left untreated, they will affect power system quality in terms of service continuity and energy loss. Thus, the occurrence of HIF must be detected immediately before a complete failure ensues, which may cause power outages that leads to loss of productivity.

3.1.6. Reliability

The reliability performance is a main issue related to HIF event. This performance can be measured based on the sensitivity and security performances. The higher level of sensitivity performance is obtained when the HIF detector had correctly recognized every downed conductor or any HIF events that happened on its feeder. Whereas high levels of security is achieved when the HIF detector does not falsely indicate a HIF from any other fault phenomena in power system.

However, there is a trade-off between sensitivity and security performances. If high level sensitivity is achieved, then it will reduce the security level and vice versa. Therefore, it is important to determine the best sensitivity and security level for the HIF detector. This efficient reliability performance can be acquired by the design and operating characteristics of the HIF detector and also by its settings.

The sensitivity performance to detect HIF and distinguish it from other type of faults can be improved by a series of staged fault tests. But, the security performance can only be enhanced by leaving the HIF detector in service for long periods of time to ensure that it is not subtle to non-HIF events.

3.1.7. Safety versus Service Continuity

After feeder where HIF occurs has been identified, the utility engineer needs to choose whether to trip the feeder or alarm the signal regarding to the event. The choice of action is taken based on the location of the fault. It is necessary to trip the feeder if the region of the event is around a school or residential area. On the other hand, if HIF occurred in the hospital or industrial areas, a better decision is to trigger the alarm. Decision to trip or alarm is crucial depending on the necessity of the power supply and hazardous caused by the continuation of the power supply during the HIF event.

The feeder is tripped right after the occurrence of HIF is identified in the distribution system. The purpose of this action is to de-energize the feeder to avoid the arcing and fire hazard. This is because the public safety is in danger due to the phenomena caused by the HIF event. Small children or unaware citizen about the fault may come closer to the fault location. Sometimes the fault occurs within the reach of the public. Due to this dangerous scenario, tripping the feeder is a wise decision to avoid unnecessary incidents

to occur. However, if this action is chosen, locating the HIF will become difficult. This is because, de-energize conductor does not show any indication of the occurrence of the HIF.

On the other hand, energize conductor during HIF will generate electric arcing or fire which can be located easily via sight. It also can be located via sound, radio frequency interference (RFI) or loss of power in an area (M. Adamiak et al., April 2006). Therefore, to allow the conductor to be energized, the alarm signal is issued instead of tripping the feeder. This alarm signal has to be taken seriously and remedial action has to be done immediately as the energized conductor can produce arcing and fire hazard. Meanwhile, a public announcement about the possibility of the occurrence of HIF and its danger has to be issued so that a precautionary action could be taken.

The reasons for this alarm action instead of tripping is to avoid possible unsafe conditions such as traffic light malfunction at busy intersections (traffic hazards). Also, life support equipments are malfunction during the power outage which will cause the patient's life in danger or loss their life. Besides, industrial customer may face huge losses due to the shutdown of the production process.

Therefore, the decision to trip or not to trip the feeder as a course of action must be based on the relative consequences of each action. Nevertheless, a quick action in locating the fault location has to be taken to expedite the power system restoration process.

3.2. Wavelet Transform

3.2.1. Introduction

The wavelet transform is a wavelike oscillation with an amplitude that starts from zero, increases and decreases in certain amount of amplitude and goes back to zero amplitude within a limited duration which has an average value of zero. Generally, wavelet is a mathematical function that satisfies certain mathematical requirements to represent the signal in time and frequency domain.

The fundamental idea behind wavelet transform is to analyse the original signal according to the scale (by dilation and translation). It can be assumed as cutting the signal of interest into various lengths with the same size of the samples and then analyse each sample separately. For example, if we sample a signal with a small “window” (small dilation) and move the window along the signal (translation), we would notice the distinct features of the signal. Similarly, if we sample a signal with a large “window” and move it, a vague features of the signal will be obtained. Therefore, by varying the size of the “window” and shifting the “window” across the signal, more significant and various features of the signal can be gained (Wavelet Transform).

Basically, wavelet transform has overcome the limitation of Fourier transform of gaining information in time and frequency domain at the same time. The Fourier transform only provide information of frequency domain and lose the time localization information during the analysis. It depicts all the frequency component present in a signal without the moment of occurrence.

Whereas wavelet transform can be viewed as a trade-off between time and frequency domains. It allows exceptional localization in both the time domain and scale (frequency) domain via translations and dilations processes of the mother wavelet respectively. Figure 3.4 shows the pattern of dilated Gaussian wavelet as mother wavelet which is scaled by parameter a. The translation and dilation operations are performed to calculate the wavelet coefficients to represent the correlation between the signal of interest and mother wavelet. Basically, wavelet coefficients are calculated for each signal segment, giving a time-scale function relating the correlation between wavelet and signal. The process of translation and dilation of the mother wavelet on the signal is shown in Figure 3.5.

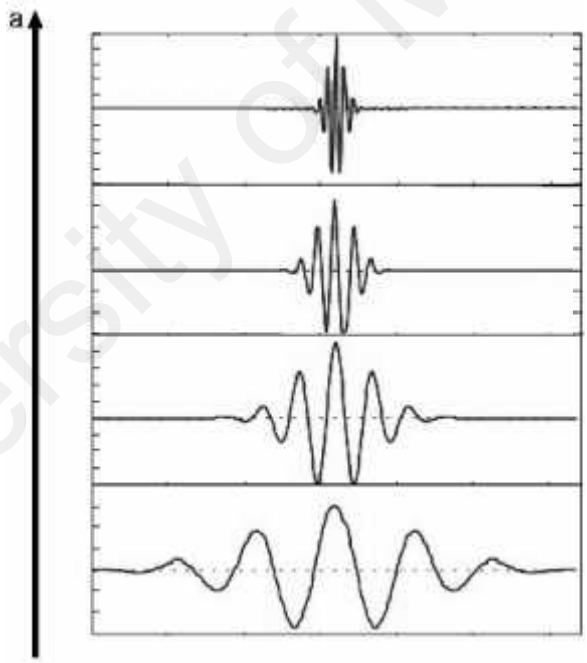

Figure 3.4 : Dilation patterns of Gaussian wavelet

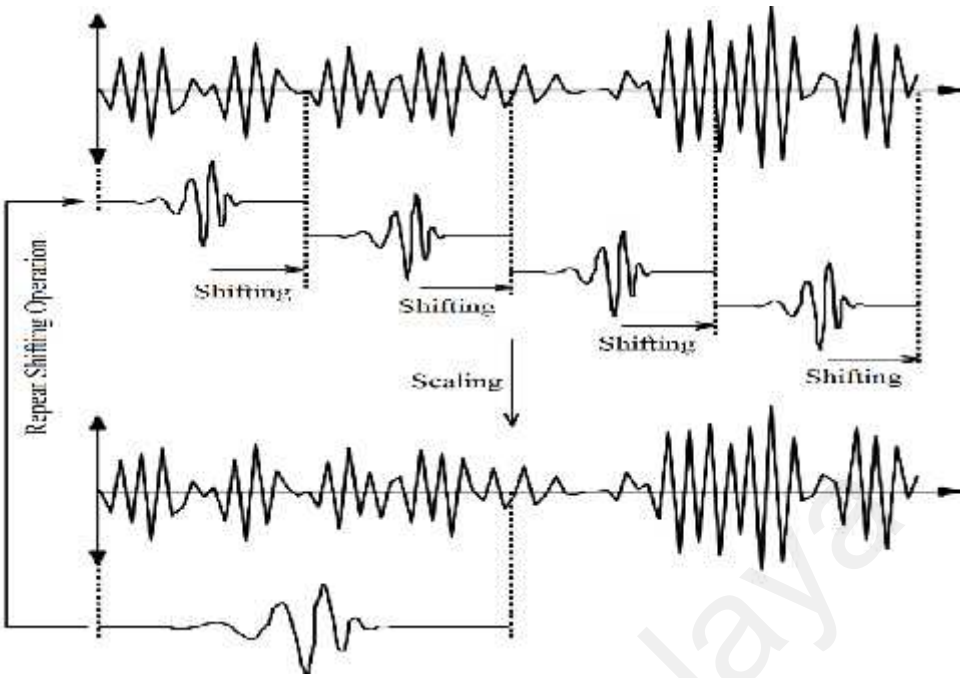

Figure 3.5 : Shifting (translation) and scaling (dilation) process of the mother wavelet

There are several types of mother wavelet such as Daubechies wavelet, Gaussian wavelet, Coiflets wavelet, Symlets wavelet, Biorthogonal wavelet and many more. Each of these mother wavelets has their own unique shape which consists of several orders of the mother wavelet as shown in the Appendix section. Also, all of the mother wavelets have to fulfil the wavelet properties such as admissibility and regularity condition before they can be called as “mother wavelet”.

In order to determine the best choice of the mother wavelet to be used for feature extraction or to analyse data, wavelet coefficients are used to calculate the energy level for each mother wavelet. In (Wenzhong et al., 2011) the energy level of wavelet coefficients was used as a criterion to choose an ideal mother wavelet. Mother wavelet with a higher energy level is selected as an appropriate mother wavelet to be utilized for that particular analysis. Whereas in (Kejun et al., 2006), the selection of mother wavelet is based on Signal to Noise Ratio (SNR). The SNR measures the disturbance energy of

the original signals with respect to the noise in the signal. The large magnitude of SNR indicates superior performance of mother wavelet.

The wavelet transform was widely used in many fields such as astronomy, signal and image processing, magnetic resonance imaging and pure mathematics applications such as solving partial differential equations. Nowadays, the application of wavelet transform has been drastically evolving in solving the power system issues such as fault detection (Akorede, et al., 2010; Sarlak, et al., 2011), power system dynamic (Avdakovic et al., 2012; Wenzhong, et al., 2011), incipient fault analysis (Sidhu et al., 2010) and power quality issue (Dilokratanatrakool et al., 2003).

3.2.2. Variety of Wavelet

There are two main types of wavelet transform:

i) Continuous Wavelet Transform (CWT)

ii) Discrete Wavelet Transform (DWT)

CWT analysis is simply a convolution of the input data sequence with the set of function generated by the mother wavelet to calculate the wavelet coefficients. Whereas in the DWT analysis, the continuous signal is digitized first before the matrix of digitized data is dot product with the matrix of discrete mother wavelet. Figure 3.6 shows the simplify operation of CWT and DWT.

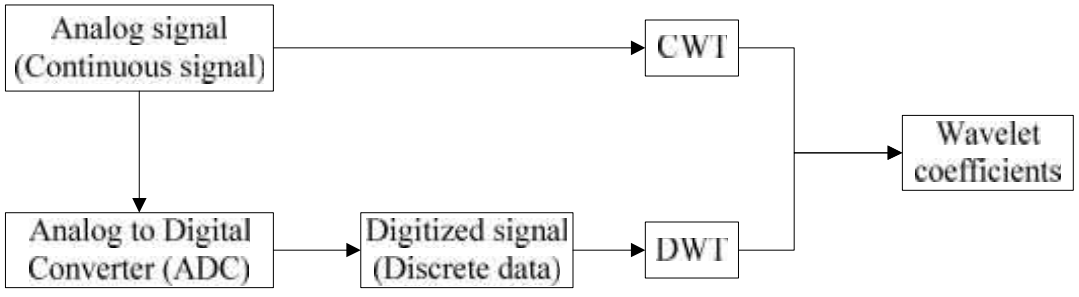

Figure 3.6 : CWT and DWT operations

DWT analysis can be expanded into two:

a. Multi-Resolution Analysis-Discrete Wavelet Transform (MRA-DWT)

b. Spanning Tree-Discrete Wavelet Transform (ST-DWT)

These expanded DWT gives a better signal representation and offer richest analysis. The operations and uniqueness of each type of wavelet transform will be explained briefly in the next sub-chapter.

3.2.3. Continuous Wavelet Transforms (CWT)

The continuous wavelet transform is like the Fourier transform that use the inner product of the signal, $f(t)$ to measure the similarity between a signal of interest and mother wavelet, $\psi(t)$. The similarity can be determined based on the wavelet coefficient value. Wavelet coefficients equal to one represent a perfect matching between the signal and mother wavelet. The CWT can be derived as below (3.1):

$$C(a,b; f(t), \cdot(t)) = \int_{-\infty}^{\infty} f(t) \frac{1}{\sqrt{a}} \cdot^{*}(\frac{t-b}{a}) dt \qquad (3.1)$$

where parameter *a* and b represents the scale (dilation) and position (translation) values respectively and $*$ denotes the complex conjugate. *C (a, b)* is the continuous wavelet transform coefficients that represent the correlation between the signal and the mother wavelet. The values of dilation, *a* and translation, *b* will affect the calculation of the value of CWT coefficients. Besides that, the choice of mother wavelet will also affect the coefficient value obtained. Therefore, it is important to choose a proper mother wavelet and also suitable value for parameter a and b to achieve an excellent analysis. This is because the higher the value of CWT coefficients approaching to one, the more similarity between the signal of interest and the wavelet signal.

There are 5 steps to construct the CWT analysis:

1) Compare the suitable mother wavelet with a section at the start of the original signal.
2) Calculate the coefficient, *C* to observe the correlation between the wavelet signal and the input signal. This is important to notice that, different values of CWT coefficients are obtained for a different mother wavelet that used on the same signal.

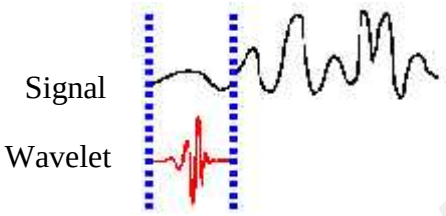

C = 0.0102

3) Repeat steps 1 and 2 by shifting the mother wavelet until the whole signal is covered.

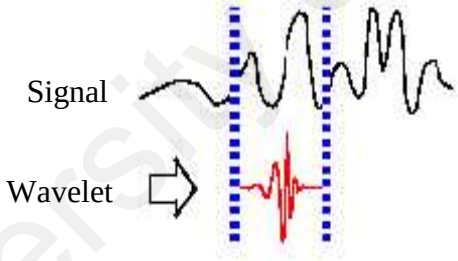

4) Step 1 until 3 is repeated with increasing the scale value of a mother wavelet. Once again, the wavelet coefficient, C is calculated to attain different correlation between input signal and wavelet signal.

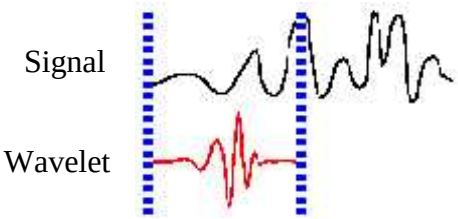

C = 0.2247

5) Finally, step 1 until 4 is repeated for different scaled mother wavelet. By doing this, variety features regarding the signal can be achieved which give a better analysis. Also, more accurate analysis can be gained if more features are available.

Figure 3.7 shows an example of a signal with abrupt transitions and smooth oscillation at t= 0.3s and t= 0.7s respectively. The anomaly in the signal can be depicted by the frequency spectrum using the CWT.

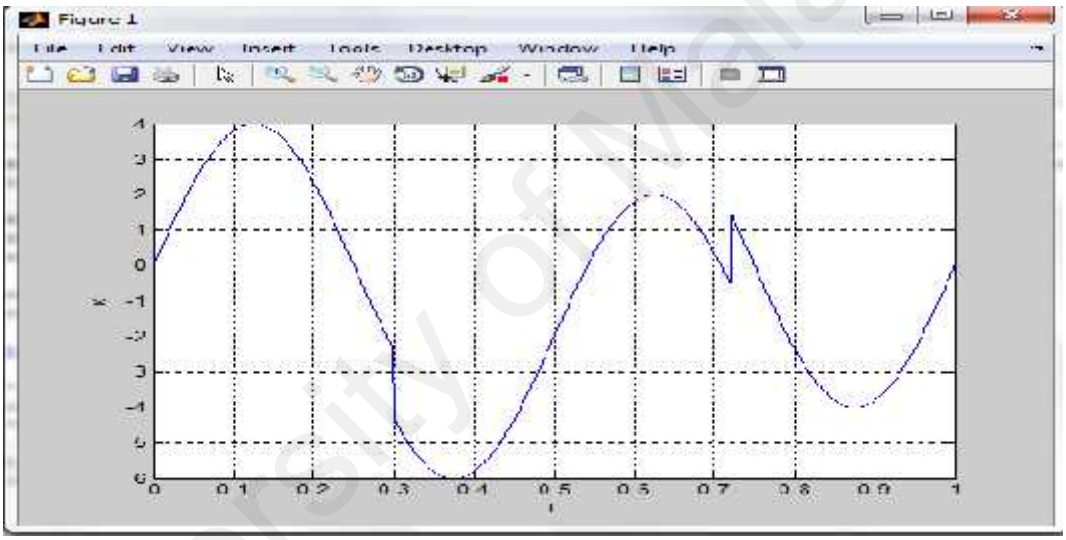

Figure 3.7 : Abrupt transitions and smooth oscillations

The faulted signal in Figure 3.7 is analysed using the fourth order of the Daubechies wavelet (dB4) to extract the features from the signal. As shown in Figure 3.8, CWT is capable of detecting the occurrence of both abrupt transition and oscillation in the signal based on the frequency spectrum at 0.3s and 0.7s respectively. On top of that, the moment of event occurrence can be identified accurately. Besides, it can be observed that the CWT coefficient in terms of frequency spectrum can identify clearly the abrupt transition at all scales. It also separates themselves from the smoother signal features at small scales.

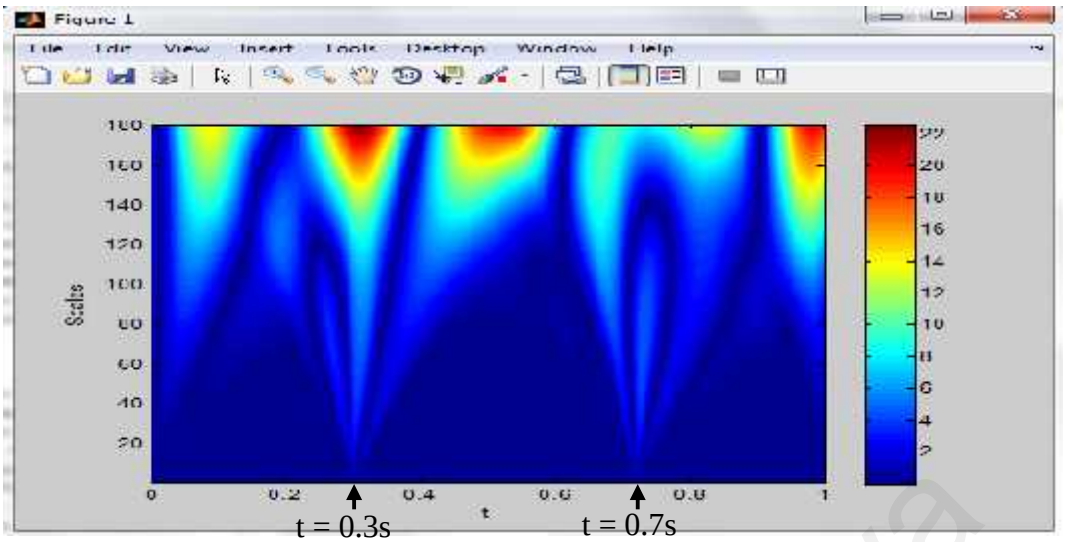

Figure 3.8 : Analysis of fault signal using Db4

There is some general principle when interpreting the Figure 3.8 based on the frequency spectrum of CWT coefficients.

- **Detecting abrupt transitions**— Wavelets are very useful for detecting abrupt changes in a signal. Abrupt changes in a signal produce relatively large wavelet coefficients (in absolute value) centred around the discontinuity at all scales. Because of the support of the wavelet, the set of CWT coefficients affected by the singularity increases with increasing scale. The most precise localization of the discontinuity based on the CWT coefficients is obtained at the smallest scales.
- **Detecting smooth oscillations**— Smooth oscillation signal features produce relatively large wavelet coefficients at scales where the oscillation in the wavelet correlates best with the signal feature. For sinusoidal oscillations, the CWT coefficients display an oscillatory pattern of scales where the oscillation in the wavelet approximates the period of the sine wave.

In (Poisson et al., 2000), CWT had been used to detect and analyse power quality disturbance in power system. Whereas in image processing research, CWT had been employed as stated in (Briassouli et al., 2010; Tria et al., 2007) for analysis. Also, CWT was employed in the medical field as reported in (Cnockaert et al., 2008; Hulzink et al., 2011) for diagnosis purposes.

3.2.4. Discrete Wavelet Transforms (DWT)

Discrete wavelet transform (DWT) is similar to CWT in terms of purpose for calculating the wavelet coefficients but in different ways. DWT is created to overcome the drawbacks of CWT and give a better performance analysis. There are three properties that cause a difficulty of utilizing CWT in the analysis (Wavelet guide)

- Redundancy

  In CWT, the wavelet coefficients are calculated by continuously shifted and dilated the mother wavelet to obtain the correlation between the signal of interest and mother wavelet. Unfortunately, it is clear that the dilated function will be nowhere near an orthogonal basis and therefore the wavelet coefficients obtained are highly redundant.

- Infinite number of wavelet

  There are an infinite number of mother wavelets in the wavelet transform by varying the dilation and translation parameter. Therefore, it is necessary to reduce this number to be more manageable count.

- No analytical solution

  CWT does not have an analytical solution and it can only be calculated numerically or by application of an optical analog computer which is time consuming. Thus, fast algorithms are required to be able to exploit the power of the wavelet transform.

As mentioned before, CWT calculates wavelet coefficients at each possible scale of the mother wavelet that shifted across a signal. Thus, it causes a lot of work, time consuming and generate numerous data. In order to overcome these problems, the DWT is introduced in which the wavelet coefficients are calculated based on a subset of scales and positions. The scales and positions are chosen based on powers of two that also known as *dyadic* scales and positions. This approach allows the DWT technique to give an efficient and accurate analysis compared to CWT.

In DWT, the original input signal is decomposed through two complementary filters (high-pass filter and low-pass filter) and emerges as two signals (high-frequency components and low-frequency components) respectively. In signal analysis, the low-frequency components are the crucial part because it gives the signal identity. Whereas, the high-frequency components are just conveyed flavour or nuance in the signal. The low-frequency components of the signal is a high-scale decomposition also called *approximations*. The high-frequency component on the other hand is a low-scale decomposition also called *details* (Wavelet Transform).

For example, when a signal consists of 1000 samples is analysed using the DWT, it will generate 1000 samples of approximation and 1000 samples of details, for a total of 2000 samples as shown in Figure 3.9. Even though, the approximation and detail signals obtained are quite interesting, but the results double up the original data sample.

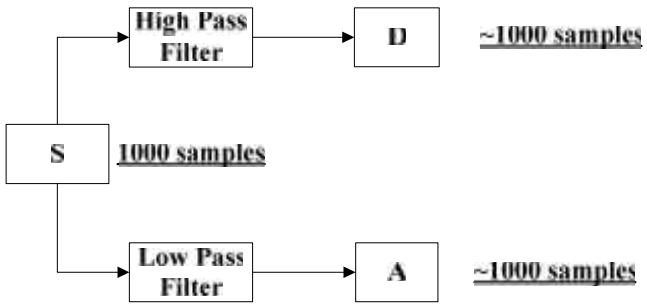

Figure 3.9 : Wavelet decomposition without downsampling

Therefore, a more subtle way to perform the decomposition process called downsampling operation is introduced. In downsampling operation, only one point out of two in each of the two 1000-length samples are analysed to obtain complete information. Through this process, two sequences called approximation coefficients, *cA* and detail coefficients, *cD* are produced. As shown in Figure 3.10, 500 approximation coefficients and 500 detail coefficients are generated through downsampling operation instead of 1000 samples for approximations and details without downsampling operation.

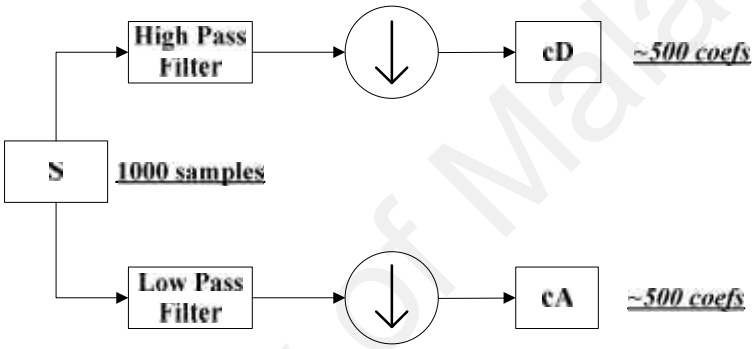

Figure 3.10 : Wavelet decomposition with downsampling

For further understanding of DWT with downsampling process, one stage DWT is performed. Figure 3.11 shows the pure sinusoidal signal with high frequency noise added to it is decomposed using the second order of Daubechies mother wavelet, Daub2. From this downsampling operation, it is clearly shown that the approximation coefficients, *cA* consists of less noise and its look similar to the original signal. While, the detail coefficients, *cD* looks like a ripple signal which contains mainly a high-frequency noise.

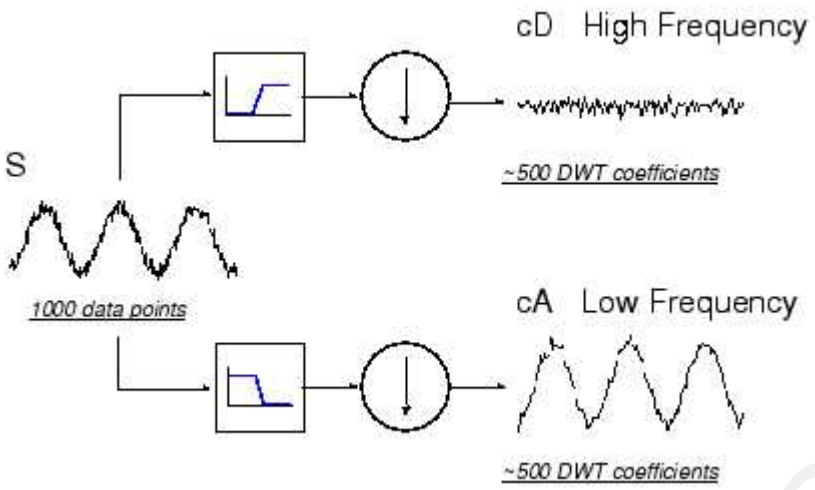

Figure 3.11 : Wavelet decomposition using Daub2

Other than that, downsampling operation can also be applied in image processing. Figure 3.12 illustrates an example of an image which decomposed using the fourth order of the Daubechies mother wavelet. As shown in the figure, same similar image can be generated from the original image which the size of the image has been reduced to half. It is usually implemented to transmit a small size image with a good quality.

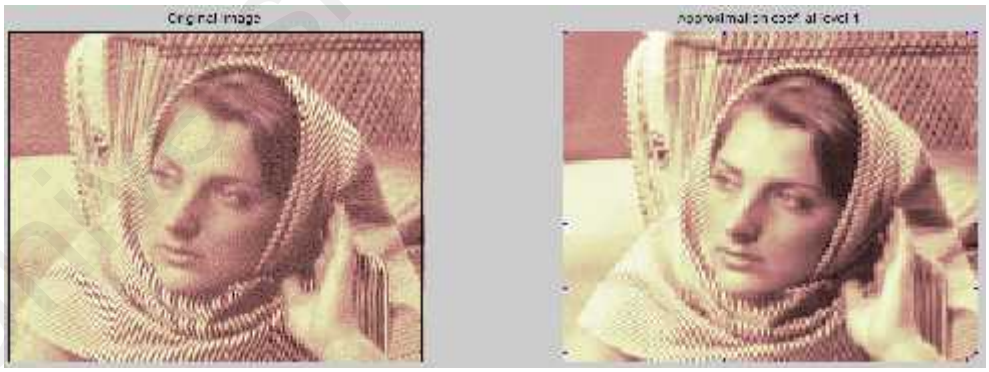

Figure 3.12 : Downsampling operation on an image using Db4

The overall decomposition operation of the image is shown in Figure 3.13. The original image had been decomposed into approximation image and three patterns of detail images.

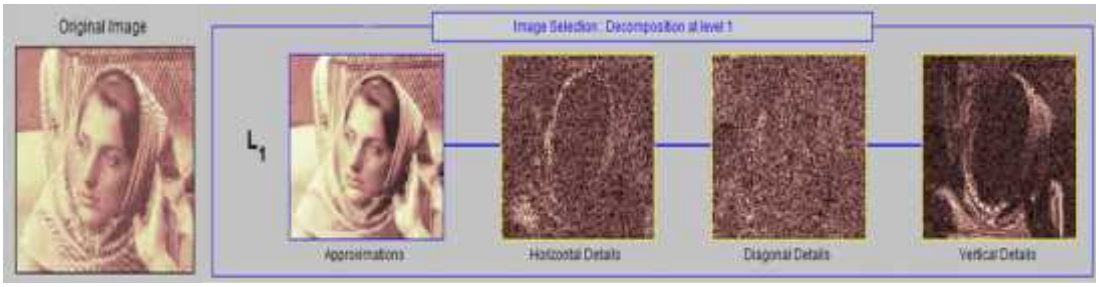

Figure 3.13 : Overall operation of decomposition on image

The DWT has been widely used in many applications and fields such as in signal, audio and video analysis and power system research. An application of DWT in power quality problem in power system has been widely investigated. In (Nath et al., 2012), power quality issue related to location of source of harmonic pollution is identified using the DWT. Detection, analysis and classification of fault event in transmission system using DWT had been proposed in (Bhalja et al., 2008; Martin et al., 2003). Besides that, DWT has been utilized to analyse and locate lower frequency oscillations during power system dynamic event which resulting in a loss of stability or blackout (Avdakovic, et al., 2012). Also, total active power imbalance in the system can be estimated from the analysis.

3.2.5. Multi-Resolution Analysis-Discrete Wavelet Transform (MRA-DWT)

The Multi-Resolution Analysis-Discrete Wavelet Transform (MRA-DWT) is similar to DWT except that the decomposition process can be iterated with successive approximations being decomposed in turn. The MRA-DWT splits the original signal, S into many lower resolution components as shown in Figure 3.14. Therefore, the MRA-DWT also can be known as the Multi- Level Decomposition. The main purpose of the MRA-DWT is to reduce the size of the signal but significantly maintains the similarity and the shape of the original signal. It can be obtained by eliminating the unnecessary noise signal that embedded in the signal.

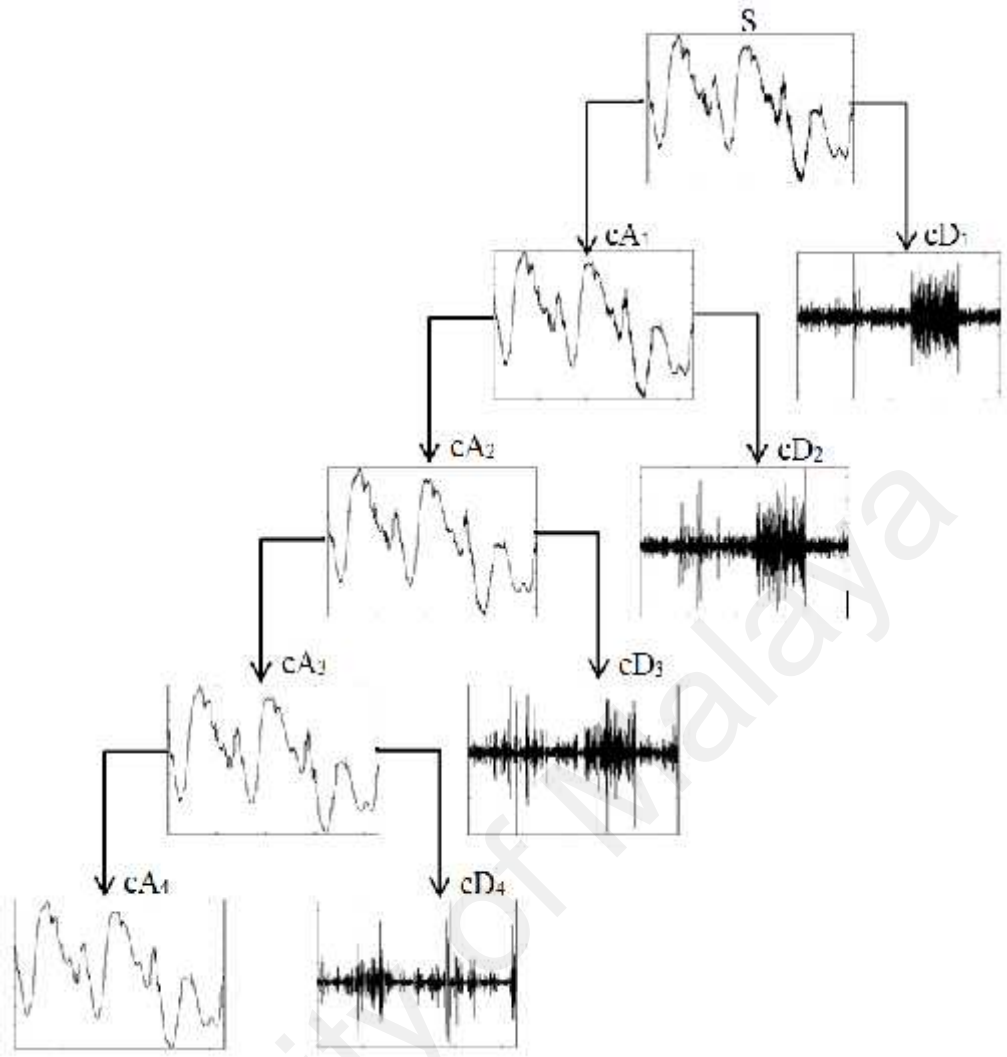

Figure 3.14 : MRA-DWT operation

For more understanding about the MRA-DWT, the process to calculate the approximation and detail coefficients is shown below. The matrix of input data consists of [y1, y2, …, y16] is multiplied with a matrix of wavelet coefficients, *M*. The size of a matrix M is dependent on the number of input data. If the number of input data is *n*, then the size of a matrix M is *n* x *n*. An example of matrix M for forth order Daubechies mother wavelet with size 10x10 is shown as follows:

M=

$$\begin{bmatrix} C_0 & C_1 & C_2 & C_3 & 0 & 0 & 0 & 0 & 0 & 0 \\ C_3 & -C_2 & C_1 & -C_0 & 0 & 0 & 0 & 0 & 0 & 0 \\ 0 & 0 & C_0 & C_1 & C_2 & C_3 & 0 & 0 & 0 & 0 \\ 0 & 0 & C_3 & -C_2 & C_1 & -C_0 & 0 & 0 & 0 & 0 \\ 0 & 0 & 0 & 0 & C_0 & C_1 & C_2 & C_3 & 0 & 0 \\ 0 & 0 & 0 & 0 & C_3 & -C_2 & C_1 & -C_0 & 0 & 0 \\ 0 & 0 & 0 & 0 & 0 & 0 & C_0 & C_1 & C_2 & C_3 \\ 0 & 0 & 0 & 0 & 0 & 0 & C_3 & -C_2 & C_1 & -C_0 \\ C_2 & C_3 & 0 & 0 & 0 & 0 & 0 & 0 & C_0 & C_1 \\ C_1 & -C_0 & 0 & 0 & 0 & 0 & 0 & 0 & C_3 & -C_2 \end{bmatrix}$$

There are four coefficients, C_0, C_1, C_2 and C_3 that represent the fourth order of Daubechies mother wavelet . The row with [C_0 C_1 C_2 C_3] represent the low pass filter, L whereas the row with [C_3 $-C_2$ C_1 $-C_0$] represent the high pass filter, H. The L and H are shifted as shown in the diagram to represent the downsampling operation.

The matrix M is multiplied with input data to generate an approximation coefficients, s and detail coefficients, d for the first level decomposition process. The coefficients s and d are permuted to split approximation and detail coefficients as shown below. The successive approximation coefficients are decomposed again to produce another approximation and detail coefficients for the next level of decomposition. The process continues until only one approximation coefficient is obtained.

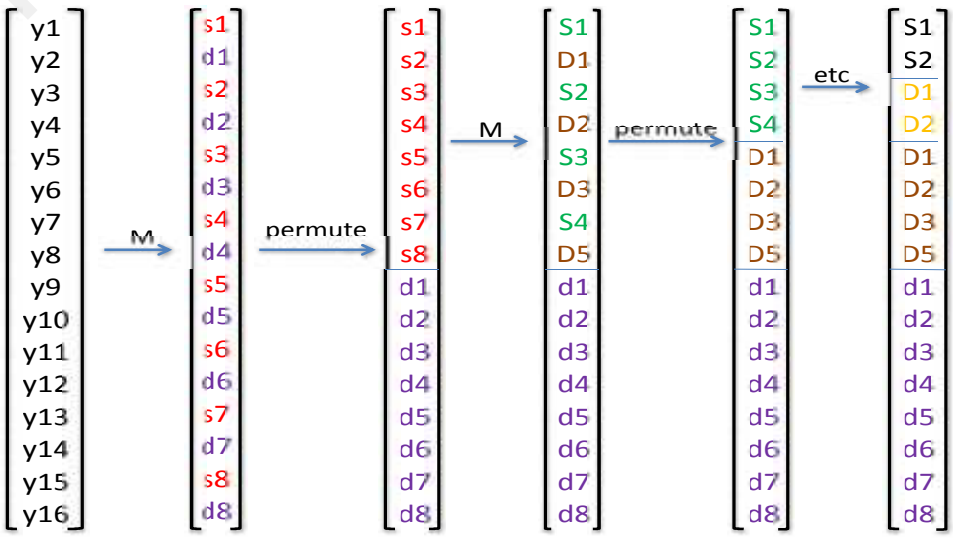

Recently, MRA-DWT had received significant attention and considered as a powerful tool for effectively representing functions at multiple levels-of-detail coefficients with many inherent advantages. Recently, MRA-DWT has been applied to many engineering problems such as:

- Power System Protection
- Power System Analysis
- Power Quality Detection and Classification

In (Gaouda et al., 1999; S. Nath, 2009), MRA-DWT was used for power quality disturbance detection and classification in power system. To indicate the fault location on transmission lines, MRA-DWT was used as reported in (Chanda et al., 2003).

3.2.6. Spanning Tree-Discrete Wavelet Transform (ST-DWT)

The Spanning Tree-Discrete Wavelet Transform (ST-DWT) technique is a generalization of wavelet decomposition that gives a richer range of possibilities for signal analysis and implies the versatility of DWT. Basically, the ST-DWT technique is similar to the MRA-DWT except that both successive approximations and detail coefficients can be decomposed into many lower resolutions as shown in Figure 3.15. This ST-DWT analysis offer superior resolution and clarification of details about the signal that cannot be shown by DWT and MRA-DWT.

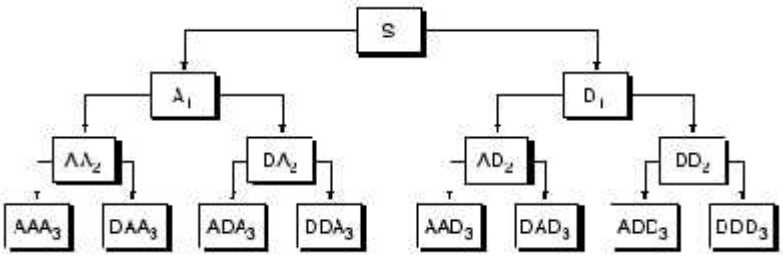

Figure 3.15 : ST-DWT operation

Using ST-DWT, various representations of the original signal can be made from the approximation and detail coefficients. For an example, the original signal can be reconstructed using the following combination:

$$S = A_1 + DD_2 + AAD_3 + DAD_3$$
$$= A_1 + AD_2 + ADD_3 + DDD_3$$
$$= D_1 + AA_2 + ADA_3 + DDA_3$$
$$= D_1 + DA_2 + AAA_3 + DAA_3$$

Various combinations can be made to represent the original signal which shows the richer analysis. Also, this combination only applicable for ST-DWT and it is not possible with DWT and MRA-DWT.

3.2.7. Advantages of Wavelet Transform

Wavelet analysis is similar to the Fourier analysis in the sense that it breaks a signal down into its component parts for analysis. Fourier transform breaks the signal into a series of sine or cosine waves of different frequencies whereas the wavelet transform split the signal into a series of wavelet function which consists of dilated and translated versions of the “mother wavelet”.

Figure 3.16 shows the comparison of signal between the sine wave and the fifth order of Daubechies mother wavelet. From the figure, it can be seen the distinct differences that make wavelet transform more enhanced from Fourier transform. This is due to the wavelet properties of irregular in shape which make it a well-suited tool for analysing signals with a discontinuity or sharp changes and impulse functions. Also, the compactly supported feature enables the determination of time localization in a signal.

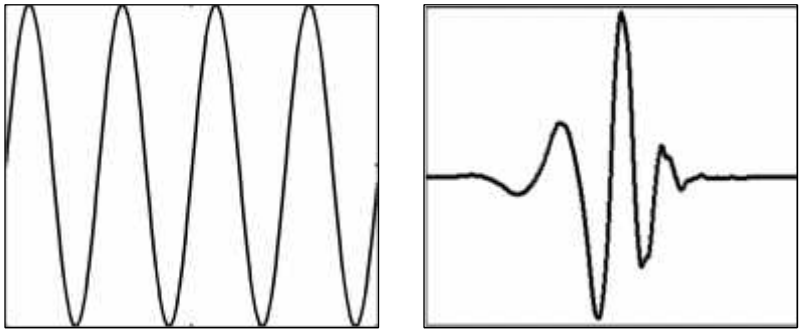

Figure 3.16 : Comparison of the sine wave and the Daubechies mother wavelet

Besides that, WT has an ability to perform a local analysis that is to analyse a localized area of a larger signal. For an example, a small discontinuity in signal can be shown clearly and the exact moment of the event can be identified through wavelet analysis. Also, WT can give a complete and efficient spectral analysis without a loss of precious information. Wavelet analysis has an ability to reveal features of data such as trends, breakdown points, discontinuities in higher derivatives and self-similarity which is other signal analysis techniques are not capable to do.

Also, WT is capable of partitioning the signal energy at different frequency bands to give an indication of the frequency content of the disturbance signal. Furthermore, WT is always used in compresses or de-noise an image without significant degradation due to its affordability of a different view of data. All of these underlying features make WT one of the most exciting tools in a research area of signal processing.

3.3. Summary

In this chapter, the background of HIF had been explained briefly in terms of characteristics, causes and effects of HIF towards the stability of the system. Also, the general definition of HIF and its objectives for detection and localization were discussed. Besides, the importance of HIF towards the reliability and the continuity of the system were described.

Then, the basic concept and types of wavelet transform has been explained in this chapter. This includes the explanation of the translation and dilation processes to determine the appropriate mother wavelet. Two different types of wavelet transform which are Continuous Wavelet Transform (CWT) and Discrete Wavelet Transform (DWT) has been discussed briefly. This is followed by detail discussion of Multi-Resolution Analysis- Discrete Wavelet Transform (MRA-DWT) and Spanning Tree-Discrete Wavelet Transform (ST-DWT) which representing the successive types of DWT. Finally, the advantages and disadvantages of each type of wavelet transform has been highlighted in this chapter.

CHAPTER 4

PROPOSED MATCHING TECHNIQUE FOR HIGH IMPEDANCE FAULT LOCATION

4.1. Introduction

In this chapter, the overall concept of the proposed method utilising the Multi Resolution Analysis-Discrete Wavelet Transform (MRA-DWT) for identification of high impedance fault (HIF) location is presented. MRA-DWT is chosen instead of ST-DWT because only detail coefficients at each level are required for the analysis. The three-phase voltage signal at the main substation is analysed and important features are extracted to be matched with the stored features in the database to determine the possible faulty section. Two different matching approaches are proposed for identifying the HIF location. In the proposed methods, multiple possible faulty sections are estimated and ranked to priorities the inspection sequence.

4.2. Overall Concept of the Proposed Method

An example of a simple radial distribution network is shown in Figure 4.1, to be considered in locating the fault using the proposed method. The network consists of one main feeder and two laterals tapped at node 2 and 3. A line section is represented by two adjacent nodes and has its own line configuration. In this diagram, a fault is assumed to have occurred in the middle of line section S-R. The three-phase voltage signal is obtained at the primary substation, which is at node 1. The voltage signal is analysed to identify the location of the fault when there is a fault occurrence at any location in the network.

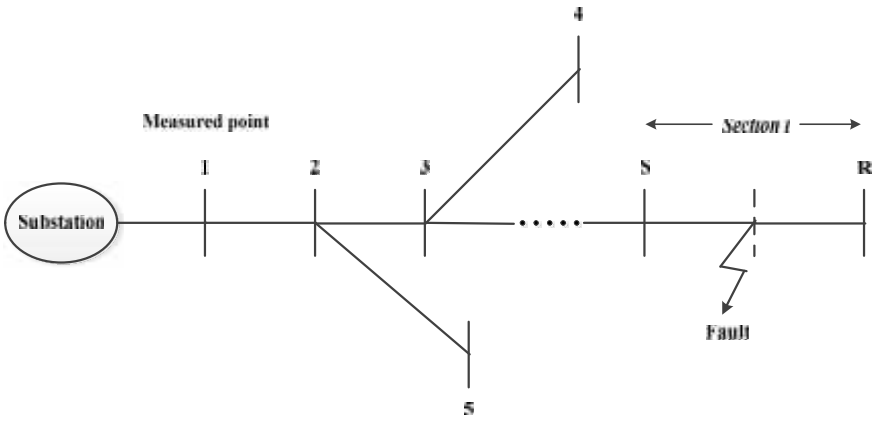

Figure 4.1 : A simple radial distribution network

The algorithm flow chart to determine the faulty section during HIF is depicted in Figure 4.2. It involves two major steps which are HIF detection and HIF location. The HIF detection involves feature extraction and fault detection. The significant features of three-phase voltage signal are extracted using the wavelet transform. Fault occurrence is detected based on the extracted detail coefficient features. The fault type identification task starts when there is a fault detected. The identification is based on the extracted approximation coefficient features.

The HIF location consists of a HIF location algorithm and ranking procedure. There are two proposed algorithms for HIF location identification. For this purpose, the measured voltage signal is analysed and compared with the database. Finally, in the ranking analysis, all the line sections are arranged based on the smallest value calculated from the proposed algorithm. In this case, the faulty section candidate with the smallest value is selected as the first possible faulty section to be inspected. The faulty section with the second lowest value is examined if the first candidate was found not the faulty section. The process continues in increment order until the faulty section is identified.

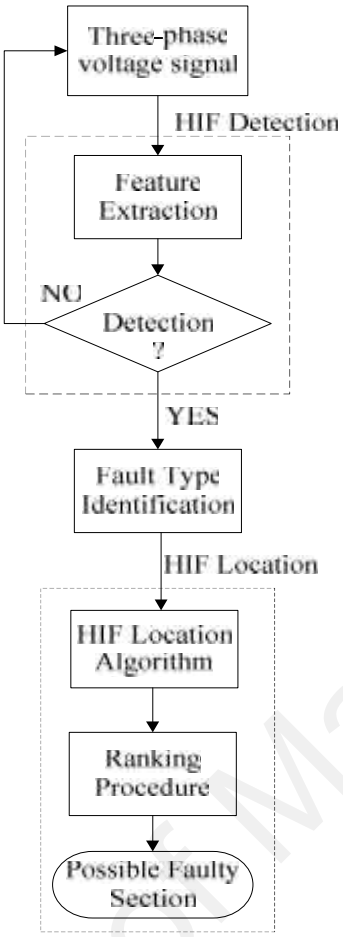

Figure 4.2 : Flowchart of HIF detection and location

4.2.1. Feature Extraction and Classification

The three-phase voltage signal obtained at main substation is analysed using the Daubechies fourth order (Daub4) wavelet. Once the HIF is detected, approximation and detail coefficients from the first and second cycles relative to the position of the HIF in the voltage signal are analysed to determine the type of HIF and its location. An example of an anomaly caused by an HIF is shown in Figure 4.3 where it occurs in the middle cycle of the signal. The cycle that contains the anomaly is considered as the first and the one that follows it is considered as the second of the post disturbance.

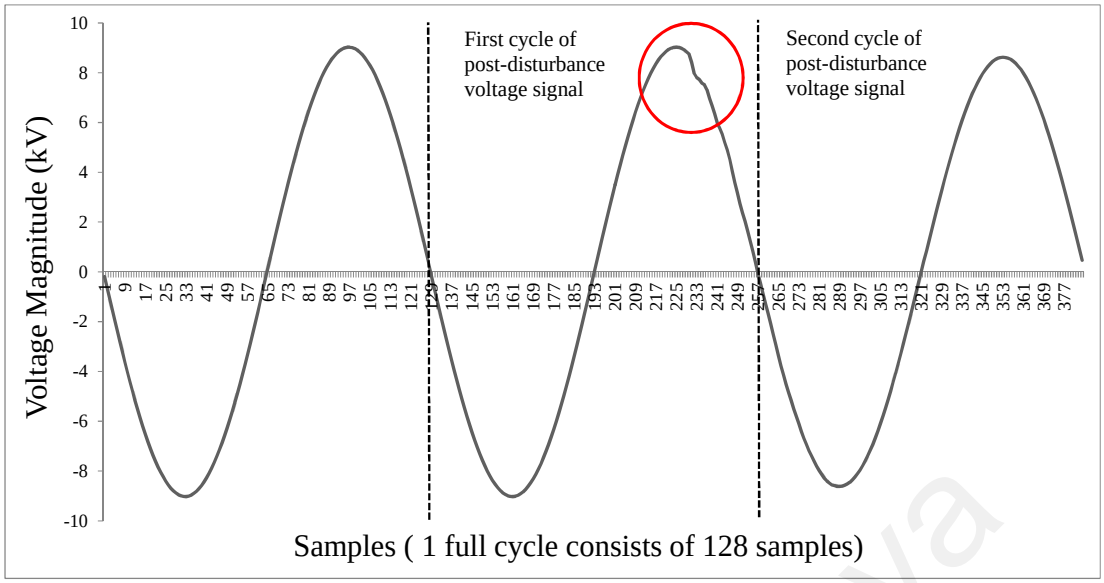

Figure 4.3 : Voltage sinusoidal obtained from a main substation

Firstly, in every cycle of the voltage signal, 128 samples are taken and transformed by the Daub4 wavelet with the downsampling operation into 64 approximation coefficients and 64 detail coefficients. The values of the 64 detail coefficients are analysed and compared to a threshold value. The threshold value is determined through analysis of HIF at various locations of the network. By observing the detail coefficients, the smallest value will be taken as the threshold value. In this work, the threshold value is set to 0.02 because in normal condition, the detail coefficient values are below than 0.02. If any of the detail coefficient values exceed the set threshold value, HIF is considered detected. This approach provides an easy means to identify an anomaly in the voltage signal.

After detecting HIF, it is necessary to classify its type and only the sum of first level approximation coefficients from the second cycle is needed. This sum is divided by the sum of first level approximation coefficients obtained from the normal cycle given by (4.1).

$$\text{Approximation Ratio, AR} = \frac{\sum a(HIF)}{\sum a(normal)} \quad (4.1)$$

Based on the observed value of this ratio, the HIF is classified into one of the four fault types and thus the database to use as follows:

i. Single Line to Ground fault (SLGF) – Faulted phase will have AR magnitude lower than 1.0 and the other two higher than 1.0

ii. Three Phase Fault (LLLF) – All of the three phases have AR magnitudes that have almost identical value.

iii. Double Line To Ground fault (LLGF) – Faulted phases will have AR magnitude lower than 1.0 and the other phase higher than 1.0.

iv. Line to Line fault (LLF) – Healthy phase will have AR magnitude the same as before the fault (AR=1), whereas the faulted phase change (one of the phases has AR magnitude lower than 1.0 and the other phase vice versa).

Then the final step is to find the section where the fault occurred. For this purpose, detail coefficients for the first and second cycles of the post-disturbance three-phase voltage signals are obtained from the MRA-DWT analysis. For each cycle, the detail coefficients at the first, second and third levels of wavelet expansion are added. So, altogether there are 18 wavelet features to be compared against sets of stored features from the selected database.

4.2.2. Database Establishment

Figure 4.4 shows the process of generating the database for each fault type starts with the first fault impedance value set to H_f = 40Ω is simulated at each node. H_f = 40Ω is assumed to be the starting value to represent the HIF phenomenon. From the obtained

three-phase voltage signal (acquired from voltage transformer), the summation of detail coefficients feature is stored in the database.

To illustrate database establishment, consider a network consists of *k* nodes. To generate database, the fault is created on each node, resulting in *k* cases data stored in the database where each case is represented by 18 wavelet features. The 18 features consists of the extracted feature of 2 cycles of post disturbance voltage signal, 3 phases voltage signal and 3 level decompositions (2cycles x 3phases x 3levels).

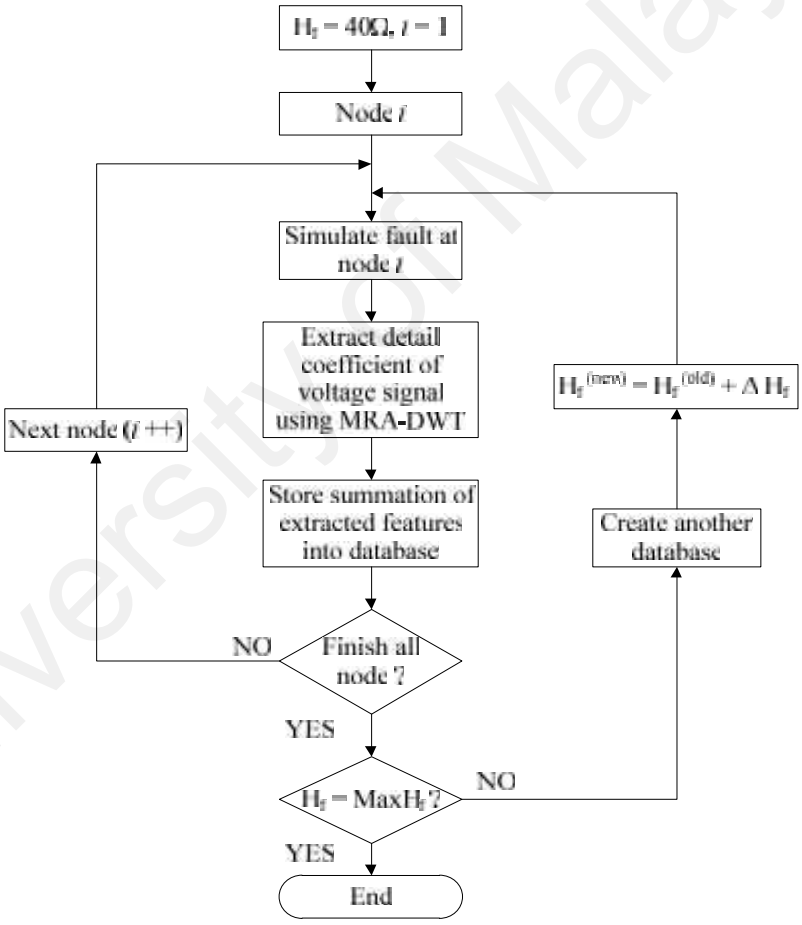

Figure 4.4 : Flowchart to develop a database

Once the database for the first fault impedance has been developed, the process is repeated with another H_f value, i.e $H_f^{(new)} = H_f^{(old)} + \Delta H_f$, where $H_f^{(old)}$ is the previous fault impedance value and ΔH_f is the defined increment of the new fault impedance

from the previous one. In this case study, the fault impedance increment, ΔH_f is set to 10Ω. It should be noted that the smaller value of ΔH_f can be set, however it will produce more cases to be stored in a database. The process continues until the simulated fault impedance value, H_f reaches the maximum defined fault impedance value, $MaxH_f$ which is set to 100Ω. Given these parameters, altogether there are *7 x k* fault cases in each of the four databases, which represent 7 different values of fault impedance and *k* cases for each fault impedance value.

The illustration of databases for different fault types and fault impedance values is shown in Figure 4.5. These databases have to be updated whenever there are changes occurring in the system such as network reconfiguration.

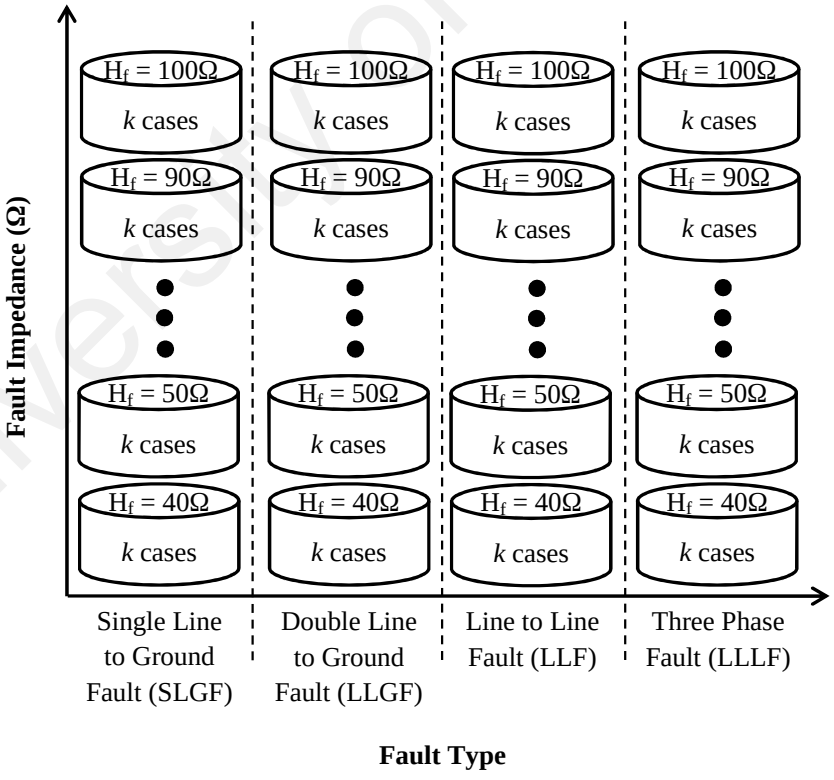

Figure 4.5 : Database of different fault types and fault impedance

4.2.3. Faulty Section Identification

Figure 4.6 shows the overall process of estimating the faulty section using the proposed method. Firstly, the detail and approximation coefficients of voltage signal are extracted and added to be used in the proposed algorithm and identify the fault type respectively. After specific database of the identified fault type has been selected, the proposed algorithm starts the analysis by matching the measured features with stored features of each line section to calculate the scores.

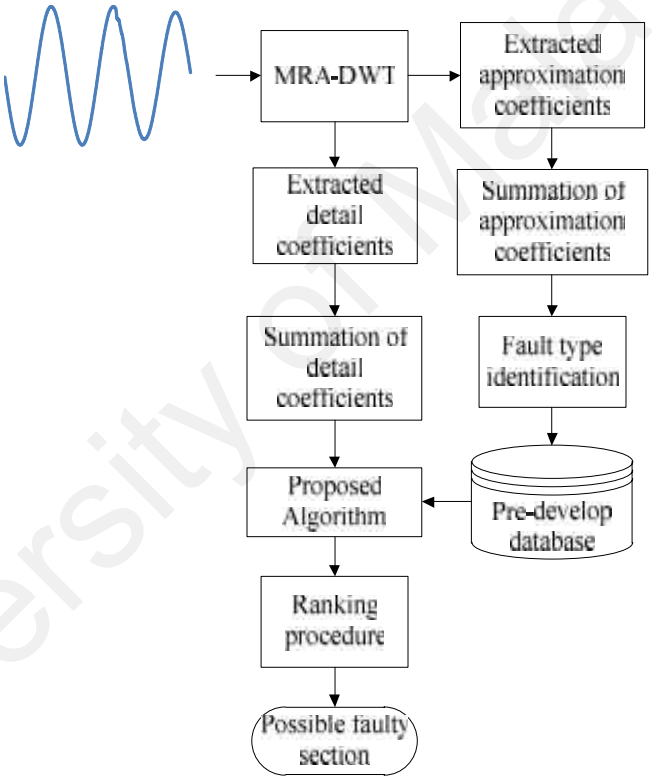

Figure 4.6 : Flowchart of the proposed fault location

Then, the scores are arranged in increment order with the line section it is associated. In ranking analysis, line section with the lowest score is ranked as the first indicate the highest possibility to be assumed as a faulty section.

4.3. Proposed Matching Approaches for Fault Location

Two algorithms to identify the possible faulty section are proposed in this work:

1. Shortest Distance (SD) Technique and Database Approach
2. Average of Absolute Difference (AAD) Technique and Database Approach

Both techniques utilise a database approach to match the measured voltage signal with the stored features of voltage signal in order to predict the possible faulty section.

4.3.1. Shortest Distance (SD) Technique and Database Approach

The proposed SD technique is simply calculating the distance between a point of interest perpendicular to the straight line. This technique is the extension of the Nearest Neighbour Rule (NNR) method. In NNR method, the unknown data is classified when its nearest neighbour comes from any collection of classified sample. For example in Figure 4.7, the unknown object is classified to the nearest object in the measurement space using Euclidean metric. As shown in the figure, the unknown object belongs to circle object class instead of square object class. However, in the proposed approach, the distance between the unknown object to each classified object in the measurement space is calculated to determine the membership of the unknown object.

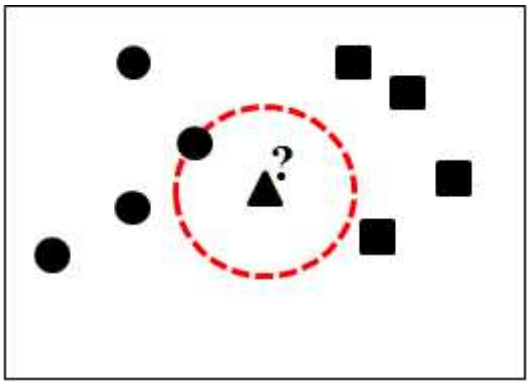

Figure 4.7 : The nearest neighbour rule method

In the proposed SD technique, the shortest distance, d_k from a point, *f* to a line, *i-j* is calculated. As shown in Figure 4.8, the points *i* and *j* form a straight line and d_k is perpendicular between point *f* and line *i-j*. Points *i*, *j* and *f* are described in three-dimensional space by means of three coordinates. The summation of detail coefficients of phases A, B and C of the voltage signal is represented by x, y and z axes respectively.

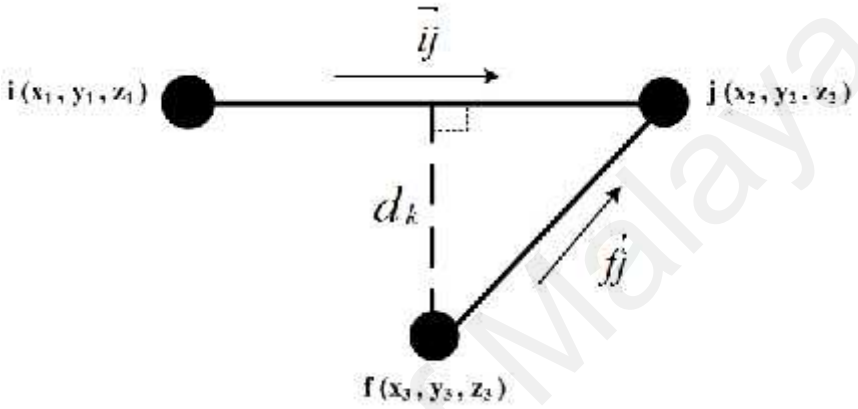

Figure 4.8 : Three coordinate diagram for each node

In this proposed method, line *i-j* is assumed to be a line section between nodes *i* and *j* while point *f* is assumed to be an unknown signal. The unknown signal is a measured signal by the application of certain fault at a certain location. While, the data for node *i* and *j* are found in the stored database. In this method, the value of d_k is used to predict the probability of the measured signal belongs to which line section. Therefore, the distance is calculated between the measured signal with all line sections using (4.2). Then, the line section that yields the smallest value of the shortest distance has a higher priority to be assumed the location of HIF occurrence.

$$\text{Shortest distance, } d_k = \frac{\left|\vec{fj} \times \vec{ij}\right|}{\left|\vec{ij}\right|} \qquad (4.2)$$

Even though the fault location can be predicted based on the first shortest distance value, there is a possibility that the fault does not belong to that line section. In these cases, the second shortest distance value is considered as the faulty section. The process is repeated until the actual fault location is identified. Thus, it is necessary to rank the shortest distance value for all line sections. They are arranged from the smallest to the highest values of the shortest distance with the smallest value is ranked as the first.

4.3.1 (a) Database Development

Before the proposed method can be implemented, the stored features of summation of detail coefficients are obtained by simulating HIF at all nodes in the network. It is observed that the extracted features obtained are different for each node with different value of fault impedance. Therefore, to generate a set of database, pre-defined high impedance fault is applied at each node. Then, the three-phase voltage signal acquired from the measurement point is analysed using the MRA-DWT. The high-frequency components (detail coefficients) are extracted from the voltage signal during the decomposition process. Three levels of detail coefficients are obtained and the sum of detail coefficients is calculated.

After HIF applied to all nodes have been simulated, a combination of two adjacent nodes that form a line section is created. For example, a line section 1 was created between nodes 3 and 4 and nodes 4 and 5 create line section 2. A pair of adjacent nodes for each line section is shown in the Appendix A.1.1. Each database has six parts which consist of the first, second and third level of summation of detail coefficients for the first and second cycle of post-disturbance voltage signal.

An example of the first three parts of the database is shown in Table 4.1 which consists the features for the first cycle of post-disturbance voltage signal for the fault type of phase B-C to ground fault. Each part consists of three data for phase A, B and C respectively.

Table 4.1 : Example of summation of the first, second and third level of detail coefficients for B-C to ground fault

	1st part (Level 1)			2nd part (Level 2)			3rd part (Level 3)		
	Phase A	Phase B	Phase C	Phase A	Phase B	Phase C	Phase A	Phase B	Phase C
Section 1	0.00666	0.01407	0.01971	0.09231	0.12126	0.09490	1.43904	1.49949	1.27941
Section 2	0.00666	0.01412	0.02065	0.09231	0.12184	0.09491	1.43904	1.49807	1.27790
…	…	…	…	…	…	…	…	…	…
Section 34	0.00666	0.02064	0.01935	0.09231	0.10113	0.09938	1.43904	1.44525	1.48736

4.3.1 (b) Faulty Section Identification

When an actual HIF event occurs, the measured three-phase voltage signal at measurement point is analysed using the MRA-DWT. Two cycles of post-disturbance voltage signal for phases A, B and C are decomposed separately using MRA-DWT. The extracted detail coefficients are added and then the distance between the measured data and line section data stored in the database is calculated. Noted that, a lookup table is used to determine the node pairs for each line section. In order to evaluate the effectiveness of the proposed method, various HIF values are applied in the middle of line section. Then, the distance is calculated using (4.2) in which the x, y and z axes are represented by the sum of detail coefficients for phases A, B and C respectively.

Table 4.2 shows an example of the shortest distance value calculated between measured signal and sample 1, 2 and 3 which represent the line section. The average value of distance is calculated for level 1, 2 and 3. The smallest average of the distance value indicate the shortest distance between the measured signal and that particular line sample.

Table 4.2 : Example of the calculated shortest distance for each level

	Simulated signal			Shortest distance		
	Phase A	Phase B	Phase C	Sample 1	Sample 2	Sample 3
LEVEL 1	0.016592	0.021358	0.008135	0.002843	0.000473	0.000321
LEVEL 2	0.199369	0.129223	0.100752	0.000836	0.000378	0.004404
LEVEL 3	1.639194	1.439835	1.335908	0.004835	0.002241	0.003382
	AVERAGE			0.002838	**0.001031**	0.002703

As shown in Table 4.2, the shortest distance belongs to sample 2 followed by sample 3 and 1. Therefore, sample 2 is inspected first as a faulty section. If the fault does not happen in line sample 2, then the second shortest distance will be the second faulty section to be inspected. The process continues until the actual faulty section is traced.

The process of calculating the first level of distance between the measured signal and sample 2 is shown below. Figure 4.9 shows a diagram of the measured signal, f to a line sample 2 represented by line *i-j*.

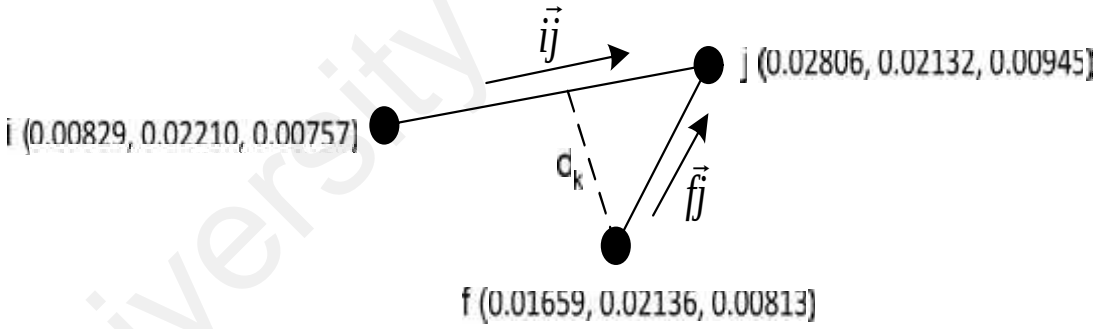

Figure 4.9 : Example of three coordinate system for node *i, j* and *f*

The input data *i* and *j* is a simulated data stored in database that represent the line section and data *f* is a measured data when a fault occurs in the system. Data *i, j* and *f* are described in three-coordinate system as follows:

$$\text{Shortest distance, } d_k = \frac{\left|\vec{fj} \times \vec{ij}\right|}{\left|\vec{ij}\right|} \qquad (4.2)$$

i = (0.00829, 0.02210, 0.00757)

j = (0.02806, 0.02132, 0.00945)

f = (0.01659, 0.02136, 0.00813)

Firstly, the vectors of $\vec{ij}$ and $\vec{fj}$ are calculated. Then, a cross product between vectors $\vec{ij}$ and $\vec{fj}$ is calculated.

$\vec{ij}$ = (0.01977, -0.00078, 0.00188)

$\vec{fj}$ = (0.01147, -4E-05, 0.00132)

$\vec{fj} \times \vec{ij}$ = (0.01147, -4E-05, 0.00132) × (0.01977, -0.00078, 0.00188)

= [(-4E-05) (0.00188) - (0.00132) (-0.00078),
(0.01147) (0.00188) - (0.00132) (0.01977),
(0.01147) (-0.00078) - (-4E-05) (0.01977)]

= (9.544E-07, -4.5328E-06, -8.1558E-06)

The magnitudes of the cross product $\left|\vec{fj} \text{ x } \vec{ij}\right|$ and $\left|\vec{ij}\right|$ are found as follows.

$$\left|\vec{fj} \text{ x } \vec{ij}\right| = \sqrt{9.544\text{E}-07^2 + -4.5328\text{E}-06^2 + -8.1558\text{E}-06^2}$$

$$= \sqrt{9.109E-13 + 2.055E-11 + 6.652E-11}$$

$$= \sqrt{8.797E-11}$$

$$= 9.379E-06$$

$$\left|\vec{ij}\right| = \sqrt{0.01977^2 + -0.00078^2 + 0.00188^2}$$

$$= \sqrt{3.9085E-04 + 6.084E-07 + 3.5344E-06}$$

$$= \sqrt{3.9499E-04}$$

$$= 0.0198744$$

Lastly, the value of d_k is calculated using (4.1)

$$d_k = \frac{9.379E-06}{0.0198744}$$

$$= 0.000472 \sim 0.000473 \text{ (from Table 4.2)}$$

The distance between the measured signal with a line section is calculated for each level separately. Then, the average distance value for all line sections are obtained and arranged from the smallest to the highest value with the line section it is represented. After the arrangement, line section with the shortest distance (smallest average distance value) is assumed as the first possible faulty section to be checked to determine the occurrence of HIF.

However, there is a possibility to incorrectly identify the faulty section from the first rank. This is due to the various uncertainty factors such as HIF values, radial network and error in measured data that contribute during the estimation of the faulty section process. Therefore, ranking analysis is important where all the line sections are considered in the inspection. Thus, it is necessary to identify the most probable faulty section to be inspected first followed by the other faulted section candidates if the first section is found health. The process continues until the actual faulty section is found.

4.3.2. Average of Absolute Difference (AAD) Technique and Database Approach

Similarly with the shortest distance and nearest neighbour rule techniques as mentioned before, the average of absolute difference, AAD technique applies the same approach. However for this technique, the difference for each point between two samples are calculated separately. For example the calculation of AAD value between two samples are shown as follows:

Sample A = (4.5, 5.9, 4.8, 6.4, 5.9)

Sample B = (4.9, 5.2, 5.7, 5.9, 6.7)

AAD = |A-B| = (0.4 + 0.7 + 0.9 + 0.5 + 0.8) / 5

= 0.66

In this proposed method, the AAD is calculated between the unknown signal data with the collection of a classified data. The unknown signal data are measured signal at the measurement point by the application of a certain HIF value at a certain location. The collection of a classified data is a simulated signal for each line section stored in the database.

To identify the fault location in a distribution system, the AAD value is calculated between the measured signal and all line sections stored in the database. Then the AAD values are arranged in increment order with the line section it is associated. A line section with the lowest AAD value has a higher priority to be assumed as a faulty section. Therefore, it will be inspected first to identify the HIF occurrence.

However in a certain situation where the first inspected line section is incorrect faulty section then, the other line sections have to be checked in order to trace the fault event. Therefore, the next line section to be inspected need to be determined directly after the first line section is found not a faulty section. Due to this reason, ranking analysis is necessary to assist an engineer to be able tracing the fault easily and immediately.

4.3.2 (a) Database Development

This technique involves a database approach to be implemented in locating a faulty section in a distribution system. In order to generate a set of database, pre-defined high

impedance fault is simulated at each node. The three-phase voltage signal obtained from the simulation is decomposed using the MRA-DWT to get three levels of detail coefficients for each voltage phase. After the fault had been simulated and the voltage signal was analysed for each node, the average of the summation of detail coefficients, A_v for two adjacent nodes is calculated. The A_v value is calculated to represent the data for that particular line section. The calculated A_v which is associated with the line section *i-j* is stored in the database. The process is performed for all line sections in the system. The A_v is calculated using (4.3)

$$A_v = \frac{\sum d_i + \sum d_j}{2} \tag{4.3}$$

where

A_v = an average of the summation of detail coefficients between two adjacent nodes

$\sum d_i$ = Summation of detail coefficients for level 1, 2 and 3 for node *i*

$\sum d_j$ = Summation of detail coefficients for level 1, 2 and 3 for node *j*

(*i* and *j* are two adjacent nodes)

There will be 18 data for each line section stored in database which consists of two cycles of post-disturbance voltage signal of phase A, B and C comprises of three levels of detail coefficients (2 cycles X 3 phases X 3 levels = 18 data). A list of all line sections between two adjacent nodes with the type of cable used is shown in the Appendix A.1.1 and A.1.2.

4.3.2 (b) Faulty Section Identification

After constructing a reference database that contains samples of A_v of HIF cases from different sections in the network, the effectiveness of the proposed method in locating

the faulty section is tested. Given a signal of an HIF case where fault is applied in the middle of a line section with defined fault impedance value, a set of wavelet features of measured voltage signal is extracted. Then the average of absolute difference, AAD between the extracted wavelet features from the signal and each set from the database is calculated.

Figure 4.10 shows an example of the first six wavelet features from the signal of interest matched against the same number of features from 4 samples (line section) that assumed as the reference database that most closely resemble them. It should be noted that only the first six coefficients data out of 18 data are shown in the figure due to the need to show the differences in their values with sufficient magnification. The AAD between the features of the interest signal and each case of the samples can be calculated using (4.4).

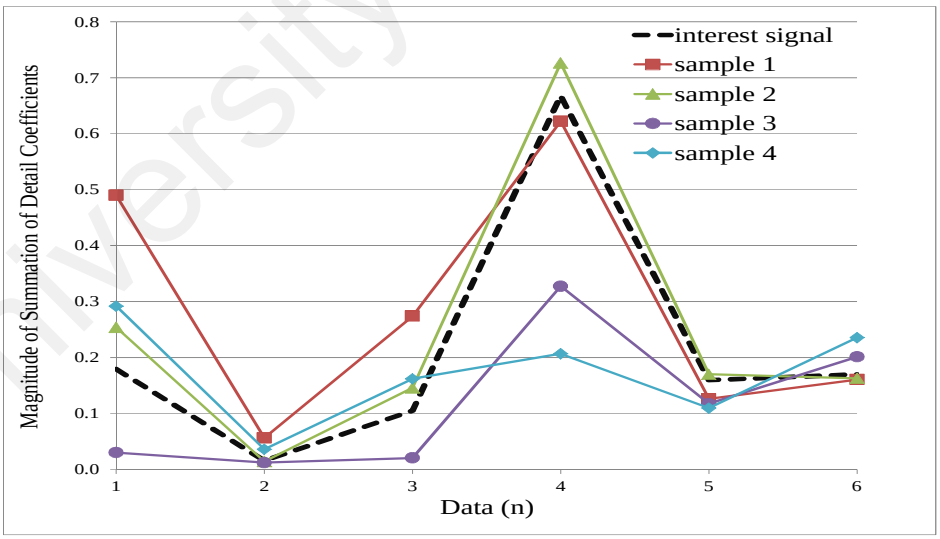

Figure 4.10 : Measured signal matching with each section in database

$$AAD_m = \frac{\sum_{k=1}^{n} \left| d_{k(measured)} - A_{v_k} \right|}{n} \qquad (4.4)$$

where

m = 1,2,..34 (number of line sections)

n = number of data, i.e. n=18

$d_{k(measured)}$ = detail coefficients of the test voltage signal

A_{V_k} = reference database.

The value of AAD is calculated using (4.4) to find the similarity of the pattern between the interest signal and sample. Table 4.3 shows an example of data for signal of interest and four different samples extracted from Figure 4.10. The result of AAD value calculated between the interest signal with each sample is depicted in Table 4.4.

Table 4.3 : Example data for interest signal and samples

Interest signal (S)	0.17926	0.01574	0.10515	0.66779	0.15961	0.16976
Sample 1 (a)	0.48996	0.05641	0.27393	0.62219	0.12622	0.16068
Sample 2 (b)	0.25403	0.01436	0.14573	0.72623	0.17017	0.16277
Sample 3 (c)	0.03029	0.01210	0.02059	0.32739	0.11747	0.20122
Sample 4 (d)	0.29174	0.03609	0.16193	0.20664	0.10969	0.23547

Table 4.4 : Example calculated AAD values

	Absolute difference value between signal of interest with samples						Total Difference	AAD
| S-a |	0.31071	0.04067	0.16878	0.04560	0.03340	0.00908	0.60823	0.10137
| S-b |	0.07477	0.00138	0.04058	0.05844	0.01056	0.00699	0.19273	**0.03212**
| S-c |	0.14897	0.00364	0.08456	0.34041	0.04214	0.03146	0.65118	0.10853
| S-d |	0.11249	0.02034	0.05679	0.46116	0.04992	0.06571	0.76640	0.12773

Once the AADs for all sets in the database have been calculated, they are arranged from the smallest to highest value where the smallest value is ranked as the first. Finally, the proposed method will check the suspected faulty sections associated with the lowest few *AAD* values that give a high probability of occurrence. The smallest value of AAD is chosen because it shows that the sample closely resembles the interest signal. It is necessary to use a few low AAD values to detect the faulty section because in some cases the lowest AAD value does not point the correct faulty section. Therefore, if the section related to the lowest AAD value is not faulty, the HIF is searched at sections

related to the second and third lowest AADs. This is done by physically inspecting the suspected locations. In practice, when any fault occurs, engineers have to go to the location where the fault occurs in order to clear the fault thus expedite the power system restoration.

4.4. Summary

In this chapter, the overall concepts of the proposed methods in identifying the HIF location have been discussed. Basically, the wavelet transform was used to extract the significant features required by the proposed methods to locate the fault. The identification of the HIF location was performed based on the matching approach between the measured features and database. The database consists of the extracted features of voltage signal corresponding to the several HIF value at each node.

Also, the classification of fault type based on the approximation ratio has been explained in this chapter. The steps to construct a database for different type of faults and fault values were described briefly. Finally, detail explanation of the HIF faulty section identification using SD and AAD methods have been discussed thoroughly in this chapter.

CHAPTER 5

RESULTS AND DISCUSSION

5.1. Introduction

In the previous chapter, the proposed method used for identification of HIF locations in underground distribution system has been presented. The algorithm of the proposed method has been developed in MATLAB to validate its effectiveness in locating the faults. The database and test data for the proposed method have been obtained through fault simulation carried out in PSCAD/EMTDC software Version X4. The test system for this research consists of a typical 132/11kV distribution network of Malaysia. All the tests and simulation have been performed on a Personal Computer with processor Intel Core Duo CPU 3.07 GHz. This chapter presents the test system, results and discussions for the proposed method.

5.2. Test System Modelling for the Proposed Method

The test system for analysing the proposed method is a 11kV, 50 Hz system as shown in Figure 5.1. The test system has 38 nodes that represent 34 line sections. All cables in the network are three-phase balanced and underground. Measurement is located at the primary substation. The complete network data are given in the Appendix A.1. The test system modelled in PSCAD/EMTDC is shown in Figure 5.2

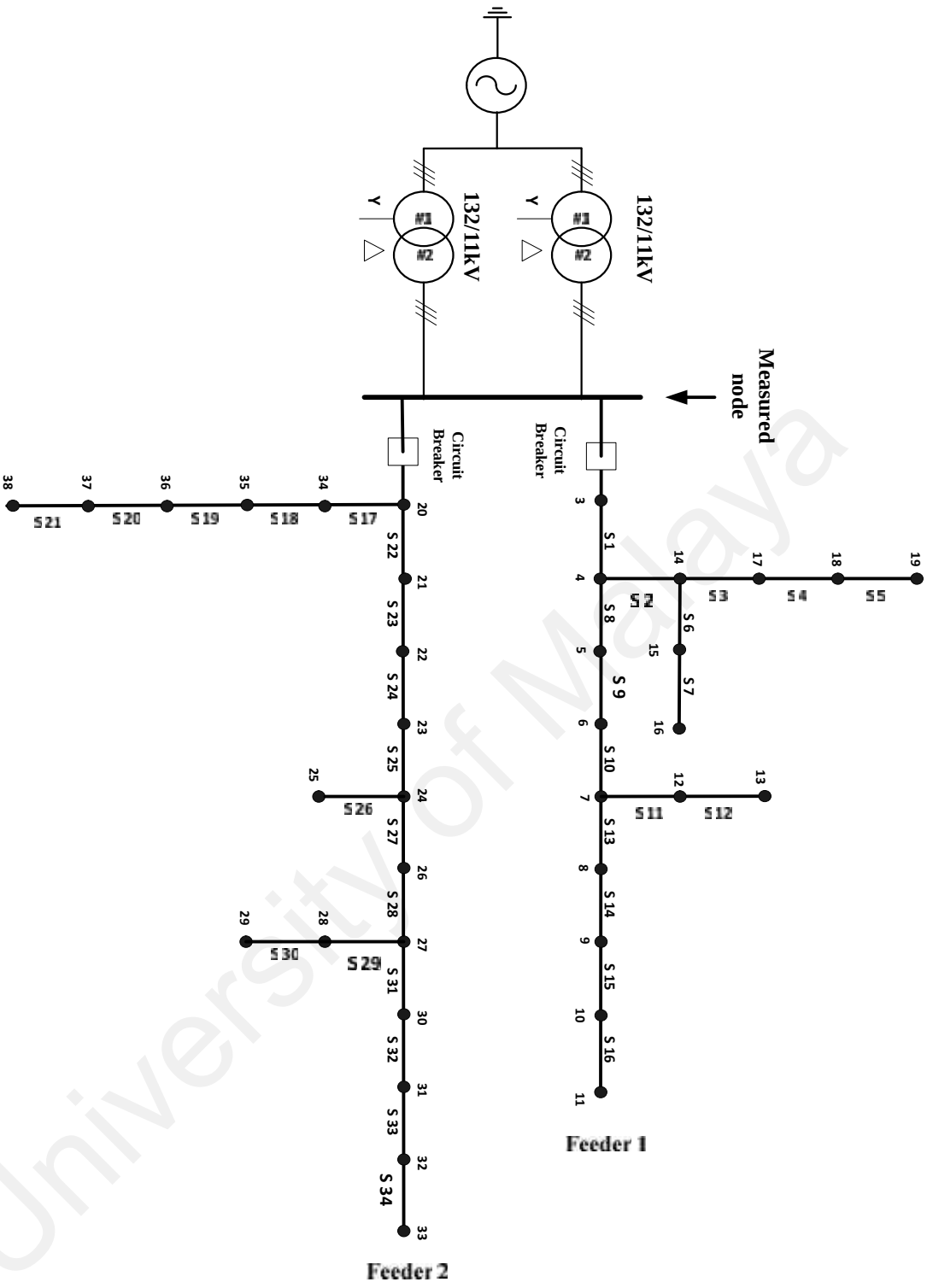

Figure 5.1 : Schematic diagram of 11kV distribution network in Malaysia

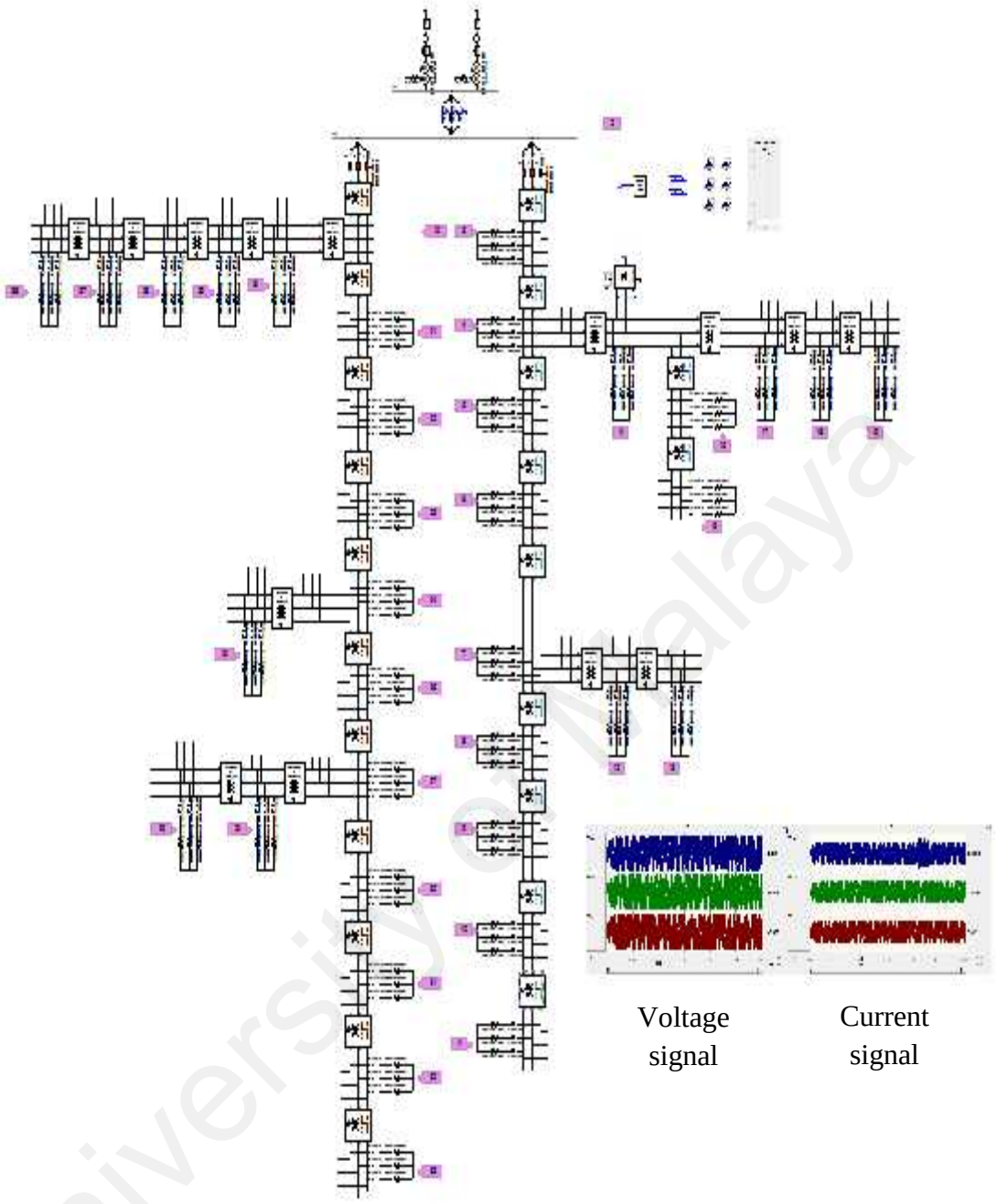

Figure 5.2 : The typical 11kV distribution network in Malaysia modelled in PSCAD/EMTDC software

The grid is modelled by using an equivalent three-phase voltage source model. The transformer consists of three-phase 2-winding transformer and the line sections are modelled by using the π-model. All of these models can be found in PSCAD/EMTDC master library. The loads are modelled as resistance (R) and inductor (L), where the values are given in Appendix A.1.3. The voltmeter from the master library was used to obtain the three-phase voltage at the primary substation. To evaluate the proposed fault

location method, a set of database has been generated for different values of high impedance fault with all types of fault, which are Single Line to Ground Fault (SLGF), Double Line to Ground Fault (LLGF), Line to Line Fault (LLF) and Three Phase Fault (LLLF).

In this research, HIF values are assumed between 40Ω - 100Ω. This assumption is done since there is no standard range of the HIF value. For example, in (Uriarte, et al., 2005) the value of HIF is recommended based on the type of surface where the conductor is contacted such as dry sand and concrete. Another example value for HIF is set to 140kΩ in a case when distribution network suffered from a fault due to leaning tree (Elkalashy, et al., 2008b). Meanwhile, in (Bretas, et al., 2006) and (Jung, et al., 2007), the maximum HIF value is set to 100Ω and 200Ω respectively.

5.2.1. Fault Simulation in PSCAD/EMTDC

To test the proposed method, the HIF of SLGF is applied in the middle of line section 6 at time 2.1s. The three-phase voltage signal obtained at the primary substation is shown in Figure 5.3. The voltage signal is used in this analysis instead of current signal because waveform disruption on voltage waveform is not too obvious (as shown in Figure 5.3) as compared to current waveform. The purpose is to show the significance of wavelet transform to extract features even a very small fluctuation.

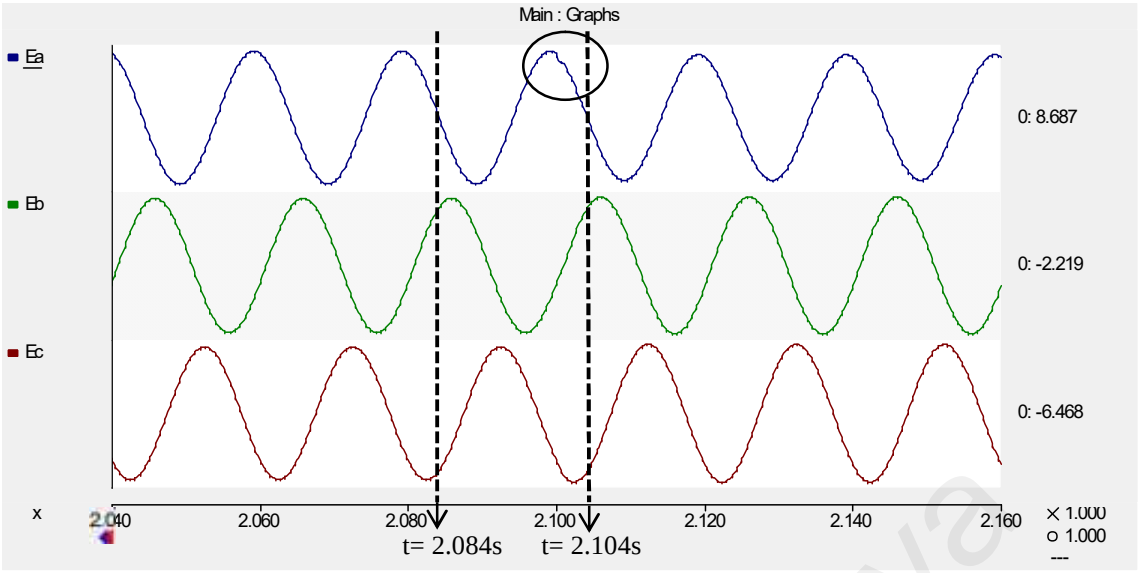

Figure 5.3 : Three-phase voltage signal due to HIF

It can be observed from the Figure 5.3 that, there is a very small fluctuation (as shown in the circle) on the voltage signal (Ea) at t = 2.1s which hardly can be seen. However, by using MRA-DWT the important features can be extracted from this small fluctuation. The features are used to detect the occurrence of HIF and to predict the fault location using the proposed method.

5.2.2. Wavelet Analysis for Fault Detection and Location

This fluctuation of voltage signal as shown in Figure 5.3 can be observed clearly by taking one complete cycle between t=2.084s and t=2.104s as shown in Figure 5.4(a). It illustrates the first cycle of post-disturbance voltage signal. Generally, this small fluctuation cannot be detected by the common impedance-based methods because it behaves like a normal signal. In order to distinguish this type of anomaly, MRA-DWT is utilised to extract the features from the signal. After the signal was decomposed using the MRA-DWT, sharp fluctuations can be seen in its detail coefficients as shown in Figure 5.4 (b) – (d). These are the detail coefficients of the first, second and third level decomposition respectively for the first cycle of the post disturbance voltage signal. This sharp fluctuation indicates the occurrence of an anomaly in the voltage signal.

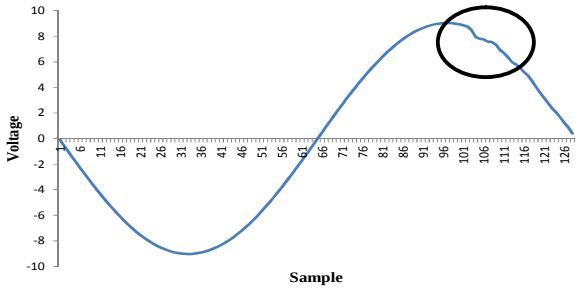

(a) : 1st cycle of post-fault

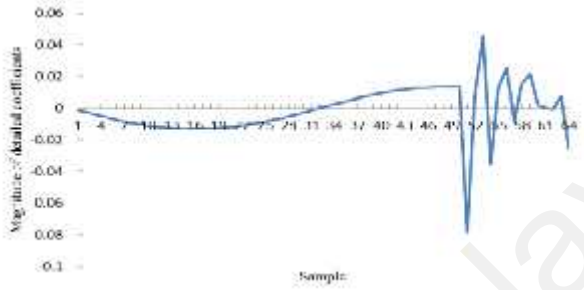

(b) : 1st level of detailed coefficients.

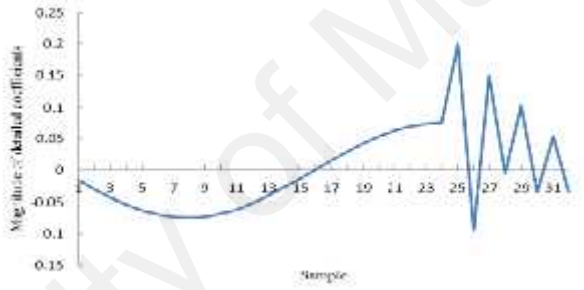

(c) : 2nd level of detailed coefficients.

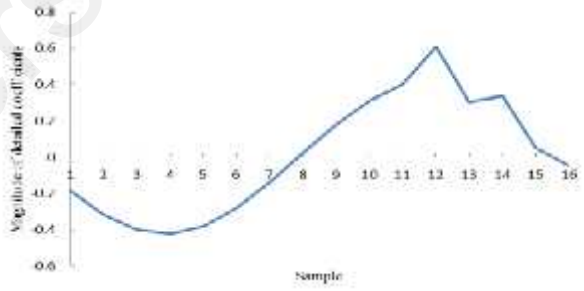

(d) : 3rd level of detailed coefficients.

Figure 5.4 : MRA-DWT analysis for post-disturbance voltage signal

As shown in Figure 5.4 (b), an obvious sharp fluctuation can be observed in the first level of detail coefficients compared to the second and third level. An indistinctive fluctuation can be seen at higher level decomposition for example in Figure 5.4 (d). This is because, at the first level decomposition, all the high frequency components

were filtered out. As the level of decomposition increases, the frequency of component decreases. Thus, a low frequency components are filtered out at a higher level of decomposition. In order to identify the faulty section, the sum of three levels detailed coefficients from the first and second cycles of post-disturbance voltage signal is calculated and compared to those in the selected database.

5.3. Performance of the Proposed Method

Line section 2 and 9 were used to represent faults at feeder 1 while line section 29 and 34 were selected to represent faults at feeder 2. The tested high impedance fault values are 45Ω, 55Ω, 65Ω, 75Ω, 85Ω and 95Ω. For this purpose, four fault types which are SLGF, LLLF, LLGF and LLF were applied in the middle of a line section. Table 5.1 summarises different type of fault, tested locations and fault impedance values used to validate the performance of the proposed method.

Table 5.1: Parameter for different fault type, faulty section and fault impedance

Fault Type	SLGF, LLLF, LLGF and LLF
Test Section	2, 9, 29 and 34
Fault Impedance Value (Ω)	45,55,65,75,85 and 95

Two different techniques which are the shortest distance technique (SD) and average of absolute difference technique (AAD) are applied to identify the faulty section. The outcomes of each technique are discussed separately using the same test system. In this chapter, a test result of SLGF is discussed in details since it is the most frequent type of fault that occurs in the distribution system. Only the results of three different fault impedances which are 75Ω, 85Ω and 95Ω are discussed in details whereas the rest of the fault impedance values and other fault types results are summarised.

5.3.1. Shortest Distance Technique

The first proposed method used to locate the faulty section is the shortest distance technique. The steps to estimate the possible faulty sections using this technique had been discussed briefly in Section 4.3.1. Using this technique, only five possible faulty section candidates with the lowest value of SD are selected for fault finding. This is due to the analysis results using the SD technique that show the actual faulty section that can be located among five candidates with the lowest SD value.

5.3.1 (a) Case Study - Single Line to Ground Fault

For the case study, SLGF is simulated at the midpoint of a line section. There are 3 types of SLGF:

i. Phase A to Ground Fault
ii. Phase B to Ground Fault
iii. Phase C to Ground Fault

In this case study, phase A to ground fault is selected. It should be noted that, the proposed algorithm is also applicable for phase B to ground fault and phase C to ground fault since all three phases are utilized in the algorithm. However, different database is used for different type of SLGF to be applied in the algorithm.

Table 5.2 summarized the tested locations and their respective fault impedance values for SLGF analysis. In Figure 5.5, it shows the location (indicated by ‘x’) of the fault applied in the middle of line section.

Table 5.2 : Parameter for different faulty section and fault impedance

Test Section		Fault Impedance Value (Ω)
Feeder 1	Section 9 (S9)	75 85 95
Feeder 2	Section 34 (S34)	75 85 95
Branch 1	Section 2 (S2)	75 85 95
Branch 5	Section 29 (S29)	75 85 95

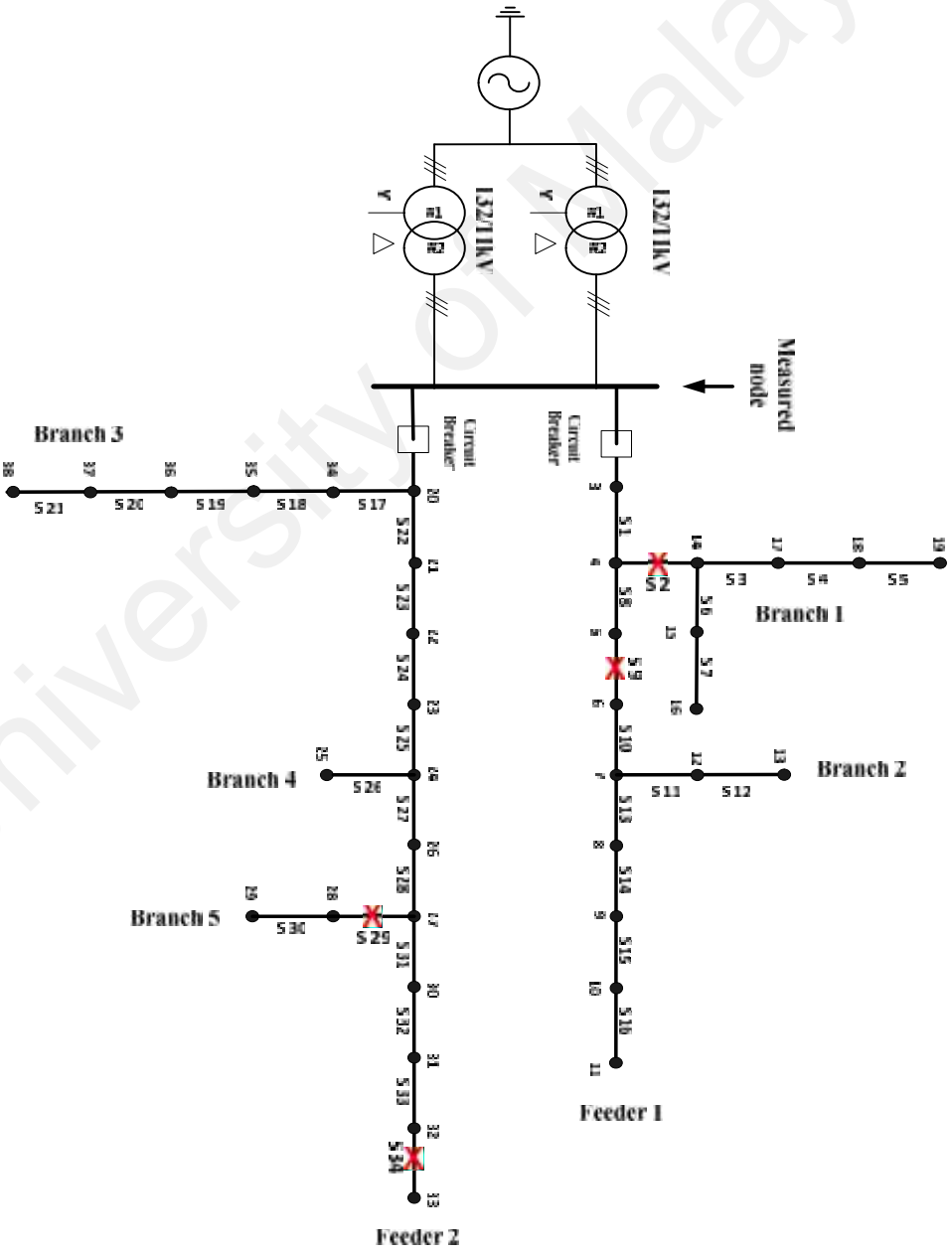

Figure 5.5 : Location of the fault

5.3.1 (b) Analysis of Fault at the Main Feeder

For the first analysis, the effectiveness of the proposed algorithm is checked when fault is applied in the main feeder line. For this purpose, sections 9 and 34 are selected to represent the line section at the main feeder for feeder 1 and 2 respectively. Three different fault impedance values are tested and the results are shown in Table 5.3 and Table 5.4. Both tables show the shortest distance value (SD), faulty section candidates and rank number of the section. The correct faulty section is indicated with a rectangle.

Table 5.3 : Fault at Feeder 1 (S9)

75ohm			85ohm			95ohm		
SD	Faulty Section Candidate	Ranking Number	SD	Faulty Section Candidate	Ranking Number	SD	Faulty Section Candidate	Ranking Number
0.00031	10	1	0.00026	10	1	0.00021	10	1
0.00041	***9***	***2***	0.00031	8	2	0.00021	8	2
0.00045	8	3	***0.00032***	***9***	***3***	***0.00024***	***9***	***3***
0.00054	13	4	0.00033	13	4	0.00025	13	4
0.00056	2	5	0.00050	2	5	0.00042	2	5

Table 5.4 : Fault at Feeder 2 (S34)

75ohm			85ohm			95ohm		
SD	Faulty Section Candidate	Ranking Number	SD	Faulty Section Candidate	Ranking Number	SD	Faulty Section Candidate	Ranking Number
0.00036	32	1	0.00021	32	1	0.00014	32	1
0.00065	33	2	0.00052	33	2	***0.00041***	***34***	***2***
0.00079	***34***	***3***	***0.00062***	***34***	***3***	0.00042	33	3
0.00105	31	4	0.00095	31	4	0.00084	31	4
0.00149	25	5	0.00127	28	5	0.00117	28	5

As shown in Table 5.3, the actual faulty section is found in the second and third rank. It is noted that section 9 is between section 8 and 10. Also, the value of SD for sections 8, 9 and 10 are close to each other. Therefore, there is a possibility that the fault happens in either one of the line section.

To illustrate the SD approach in determining the faulty section, fault at section 9 with 85ohm is taken as an example. Figure 5.6 shows the measured features (* sign) and line section (straight line) with respect to section 8, 9, and 10 described in 3-dimensional coordinate. The value on x, y and z axes are the sum of detail coefficients of Phase A, B and C of the voltage signal respectively. The dash lines are the perpendicular line of shortest distance between the measured signal with line section 8, 9 and 10. As shown in the figure, the shortest distance belongs to Section 10. However, the actual faulty section belongs to Section 9 (third shortest distance value).

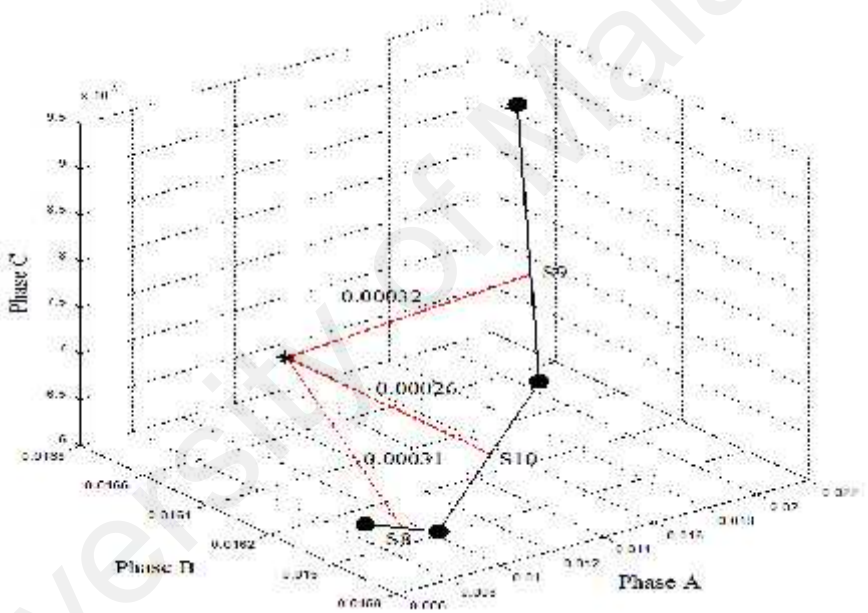

Figure 5.6 : Shortest distance for measured signal

In Table 5.4, it is also noticed that the actual faulty section is traced in the third rank for fault impedance of 75Ω and 85Ω and second rank for 95Ω fault impedance. In all three cases, the top three candidates of faulty section are section 32,33 and 34. From the analyses, it can be observed that the top three candidates of the faulty section fall in one straight line and adjacent to each other. Therefore, it can reduce the time taken to locate the actual faulty section.

From Table 5.3 and Table 5.4, it can be seen that the fault has been successfully located within the first three smallest values of SD in section 9 and section 34 respectively. Furthermore, it can be observed that the proposed method work successfully regardless of fault impedance value.

5.3.1 (c) Analysis of Fault on a Branch Section

The capability of the proposed algorithm in locating the faulty section at a branch section is analysed. In this analysis, sections 2 and 29 are chosen to represent the branch section at feeder 1 and 2 respectively. As shown in Figure 5.8, section 2 is in between sections 1,3,6 and 8 whereas section 29 is next to section 28, 30 and 31. The test results of the analysis are shown in Table 5.5 and 5.6.

Table 5.5 : Fault at Branch 1 (S2)

75ohm			85ohm			95ohm		
SD	Faulty Section Candidate	Ranking Number	SD	Faulty Section Candidate	Ranking Number	SD	Faulty Section Candidate	Ranking Number
0.00054	***2***	***1***	***0.00047***	***2***	***1***	***0.00039***	***2***	***1***
0.00075	7	2	0.00052	7	2	0.00043	7	2
0.00089	3	3	0.00065	3	3	0.00048	3	3
0.00100	5	4	0.00082	8	4	0.00064	4	4
0.00106	9	5	0.00084	9	5	0.00065	8	5

Table 5.6 : Fault at Branch 5 (S29)

75ohm			85ohm			95ohm		
SD	Faulty Section Candidate	Ranking Number	SD	Faulty Section Candidate	Ranking Number	SD	Faulty Section Candidate	Ranking Number
0.00016	30	1	0.00015	30	1	***0.00011***	***29***	***1***
0.00018	32	2	***0.00016***	***29***	***2***	0.00014	30	2
0.00022	***29***	***3***	0.00017	31	3	0.00014	31	3
0.00022	31	4	0.00018	32	4	0.00017	32	4
0.00040	28	5	0.00026	28	5	0.00017	28	5

From Table 5.5 and Table 5.6, it can be observed that the fault has been successfully located within five possible candidates regardless of the fault impedance value. In Table 5.6, the fault is identified in the first rank for the fault impedance value of 95Ω.

Whereas, for the fault impedance value of 85Ω and 75Ω, the fault is located in the second and third rank respectively. It can be seen also that some of the sections have similar SD value. In this case, the program will increase the number of decimal points of the values. It should be noticed that all the values had been rounded off into five decimal points. The proposed algorithm can be considered to provide a good approximation since all the faulty section can be found within three possible sections.

5.3.1 (d) Overall Test Results for Various Fault Impedance Values

Different fault impedance values are applied in the middle of line section 2, 9, 29 and 34 with the result is presented in Table 5.7. The rank number of actual faulty sections on various fault impedance values are shown in column 2 until 7. Four different sections and six different HIF values are chosen as the test study.

Table 5.7 : Results of SLGF for Various HIF value

	Rank Number of the actual faulty section					
	45Ω	55Ω	65Ω	75Ω	85Ω	95Ω
Section 2	1	1	1	1	1	1
Section 9	2	3	2	2	3	3
Section 29	2	2	3	3	2	1
Section 34	1	3	3	3	3	2

As shown in the Table 5.7, all the faults could be successfully located within the first three possible faulty sections. It shows that the proposed algorithm has restrict all the faulty section candidates from 34 possible faulty sections into 3 most likely the location of fault occurrence.

For any fault occurrence at Section 9, 29 and 34, the algorithm has identified the actual fault location either in the first, second or third rank. Even though the actual faulty section cannot be located in the first rank candidate, it still considered that the proposed algorithm had given good performance in estimating the location of the fault. This is

because, from the test results, it can be observed that mostly the differences of SD value between the first, second and third rank faulty section are quite close to each other. Furthermore, it can be seen from the test results that the top three candidates of the possible faulty section are the same for any fault impedance value as shown in Table 5.3 and 5.4. It means that, the fault applied to a particular location, regardless of the fault impedance value, the proposed algorithm will estimate the same three candidates with the smallest value of SD. In this proposed method, it should be noted that, even though the actual fault location is traced from the third rank candidate, the first and second rank faulty section has to be inspected first.

5.3.1 (e) Overall Test Results on Various Test Sections

The same fault impedance values are tested in the middle of each line section on the distribution network. The results from the testing are shown in Figure 5.7. In the figure, it shows the total number of test section found correctly at various ranks on the SLGF for different fault impedance values.

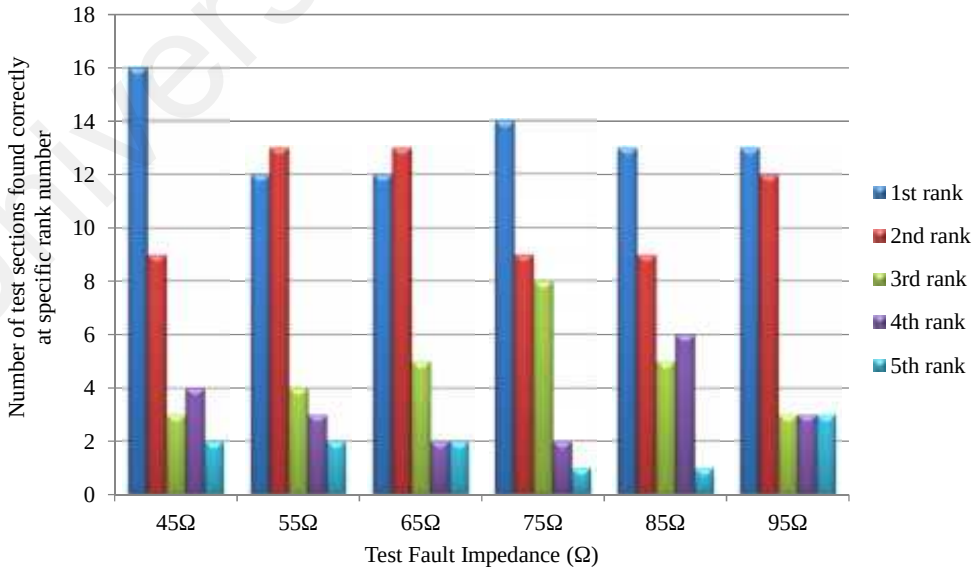

Figure 5.7 : Overall Performance for SLGF

It turns out that the majority of the test section was found correctly in the first or second rank. There are few faulty cases associated with the candidate with the third, fourth and fifth rank. From the analysis, it has been found that all the test section fall within third, fourth and fifth rank are the branch section. An example of test section found correctly at a higher rank number is illustrated in Table 5.8.

Table 5.8: Fault at Branch 2 (S13) and Branch 4 (S27)

85Ω					
SD	Faulty Section Candidate	Ranking Number	SD	Faulty Section Candidate	Ranking Number
0.000301	14	1	0.000088	28	1
0.000302	11	2	0.000117	25	2
0.000379	12	3	0.000123	26	3
0.000447	10	4	***0.000139***	***27***	***4***
0.000450	***13***	***5***	0.000202	24	5

Table 5.8 shows an example of fault cases where 85Ω is applied in the middle of line section 13 and 27. As shown in the Table 5.8, both cases identified the real faulty section in the fourth and fifth rank. It could be noted that all the possible faulty section candidates are adjacent to each other as shown in Figure 5.6. Also, it was observed that the SD value for each candidate is near to each other. Therefore due to the effect of branches, more than one possible faulty section could be found.

It is also important to note that the tested HIF value of 45Ω, 55Ω, 65Ω, 75Ω, 85Ω and 95Ω is different from the values used to construct the databases which are 40Ω, 50Ω, 60Ω, 70Ω, 80Ω, 90Ω and 100Ω. Therefore, it is acceptable to identify the actual faulty section by inspecting at maximum five possible candidates of fault location.

5.3.1 (f) Overall Test Results on Various Fault Types

Similar test as in SLGF was repeated for another type of faults. The effectiveness of the proposed method is evaluated based on the number of times the actual faulty section is found in the section associated with the lowest SD (1st in rank), the second (2nd in rank), the third (3rd in rank), the fourth (4th in rank) and the fifth lowest SD (5th in rank) for LLLF, LLGF and LLF. The overall results are shown in Figure 5.8.

It can be seen in Figure 5.8 that most of the faulty section was found correctly in the first rank. There are only a few test sections identified by the proposed algorithm in the higher ranked. It can be observed that, there is no faulty section traced in the fifth rank for LLGF and LLF. Also, only one test section has been found in the fourth rank. By examining all the test sections, it was found that the actual faulty section falls in the fourth rank is a branch section. By its nature of branches, multiple faulty section are estimated and inspected before the real one is identified. Furthermore, it can be noticed that the total number of test section found correctly in the first rank increases as the fault impedance value increases for LLGF. Consequently, the total number of test section successfully identified in the higher ranked decreases with the increasing of fault impedance value.

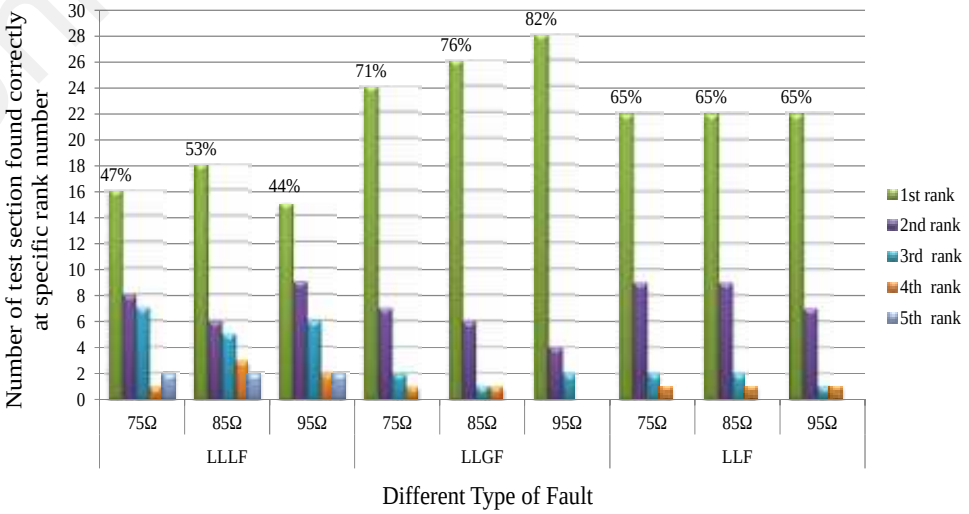

Figure 5.8 : Overall Performance for Various Type of Faults

From the test results, it can be noticed that the proposed method gives a good accuracy in locating the HIF location in the first rank for LLGF and LLF. For example in LLGF, 71% (24 cases), 76% (26 cases) and 82% (28 cases) accuracies were achieved for fault impedance value of 75Ω, 85Ω and 95Ω respectively. Besides, it can be observed that, the accuracy in LLLF is less as compared to LLGF and LLF. Only 47% (16 cases), 53% (18 cases) and 44% (15 cases) accuracies are recorded in locating LLLF for the fault impedance value of 75Ω, 85Ω and 95Ω respectively. However, it is still acceptable since the actual faulty section can be identified in a reasonably low rank. Furthermore, limitation of database and wide range of fault impedance value proves that the proposed method is effective in locating a faulty section in an underground distribution network.

5.3.2. Average of Absolute Difference Technique

The second proposed method used to locate the fault during HIF occurrence is the average of absolute difference (AAD) technique. The steps to estimate the possible faulty section using the proposed technique had been discussed in Section 4.3.2. Utilizing this proposed technique, only three faulty section candidates with the smallest value of AAD are selected to assist in identifying the faulty section. It is because the actual faulty section can be located within three candidates with the smallest value of AAD.

5.3.2 (a) Case Study - Single Line to Ground Fault

As performed in the SD case study, SLGF is used to show in details the effectiveness of the AAD technique in locating the faulty section. Phase A to ground fault type is simulated at the middle of a line section. In order to make a better comparison between this technique with the previous technique, the fault is applied at the same location with the same fault impedance values as the previous one. The summarised table of test

locations and their respective fault impedance values for phase A to ground fault is shown in Table 5.2. The location in which the fault is applied in the middle of a line section is shown in Figure 5.5.

5.3.2 (b) Analysis of Fault at a Main Feeder

Table 5.9 and 5.10 shows the test results of the analysis using the AAD technique. The tables show the calculated AAD value, faulty section candidates and also rank number of the section candidates.

Table 5.9 : Fault at Feeder 1 (S9)

75ohm			85ohm			95ohm		
AAD	Faulty Section candidate	Ranking Number	AAD	Faulty Section candidate	Ranking Number	AAD	Faulty Section candidate	Ranking Number
0.00031	***9***	***1***	***0.00024***	***9***	***1***	***0.00020***	***9***	***1***
0.00075	8	2	0.00068	8	2	0.00063	8	2
0.00083	2	3	0.00072	2	3	0.00065	2	3
0.00133	10	4	0.00106	10	4	0.00087	10	4
0.00202	11	5	0.00165	2	5	0.00138	11	5

Table 5.10 : Fault at Feeder 2 (S34)

75ohm			85ohm			95ohm		
AAD	Faulty Section Candidate	Ranking Number	AAD	Faulty Section Candidate	Ranking Number	AAD	Faulty Section Candidate	Ranking Number
0.00060	***34***	***1***	***0.00049***	***34***	***1***	***0.00041***	***34***	***1***
0.00078	33	2	0.00065	33	2	0.00055	33	2
0.00200	32	3	0.00163	32	3	0.00137	32	3
0.00266	31	4	0.00222	31	4	0.00189	31	4
0.00282	29	5	0.00234	30	5	0.00198	30	5

As shown in Table 5.9 and Table 5.10, the actual faulty section is found in the first rank candidate with the lowest AAD value in all cases. It indicates that the proposed algorithm pinpoints the actual faulty section in the first attempt. Also, it can be observed that regardless of fault impedance value, the proposed algorithm works effectively in locating the fault location.

5.3.2 (c) Analysis of Fault on a Branch Section

As the previous analysis, fault is tested on a branch section. The test results are shown in Table 5.11 and Table 5.12 for different fault impedance values.

Table 5.11 : Fault at Branch 1 (S2)

75ohm			85ohm			95ohm		
AAD	Faulty Section Candidate	Ranking Number	AAD	Faulty Section Candidate	Ranking Number	AAD	Faulty Section Candidate	Ranking Number
0.00052	***2***	***1***	***0.00048***	***2***	***1***	***0.00045***	***2***	***1***
0.00111	9	2	0.00099	9	2	0.00085	10	2
0.00119	10	3	0.00099	10	3	0.00092	9	3
0.00141	6	4	0.00120	6	4	0.00105	11	4
0.00151	3	5	0.00127	11	5	0.00106	6	5

Table 5.12 : Fault at Branch 5 (S29)

75ohm			85ohm			95ohm		
AAD	Faulty Section Candidate	Ranking Number	AAD	Faulty Section Candidate	Ranking Number	AAD	Faulty Section Candidate	Ranking Number
0.00010	30	1	0.00009	30	1	***0.00008***	***29***	***1***
0.00018	***29***	***2***	***0.00011***	***29***	***2***	0.00008	30	2
0.00034	31	3	0.00026	31	3	0.00024	31	3
0.00055	28	4	0.00047	28	4	0.00042	28	4
0.00103	27	5	0.00089	27	5	0.00079	27	5

In Table 5.11, it can be observed that faulty section was identified in line section candidate associated with the lowest AAD value. Also, a distinctive difference of AAD value between the first and second rank candidate can be seen. It indicates the highest possibility of fault occurs at the first rank candidate.

From the Table 5.12, when a fault impedance of 75Ω and 85Ω were applied in the middle of line Section 29, it can be observed that the lowest AAD value belongs to Section 30 although Section 29 is the actual faulty section. According to this approach, since the fault does not occur in Section 30, the next section with the second lowest AAD value is checked and it is found that Section 29 is where the actual fault occurred. Although the actual faulty section is successfully located after the second attempt, in

practice, when any fault occurs, engineers have to do a physical inspection by visiting the suspected location. Hence, the proposed method reduces the number of line section to be inspected.

5.3.2 (d) Overall Test Results for Various Fault Impedance Values

The effectiveness of the proposed method in locating faults for various fault impedance values have been studied. The performance of the proposed method is based on the number of attempts before the real fault location is identified regardless of fault impedance value. The test results are presented in Table 5.13, consists of the rank number of the actual faulty section is found in different HIF value as shown in the second until seventh columns.

Table 5.13 : Results of SLGF for Various HIF value

	Rank Number of the actual faulty section					
	45Ω	55Ω	65Ω	75Ω	85Ω	95Ω
Section 2	1	1	1	1	1	1
Section 9	1	1	1	1	1	1
Section 29	2	2	2	2	2	1
Section 34	1	1	1	1	1	1

As shown in the table, all the faults can be successfully located after one or two attempts in tracing the fault. It is observed that when a fault is applied regardless of fault value to Sections 2, 9 and 34, the proposed algorithm accurately estimate the actual faulty section. The actual faulty section is identified from the first rank of the possible faulty section candidate. For the case when the fault occurs in Section 29, the actual faulty section is identified after it was found that the first inspected line section is not faulted except for 95Ω fault impedance value. From the test results, it can be concluded that the proposed algorithm manages to accurately estimate the fault location regardless of fault impedance values.

5.3.2 (e) Overall Test Results on Various Test Sections

In this case, similar HIF values as used in previous analyses, have been applied to test for all line sections in the distribution network. The performance of the proposed algorithm is evaluated based on the number of test sections found correctly at a specific rank number. The results are shown in Figure 5.9 for the SLGF applied in the middle of each line section.

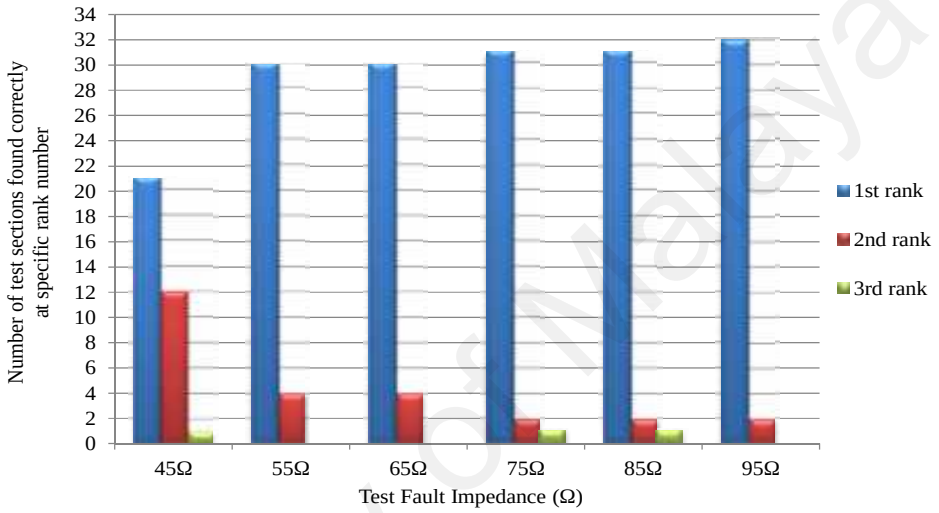

Figure 5.9 : Overall Performance for SLGF

From the Figure 5.9, it can be observed that the majority of the faulty cases are associated with the candidates having the lowest AAD value (first in rank). The remaining faulty sections are mainly located in the section of the second lowest AAD value and a few can be traced with sections of the third lowest AAD value. Only one case of the faulty section found correctly in the third rank for fault impedance of 45Ω, 75Ω and 85Ω while in the other cases, faulty sections were found in first or second rank. Based on the test results, it can be concluded that the proposed method is able to narrow down 34 possible faulty section candidates into 3 most likely the location of fault occurrence which has the lowest AAD value.

5.3.2 (f) Overall Test Results on Various Fault Types

The overall performance of the proposed method in terms of effectiveness in identifying the actual faulty section is studied for various other types of fault (LLLF, LLGF and LLF). Only three difference HIF values (75Ω, 85Ω and 95Ω) applied in the middle of each line section are tested and then the capability of the proposed method to locate the fault is analysed. The effectiveness of the proposed method is evaluated based on the number of times the actual faulty section is found in the section associated with the lowest AAD (1^{st} in rank), the second (2^{nd} in rank) and the third lowest AAD (3^{rd} in rank) for LLLF, LLGF and LLF.

As shown in Figure 5.10, it can be observed that most of the faulty section can be located in the first rank section, which is the first attempt. For the fault type of LLGF and LLF, 97% (33 sections) and 100% (34 sections) accuracies are recorded for locating the actual faulty section in the first rank sections. There is no faulty section identified in the third rank and only one case is recorded in the second rank candidate for LLGF. For LLF, the proposed algorithm works magnificently because all the faulty section can be located easily in the first rank. Whereas, in LLLF case, there are two test sections found correctly in the third rank and few can be traced in the second rank candidates (5-6 cases). The remaining test sections were successfully identified from the first inspection (26-27 cases).

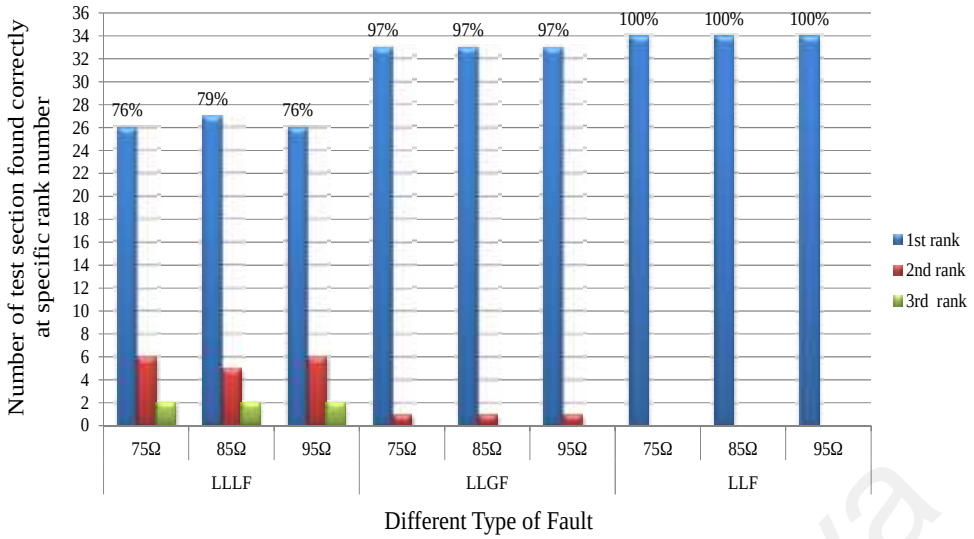

Figure 5.10 : Overall Performance for Various Type of Faults

From the theoretical point of view, it is acceptable to identify the actual faulty section by inspecting at maximum three sections because locating the faulty section in a distribution system is quite difficult especially due to the branch topology of the network that result in variations in faulty section. Also, the tested HIF value of 75Ω, 85Ω and 95Ω are different from the values used to construct the databases which are 70Ω, 80Ω, 90Ω and 100Ω.

From the test results, it can be concluded that the proposed method works well in determining the HIF location. Even though there are a few test sections found in the second or third rank candidates, but due to the limitation of the database and a wide range of fault impedance value, the proposed method is considered successful in identifying the faulty section.

5.3.3. Computational Time

It is important to observe the computational time to extract features from the voltage signal and estimate all possible faulty sections. This is because, faster computational time results in faster restoration process of the power system. The computational time

taken by the proposed SD and AAD techniques in analysing the extracted features and listing out all faulty section candidates is shown in Figure 5.11.

From the Figure 5.11, it can be observed that the proposed SD technique takes shorter time than AAD technique. Furthermore, the computational time is almost the same for all types of fault. The reason is that, all three phases of voltage signal are considered in this analysis regardless of fault type.

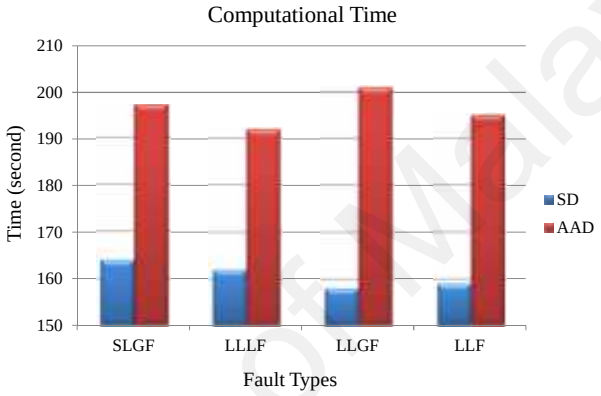

Figure 5.11 : Computational time for different type of faults

5.3.4. Limitation of High Impedance Fault Value

Since the proposed method is based on the features extracted from the waveform of voltage, there is a possibility that such waveform is not significant. This section presents the studies to determine the maximum value of fault impedance in which the significant features are able to be extracted. Maximum value of fault impedance is achieved when the features extracted during the HIF is similar to the normal condition. It can be determined using the summation of detail coefficient value. In Table 5.14, it shows various fault impedance values applied in the middle of line section 6 with fault type of SLGF, phase A to ground fault. Phase A of the voltage signal is analysed using the wavelet transform to extract the detail coefficients. Then, the value of the coefficients is added. It is also possible to use other phases of voltage signal for this purpose.

Table 5.14 : Summation value of detail coefficients for different values of HIF

Fault Impedance Value (Ω)	Summation of Detail Coefficients (Phase A)
Normal	**0.00669**
150	0.01149
250	0.00848
500	0.00713
1000	0.00678
1500	0.00672
1600	0.00671
1700	0.00670
1800	0.00670
1900	**0.00669**
2000	0.00669
2100	0.00669

It can be noticed from Table 5.14, the value of the summation of detail coefficients varies with the value of fault impedance. The summation of detail coefficient value remains unchanged (1900Ω - 2100Ω) and same to the value of sum of detail coefficients during normal condition. Therefore, the limit of the fault impedance value that can be applied to the proposed method is 1800Ω for SLGF. It should be noted that different fault types and test system could have different limitation of high impedance fault value. Similar approach as shown in this section could be applied to determine the maximum fault impedance.

5.3.5. Overall Comparison Between SD and AAD Techniques

The performance of SD and AAD can be analysed in terms of reliability, computational time and the accuracy in identifying the actual faulty section in the first rank. The following summarised the comparisons for each technique:

- **Reliability**

  The reliability of the proposed method can be evaluated based on the maximum number of attempts to trace the actual fault location. From the test results, it can be observed that both techniques are reliable in estimating the possible faulty sections. This can be seen in the test results, whereby the actual faulty section

can be found within five possible faulty sections. Nevertheless, the AAD technique is more reliable as compared to the SD technique. This is because, the SD technique requires at least five estimations of the faulty section candidate before the actual faulty section can be identified. Whereas, the AAD technique only requires three possible faulty sections to be estimated for fault finding.

- **Computational time**

  In order to estimate the faulty section, the proposed methods have to extract important features from the measured three-phase voltage signal using MRA-DWT. After extracting the detail coefficients, the proposed algorithm is used to estimate all possible faulty sections. Generally, there will be 34 possible faulty sections because there are 34 line sections of the tested underground distribution system. AAD and SD techniques are compared based on the time taken to analyse the voltage signal and list out all the possible faulty sections. Using the same database and tested signal, it has been observed that the time taken by SD is shorter than AAD to estimate all possible faulty section candidates. It is important to estimate and rank all possible faulty sections immediately before the faulty cable can be checked and repaired in order to expedite the restoration process of the power system.

- **Accuracy**

  The effectiveness of the proposed method can be measured based on the accuracy of the proposed method to successfully identify the actual faulty section in the first attempt (first rank of possible faulty section that is estimated). This is crucial because, if the first inspected line section is found healthy, the next line section has to be checked until the actual faulty section is identified. This will consume a lot of time and energy. Therefore, an effective method must have the capability to accurately identify the actual faulty section in the first

rank candidate, so that fast power system restoration can be achieved. From the analysis, it has been observed that AAD technique has a higher degree of accuracy as compared to SD technique.

5.3.6. Summary

This research proposes two techniques for identifying the faulty section. First is the shortest distance (SD) and the second is average of absolute difference (AAD) techniques. Both techniques have provided an excellent result for identifying the fault location in the underground distribution system.

Based on the observation, it can be seen that AAD technique is more superior than SD technique in terms of reliability and accuracy. Therefore, the proposed AAD technique is more effective and suitable to be implemented for locating the fault in underground distribution system. Although SD technique yields a poor estimation compared to AAD technique, however it still provides good result in identifying the faulty section. In some test sections, SD technique provides a magnificent performance, because the actual faulty section can be found quickly in the first rank candidate. It can be concluded that, regardless of fault impedance values, both techniques can successfully estimate the possible faulty section.

However, both techniques require a reliable and accurate database in order to give good performance in estimating the possible faulty sections. Also, the proposed techniques will not work accurately when the occurring fault value is not in the range of database fault value. Furthermore, the proposed methods give poor performance when analysing the Low Impedance Fault (LIF) phenomenon.

CHAPTER 6

CONCLUSION AND FUTURE WORK

6.1. Conclusion

In this research, the fault location of High Impedance Fault (HIF) in an underground distribution system was successfully estimated using Multi Resolution Analysis - Discrete Wavelet Transform (MRA-DWT) and a predefined database containing faulty cases. MRA-DWT work effectively in extracting important features from the three-phase voltage signal, obtained at the primary substation. Three levels of detail coefficients were extracted from two full cycles of post disturbance voltage signal in order to give more input data which can lead to better performance in estimating the faulty section.

In his work, the database approach was utilised to determine the faulty section in the radial distribution system having several lateral. In database approach, the extracted features of the actual voltage signal were matched with the stored features of simulated one to determine the possible faulty section. Two different techniques were proposed in this research, namely the Shortest Distance (SD) technique and the Average of Absolute Difference (AAD) technique to estimate the possible faulty section.

In AAD approach, the extracted features from MRA-DWT were applied as an input data for the proposed technique to be compared against sets of stored features in the database. Whereas in SD approach, the extracted features will be used to calculate the distance between the measured point perpendicular to a straight line. The straight line represents the line section between two adjacent nodes where the features are stored in

the database. For both techniques, several possible faulty sections could be found due to the complexity of the distribution network such as non-homogenous cable, lateral network, HIF and a single measurement point. In order to determine the sequence of line section to be inspected first, all the possible faulty sections are ranked. The ranking is based on the matching value of the proposed algorithm with the smallest value is ranked as the first.

From the test results, it is shown that most of the faulty section can be located correctly in the first rank. However, there are a few faulty sections found in the second or third ranked sections and less than 4 test sections are located in the fourth or fifth ranked. AAD technique was found to be more accurate than SD technique for locating the actual faulty section in the first rank sections. It is also observed that SD technique requires five possible faulty sections to be inspected in order to trace the actual location of HIF occurrence. Whereas, AAD technique only requires three possible faulty section candidates. The actual location of HIF can only be confirmed by physical inspection at the suspected location. In summary, the proposed method is a simple algorithm to identify the underground cable fault location accurately and with less computational time. Furthermore, the method is inexpensive for practical application since it requires single measurement at the primary substation.

6.2. Future Work

There are some suggestions which can be made to improve the proposed HIF location technique. The following are the suggestions:

- Hybrid technique

  In order to reduce the computational time and to achieve a more accurate result, SD and AAD techniques can be combined as a hybrid technique. In the first step, SD technique will be used to determine the possible faulty section. The reason of using the SD technique is because it has shorter computational time than AAD technique. Once, the possible faulty sections have been identified, AAD technique will be used to rank the selected sections. AAD technique is used in the ranking because it produces more accurate result as compared to SD technique. Through this hybrid technique, it is expected more accurate result will be produced with a minimum computation time.

- Signal processing method

  In these proposed methods, wavelet transform was utilized to analyse the whole cycle of the voltage signal. However, it was observed that when a fault occurs, it only affects a certain part of the voltage signal where there will be a slight fluctuation. Also, the fault may not occur at the beginning of the voltage cycle. Therefore, it will be more effective to analyse only part of the voltage signal in which the fault is occurring. In order to do this, the voltage signal is analysed using the discrete wavelet transform to extract the detail coefficients. From the detail coefficients, the starting point of an anomaly due to the occurrence of HIF on the voltage signal can be identified. Then, the specific part of the voltage signal containing the anomaly is analysed again using another type of digital

signal processing. For that purpose, Short Time Fourier Transform (STFT) method is suggested to be used due to its capability to analyse a small part of the voltage signal separately.

Beside improving the accuracy in identifying the faulty section, it is also possible to calculate the fault distance between the measurement point to the point of fault. By doing this, it might reduce the time in pinpointing the exact location of the fault.

REFERENCES

Abdel Aziz, M. S., Hassan, M. A. M., & El-Zahab, E. A. (2012). An Artificial Intelligence Based Approach for High Impedance Faults Analysis in Distribution Networks (pp. 44-59): IGI Global.

Adamiak, M., Wester, C., Thakur, M., & Jensen, C. (April 2006). High impedance fault detection on distribution feeders. *Protection and Control Journal*.

Aggarwal, R. K., Aslan, Y., & Johns, A. T. (1997). New concept in fault location for overhead distribution systems using superimposed components. *IEE Proceedings-Generation, Transmission and Distribution, 144*(3), 309-316. doi: 10.1049/ip-gtd:19971137

Akorede, M. F., & Katende, J. (2010). Wavelet Transform Based Algorithm for High-Impedance Faults Detection in Distribution Feeders. *European Journal of Scientific Research, 41*(2), pp.238-248.

Ancell, G. B., & Pahalawaththa, N. C. (1994). Maximum likelihoo d estimation of fault location on transmission lines using travelling waves. *IEEE Transactions on Power Delivery, 9*(2), 680-689. doi: 10.1109/61.296245

Avdakovic, S., Nuhanovic, A., Kusljugic, M., & Music, M. (2012). Wavelet transform applications in power system dynamics. *Electric Power Systems Research, 83*(1), 237-245. doi: 10.1016/j.epsr.2010.11.031

Bansal, A., & Pillai, G. N. (2007). High impedance fault detection using LVQ neural networks. *International Journal of Computer, Information, Systems Science, and Engineering, 1*(3), pp. 148–152.

Bernadić, A., & Leonowicz, Z. (2012). Fault location in power networks with mixed feeders using the complex space-phasor and Hilbert–Huang transform. *International Journal of Electrical Power and Energy Systems, 42*(1), 208-219. doi: 10.1016/j.ijepes.2012.04.012

Bhalja, B., & Maheshwari, R. P. (2008). Wavelet-based Fault Classification Scheme for a Transmission Line Using a Support Vector Machine. *Electric Power Components and Systems, 36*(10), 1017-1030. doi: 10.1080/15325000802046496

Bo, Z. Q., Weller, G., & Redfern, M. A. (1999). Accurate fault location technique for distribution system using fault-generated high-frequency transient voltage signals. *IEE Proceedings-Generation, Transmission and Distribution, 146*(1), 73-79. doi: 10.1049/ip-gtd:19990074

Bretas, A. S., Moreto, M., Salim, R. H., & Pires, L. O. (2006, 15-18 Aug. 2006). *A Novel High Impedance Fault Location for Distribution Systems Considering Distributed Generation.* Paper presented at the Transmission & Distribution Conference and Exposition: Latin America, 2006. TDC '06. IEEE/PES.

Briassouli, A., Matsiki, D., & Kompatsiaris, I. (2010). Continuous wavelet transform for time-varying motion extraction. *IET Transactions on Image Processing, 4*(4), 271-282. doi: 10.1049/iet-ipr.2008.0253

Cardoso, G., Jr., Rolim, J. G., & Zurn, H. H. (2004). Application of neural-network modules to electric power system fault section estimation. *IEEE Transactions on Power Delivery, 19*(3), 1034-1041. doi: 10.1109/tpwrd.2004.829911

Chanda, D., Kishore, N. K., & Sinha, A. K. (2003). A wavelet multiresolution analysis for location of faults on transmission lines. *International Journal of Electrical Power and Energy Systems, 25*(1), 59-69. doi: 10.1016/s0142-0615(02)00021-2

Cnockaert, L., Migeotte, P. F., Daubigny, L., Prisk, G. K., Grenez, F., & Sa, R. C. (2008). A Method for the Analysis of Respiratory Sinus Arrhythmia Using Continuous Wavelet Transforms. *IEEE Transactions on Biomedical Engineering, 55*(5), 1640-1642. doi: 10.1109/tbme.2008.918576

Dilokratanatrakool, C., Na Ayudhya, P. N., Chayavanich, T., & Prapanavarat, C. (2003, 8-13 Oct. 2003). *Automatic detection-localization of fault point on waveform and classification of power quality disturbance waveshape fault using wavelet and neural network.* Paper presented at the IEEE Proceedings International Conference on Robotics, Intelligent Systems and Signal Processing, 2003.

Dutra, C. A., Matos, R. R., Zimath, S. L., Oliveira, J. P. d., Resende, J. H. M. d., & Moutinho, J. A. P. Fault Location by Traveling Waves: Application in High Impedance Events

Dwivedi, U. D., Singh, S. N., & Srivastava, S. C. (2008, 11-13 Dec. 2008). *A wavelet based approach for classification and location of faults in distribution systems.* Paper presented at the Annual IEEE India Conference, INDICON 2008.

El-Hami, M., Lai, L. L., Daruvala, D. J., & Johns, A. T. (1992). A new travelling-wave based scheme for fault detection on overhead power distribution feeders. *IEEE Transactions on Power Delivery, 7*(4), 1825-1833. doi: 10.1109/61.156985

Elkalashy, N. I., Lehtonen, M., Darwish, H. A., Taalab, A. M. I., & Izzularab, M. A. (2007). DWT-based extraction of residual currents throughout unearthed MV networks for detecting high-impedance faults due to leaning trees. *European Transactions on Electrical Power, 17*(6), 597-614.

Elkalashy, N. I., Lehtonen, M., Darwish, H. A., Taalab, A. M. I., & Izzularab, M. A. (2008a). DWT-Based Detection and Transient Power Direction-Based Location of High-Impedance Faults Due to Leaning Trees in Unearthed MV Networks. *IEEE Transactions on Power Delivery, 23*(1), 94-101. doi: 10.1109/tpwrd.2007.911168

Elkalashy, N. I., Lehtonen, M., Darwish, H. A., Taalab, A. M. I., & Izzularab, M. A. (2008b). A novel selectivity technique for high impedance arcing fault detection in compensated MV networks. *European Transactions on Electrical Power, 18*(4), 344-363.

Elkalashy, N. I., Lehtonen, M., Darwish, H. A., Taalab, A. M. I., & Izzularab, M. A. (2008c, 17-20 March 2008). *Verification of DWT-Based Detection of High Impedance Faults in MV Networks.* Paper presented at the IET 9th International Conference on Developments in Power System Protection, DPSP 2008.

Etemadi, A. H., & Sanaye-Pasand, M. (2008). High-impedance fault detection using multi-resolution signal decomposition and adaptive neural fuzzy inference system. *IET Transactions on Generation, Transmission & Distribution, 2*(1), 110-118. doi: 10.1049/iet-gtd:20070120

Filomena, A. D., Resener, M., Salim, R. H., & Bretas, A. S. (2009). Fault location for underground distribution feeders: An extended impedance-based formulation with capacitive current compensation. *International Journal of Electrical Power and Energy Systems, 31*(9), 489-496. doi: 10.1016/j.ijepes.2009.03.026

Final report of the CIRED Working Group WG03 Fault Management, 'Fault management in electrical distribution systems'. (pp. www.cired.be/WG03-Final%20Report.pdf).

Gale, P. F., Stokoe, J., & Crossley, P. A. (1997, 25-27 Mar 1997). *Practical experience with travelling wave fault locators on Scottish Power's 275 and 400kV transmission system.* Paper presented at the Sixth International Conference on Developments in Power System Protection, (Conf. Publ. No. 434).

Gaouda, A. M., Salama, M. M. A., Sultan, M. R., & Chikhani, A. Y. (1999). Power quality detection and classification using wavelet-multiresolution signal decomposition. *IEEE Transactions on Power Delivery, 14*(4), 1469-1476. doi: 10.1109/61.796242

Garcia-Santander, L., Bastard, P., Petit, M., Gal, I., Lopez, E., & Opazo, H. (2005). Down-conductor fault detection and location via a voltage based method for radial distribution networks. *IEE Proceedings-Generation, Transmission and Distribution, 152*(2), 180-184. doi: 10.1049/ip-gtd:20041300

Girgis, A. A., Fallon, C. M., & Lubkeman, D. L. (1993). A fault location technique for rural distribution feeders. *IEEE Transactions on Industry Applications, 29*(6), 1170-1175. doi: 10.1109/28.259729

Girgis, A. A., Hart, D. G., & Peterson, W. L. (1992). A new fault location technique for two- and three-terminal lines. *IEEE Transactions on Power Delivery, 7*(1), 98-107. doi: 10.1109/61.108895

Glinkowski, M. T., & Wang, N. C. (1995). ANNs pinpoint underground distribution faults. *IEEE Transactions on Computer Applications in Power, 8*(4), 31-34. doi: 10.1109/67.468291

Gohokar, V. N., & Khedkar, M. K. (2005). Faults locations in automated distribution system. *Electric Power Systems Research, 75*(1), 51-55. doi: 10.1016/j.epsr.2005.01.003

Haghifam, M. R., Sedighi, A. R., & Malik, O. P. (2006). Development of a fuzzy inference system based on genetic algorithm for high-impedance fault detection. *IEE Proceedings-Generation, Transmission and Distribution, 153*(3), 359-367. doi: 10.1049/ip-gtd:20045224

Hizman, H., Crossley, P. A., Gale, P. F., & Bryson, G. (2002, 25-25 July 2002). *Fault section identification and location on a distribution feeder using travelling waves.* Paper presented at the 2002 IEEE Power Engineering Society Summer Meeting.

Hulzink, J., Konijnenburg, M., Ashouei, M., Breeschoten, A., Berset, T., Huisken, J., Stuyt, J., de Groot, H., Barat, F., David, J., & Van Ginderdeuren, J. (2011). An Ultra Low Energy Biomedical Signal Processing System Operating at Near-Threshold. *IEEE Transactions on Biomedical Circuits and Systems, 5*(6), 546-554. doi: 10.1109/tbcas.2011.2176726

Ibe, A. O., & Cory, B. J. (1986). A Travelling Wave-Based Fault Locator for Two- and Three-Terminal Networks. *IEEE Transactions on Power Delivery, 1*(2), 283-288. doi: 10.1109/tpwrd.1986.4307961

IEEE Guide for Determining Fault Location on AC Transmission and Distribution Lines. (2005). *IEEE Std C37.114-2004*, 1-36. doi: 10.1109/ieeestd.2005.96207

Jarventausta, P., Verho, P., & Partanen, J. (1994). Using fuzzy sets to model the uncertainty in the fault location process of distribution networks. *IEEE Transactions on Power Delivery, 9*(2), 954-960. doi: 10.1109/61.296278

Jensen, K. J., Munk, S. M., & Sorensen, J. A. (1998, 12-15 May 1998). *Feature extraction method for high impedance ground fault localization in radial power distribution networks.* Paper presented at the Proceedings of the 1998 IEEE International Conference on Acoustics, Speech and Signal Processing.

John Tengdin, C., Ron Westfall, V. C., & Kevin Stephan, S. (1996). High Impedance Fault Detection Technology Report of PSRC Working Group D15.

Johns, A. T., Lai, L. L., El-Hami, M., & Daruvala, D. J. (1991). New approach to directional fault location for overhead power distribution feeders. *IEEE Proceedings on Generation, Transmission and Distribution, 138*(4), 351-357.

Jung, C. K., Kim, K. H., Lee, J. B., & Klöckl, B. (2007). Wavelet and neuro-fuzzy based fault location for combined transmission systems. *International Journal of Electrical Power and Energy Systems, 29*(6), 445-454. doi: 10.1016/j.ijepes.2006.11.003

Kejun, M., Rovnyak, S. M., & Chee-Mun, O. (2006, 0-0 0). *Dynamic event detection using wavelet analysis.* Paper presented at the IEEE Power Engineering Society General Meeting, 2006.

Krajnak, D. J. (2000, 2000). *Faulted circuit indicators and system reliability.* Paper presented at the Rural Electric Power Conference, 2000.

Kumano, S., Ito, N., Goda, T., Uekubo, Y., Kyomoto, S., Kourogi, H., & Ariura, Y. (1993). Development of expert system for operation at substation. *IEEE Transactions on Power Delivery, 8*(1), 56-65. doi: 10.1109/61.180319

Lai, T. M., Snider, L. A., Lo, E., & Sutanto, D. (2005). High-impedance fault detection using discrete wavelet transform and frequency range and RMS conversion. *IEEE Transactions on Power Delivery, 20*(1), 397-407. doi: 10.1109/tpwrd.2004.837836(410) 2

Lee, H., & Mousa, A. M. (1996). GPS travelling wave fault locator systems: investigation into the anomalous measurements related to lightning strikes. *IEEE Transactions on Power Delivery, 11*(3), 1214-1223. doi: 10.1109/61.517474

Li, H., Mokhar, A. S., & Jenkins, N. (2005). Automatic fault location on distribution network using voltage sags measurements. *IEEE Conference Publications, 2005*(CP504), v3-98-v93-98.

Magnago, F. H., & Abur, A. (1999, 18-22 Jul 1999). *A new fault location technique for radial distribution systems based on high frequency signals.* Paper presented at the IEEE Power Engineering Society Summer Meeting, 1999.

Mahmoud, G., Doaa khalil, I., & El Sayed Tag, E. (2007). Traveling-Wave-Based Fault-Location Scheme for Multiend-Aged Underground Cable System. *IEEE Transactions on Power Delivery, 22*(1), 82-89. doi: 10.1109/tpwrd.2006.881439

Martin, F., & Aguado, J. A. (2003). Wavelet-based ANN approach for transmission line protection. *IEEE Transactions on Power Delivery, 18*(4), 1572-1574. doi: 10.1109/tpwrd.2003.817523

Martinez, E. M., & Richards, E. F. (1991, 28-30 Apr 1991). *An expert system to assist distribution dispatchers in the location of system outages.* Paper presented at the 35th Annual Conference of Rural Electric Power Conference, 1991.

Michalik, M., Lukowicz, M., Rebizant, W., Seung-Jae, L., & Sang-Hee, K. (2007). Verification of the Wavelet-Based HIF Detecting Algorithm Performance in Solidly Grounded MV Networks. *IEEE Transactions on Power Delivery, 22*(4), 2057-2064. doi: 10.1109/tpwrd.2007.905283

Michalik, M., Rebizant, W., Lukowicz, M., Seung-Jae, L., & Sang-Hee, K. (2006). High-impedance fault detection in distribution networks with use of wavelet-based algorithm. *IEEE Transactions on Power Delivery, 21*(4), 1793-1802. doi: 10.1109/tpwrd.2006.874581

Mohamed, S. S., El-Saadany, E. F., Abdel-Galil, T. K., & Salama, M. M. A. (2003, 27-30 Dec. 2003). *ANN-based technique for fault location estimation using TLS-ESPRIT.* Paper presented at the IEEE 46th Midwest Symposium on Circuits and Systems, 2003.

Mokhlis, H., Li, H. Y., & Khalid, A. R. (2010). The application of voltage sags pattern to locate a faulted section in distribution network. *International Review of Electrical Engineering, 5*(1), 173-179.

Mokhlis, H., Li, H. Y., Mohamad, H., & Bakar, A. H. A. (2010). A comprehensive fault location estimation using voltage sag profile for non-homogenous distribution networks. *International Review of Electrical Engineering, 5*(5), 2310-2316.

Mokhlis, H., Mohamad, H., Bakar, A. H. A., & Li, H. Y. (2011). Evaluation of fault location based on voltage sags profiles: A study on the influence of voltage sags patterns. *International Review of Electrical Engineering, 6*(2), 874-880.

Mokhlis, H., Mohamad, H., Li, H., & Bakar, A. H. A. (2011). Voltage Sags Matching to Locate Faults for Underground Distribution Networks. *Advances in Electrical and Computer Engineering, 11*(2), pp. 43-48. doi: 10.4316/AECE.2011.02007

Nath, S., Sinha, P., & Goswami, S. K. (2012). A wavelet based novel method for the detection of harmonic sources in power systems. *International Journal of Electrical Power and Energy Systems, 40*(1), 54-61. doi: 10.1016/j.ijepes.2012.02.005

Novosel, D., Hart, D. G., Udren, E., & Garitty, J. (1996). Unsynchronized two-terminal fault location estimation. *IEEE Transactions on Power Delivery, 11*(1), 130-138. doi: 10.1109/61.484009

Pinnegar, C. R., & Mansinha, L. (2003). A method of time–time analysis: The TT-transform. *Digital Signal Processing, 13*(4), 588-603. doi: 10.1016/s1051-2004(03)00022-8

Poisson, O., Rioual, P., & Meunier, M. (2000). Detection and measurement of power quality disturbances using wavelet transform. *IEEE Transactions on Power Delivery, 15*(3), 1039-1044. doi: 10.1109/61.871372

S. Nath, A. D., A. Chakrabarti. (2009). Detection of power quality disturbances using wavelet transform. *World Academy of Science Engineering and Technology, 49*, pp. 869-873.

Samantaray, S. R., Panigrahi, B. K., & Dash, P. K. (2008). High impedance fault detection in power distribution networks using time-frequency transform and probabilistic neural network. *IET Transactions on Generation, Transmission & Distribution, 2*(2), 261-270. doi: 10.1049/iet-gtd:20070319

Santoso, S., Dugan, R. C., Lamoree, J., & Sundaram, A. (2000, 2000). *Distance estimation technique for single line-to-ground faults in a radial distribution system.* Paper presented at the IEEE Power Engineering Society Winter Meeting, 2000.

Sarlak, M., & Shahrtash, S. M. (2011). High impedance fault detection using combination of multi-layer perceptron neural networks based on multi-resolution morphological gradient features of current waveform. *IET Transactions on Generation, Transmission & Distribution. 5*(5), 588-595. doi: 10.1049/iet-gtd.2010.070

Sidhu, T. S., & Zhihan, X. (2010). Detection of Incipient Faults in Distribution Underground Cables. *IEEE Transactions on Power Delivery, 25*(3), 1363-1371. doi: 10.1109/tpwrd.2010.2041373

Spoor, D., & Jian Guo, Z. (2006). Improved single-ended traveling-wave fault-location algorithm based on experience with conventional substation transducers. *IEEE Transactions on Power Delivery, 21*(3), 1714-1720. doi: 10.1109/tpwrd.2006.878091

Stockwell, R. G., Mansinha, L., & Lowe, R. P. (1996). Localization of the complex spectrum: the S transform. *IEEE Transactions on Signal Processing, 44*(4), 998-1001. doi: 10.1109/78.492555

Takagi, T., Yamakoshi, Y., Yamaura, M., Kondow, R., & Matsushima, T. (1982). Development of a New Type Fault Locator Using the One-Terminal Voltage and Current Data. *IEEE Transactions on Power Apparatus and Systems, PAS-101*(8), 2892-2898. doi: 10.1109/tpas.1982.317615

Tria, M., Ovarlez, J. P., Vignaud, L., Castelli, J. C., & Benidir, M. (2007). Discriminating real objects in radar imaging by exploiting the squared modulus of the continuous wavelet transform. *IET Transactions on Radar, Sonar & Navigation, , 1*(1), 27-37. doi: 10.1049/iet-rsn:20050124

Uriarte, F. M., & Centeno, V. (2005, 23-25 Oct. 2005). *High-impedance fault detection and localization in distribution feeders with microprocessor based devices.* Paper presented at the Proceedings of the 37th Annual North American Power Symposium, 2005.

Vazquez, E., Castruita, J., Chacon, O. L., & Conde, A. (2007). A New Approach Traveling-Wave Distance Protection - Part I: Algorithm. *IEEE Transactions on Power Delivery, 22*(2), 795-800. doi: 10.1109/tpwrd.2007.893376

Wavelet guide. Available at http://www.polyvalens.com/blog/?page_id=15 [assessed on 13-09-2012].

Wavelet Transform. Available at: MATLAB Toolbox.

Wen-Hui, C., Chih-Wen, L., & Men-Shen, T. (2000). On-line fault diagnosis of distribution substations using hybrid cause-effect network and fuzzy rule-based method. *IEEE Transactions on Power Delivery, 15*(2), 710-717. doi: 10.1109/61.853009

Wen, F., & Han, Z. (1995). Fault section estimation in power systems using a genetic algorithm. *Electric Power Systems Research, 34*(3), 165-172. doi: 10.1016/0378-7796(95)00974-6

Wenzhong, G., & Jiaxin, N. (2011). Wavelet-Based Disturbance Analysis for Power System Wide-Area Monitoring. *IEEE Transactions on Smart Grid, , 2*(1), 121-130. doi: 10.1109/tsg.2011.2106521

Ying-Hong, L., Chih-Wen, L., & Chi-Shan, Y. (2002). A new fault locator for three-terminal transmission lines using two-terminal synchronized voltage and current phasors. *IEEE Transactions on Power Delivery, 17*(2), 452-459. doi: 10.1109/61.997917

Yuan-Yih, H., Lu, F. C., Chien, Y., Liu, J. P., Lin, J. T., Yu, P. H. S., & Kuo, R. R. T. (1991). An expert system for locating distribution system faults. *IEEE Transactions on Power Delivery, 6*(1), 366-372. doi: 10.1109/61.103760

Zadeh, H. K. (2005). An ANN-Based High Impedance Fault Detection Scheme: Design and Implementation. *International Journal of Emerging Electric Power Systems, 4*(2). doi: http://dx.doi.org/10.2202/1553-779X.1046

Zeng, X., Li, K. K., Liu, Z., & Yin, X. (2004, 3-7 Oct. 2004). *Fault location using traveling wave for power networks.* Paper presented at the 39th IAS Annual Meeting of Industry Applications Conference, 2004.

LIST OF PUBLICATIONS

Ali, M.S. ; Bakar, A.H.A. ; Mokhlis, H. ; Aroff, H. ; Illias, H.A. ; Aman, M.M. "High Impedance Fault Localization in a Distribution Network Using the Discrete Wavelet Transform", *2012 IEEE International Power Engineering and Optimization Conference*, *PEOCO2012* Melaka, Malaysia, 6-7 June 2012, pp. 349 – 354, doi : 10.1109/PEOCO.2012.6230888 [ISBN: 978-1-4673-0660-7]

Ali, M.S. ; Bakar, A.H.A. ; Mokhlis, H. ; Aroff, H. ; Illias, H.A. "Wavelet-Based and Database Approach for Locating Faulty Section of High Impedance Fault in a Distribution System", *Przegląd Elektrotechniczny*, vol : 01a/2013, [ISSN 0033-2097]

Ali, M.S. ; Bakar, A.H.A. ; Mokhlis, H. ; Aroff, H. ; Illias, H.A. "High Impedance Fault Location Using Matching Technique and Wavelet Transform for Underground Cable Distribution Network", *The Institute of Electrical Engineers of Japan, IEEJ* [Accepted]

A.H.A. Bakar, M.S. Ali, H. Mokhlis, H. Arof, H. A. Illias, "Cable Fault Location for High Impedance Fault in 11kV Underground Distribution System" *International Journal of Electrical Power & Energy Systems, IJEPES*. [Under review]

APPENDICES

A.1 Parameters for typical distribution system in Malaysia

A.1.1 Line data of radial distribution network

Section	Node		Length (km)	Type of Cable
	From	To		
Main line				
	2	3	0.5	A11UG300
1	3	4	1.254	A11UG300
2	4	14	1.29	A11UG185
3	14	17	0.5	A11UG185
4	17	18	0.5	A11UG185
5	18	19	0.25	A11UG300
6	14	15	0.395	A11UG185
7	15	16	0.51	A11UG185
8	4	5	0.14	A11UG185
9	5	6	0.4	A11UG185
10	6	7	0.35	A11UG185
11	7	12	0.3	A11UG300
12	12	13	0.75	A11UG300
13	7	8	0.2	A11UG300
14	8	9	0.5	A11UG300
15	9	10	0.27	A11UG300
16	10	11	0.5	A11UG300
	2	20	5	A11UG300
17	20	34	0.5	A11UG240X
18	34	35	0.473	A11UG185
19	35	36	1.3	A11UG300
20	36	37	0.3	A11UG300
21	37	38	0.5	A11UG300
22	20	21	0.04	A11UG240X
23	21	22	0.884	A11UG185
24	22	23	0.54	A11UG185
25	23	24	0.716	A11UG240X
26	24	25	0.9	A11UG185
27	24	26	0.1	A11UG150X
28	26	27	0.5	A11UG185
29	27	28	0.723	A11UG185
30	28	29	0.45	A11UG185
31	27	30	0.594	A11UG185
32	30	31	0.908	A11UG185
33	31	32	0.5	A11UG185
34	32	33	0.5	A11UG185

A.1.2 Cable parameter

Type Of Cable	Positive Sequence (p.u/km)		Zero Sequence (p.u/km)	
	R	X	R	X
A11UG300	0.12	0.0787	1.779	0.0396
A11UG185	0.195	0.0829	2.39	0.0406
A11UG240X	0.1609	0.1524	0.1814	0.0312
A11UG150X	0.2645	0.1603	0.2960	0.0352

A.1.3 Loads parameters and the equivalent impedance

Node	P (kW)	P (kW/phase)	Q (kVar)	Q (kVar/phase)	Equivalent Impedance/ phase	
					R (ohm)	X (H)
2	1028.5710	342.8570	637.4510	212.4837	97.7642	0.5021
3	3.3460	1.1153	2.2050	0.7350	32791.2373	158.3686
4	370.0600	123.3533	243.8750	81.2917	296.5029	1.4319
5	40.8630	13.6210	26.9290	8.9763	2685.1200	12.9678
6	40.8630	13.6210	26.9290	8.9763	2685.1200	12.9678
7	81.7260	27.2420	53.8590	17.9530	1342.5948	6.4840
8	81.7260	27.2420	53.8590	17.9530	1342.5948	6.4840
9	81.7260	27.2420	53.8590	17.9530	1342.5948	6.4840
10	40.8630	13.6210	26.9290	8.9763	2685.1200	12.9678
11	40.8630	13.6210	26.9290	8.9763	2685.1200	12.9678
12	81.7260	27.2420	53.8590	17.9530	1342.5948	6.4840
13	71.5100	23.8367	47.1270	15.7090	1534.4239	7.4103
14	30.6470	10.2157	20.1970	6.7323	3580.2917	17.2907
15	30.6470	10.2157	20.1970	6.7323	3580.2917	17.2907
16	40.8630	13.6210	26.9290	8.9763	2685.1200	12.9678
17	40.8630	13.6210	26.9290	8.9763	2685.1200	12.9678
18	81.7260	27.2420	53.8590	17.9530	1342.5948	6.4840
19	40.8630	13.6210	26.9290	8.9763	2685.1200	12.9678
20	Switching Station					
21	2.715	0.9050	1.741	0.5803	38890.9977	193.0252
22	4.525	1.5083	2.902	0.9673	23338.3976	115.8207
23	9.05	3.0167	5.804	1.9347	11669.1988	57.9103
24	9.05	3.0167	5.804	1.9347	11669.1988	57.9103
25	6.787	2.2623	4.353	1.4510	15561.7025	77.2218
26	894.427	298.1423	573.63	191.2100	118.0745	0.5860
27	0.25	0.0833	0.125	0.0417	289895.1761	1845.2907
28	0.5	0.1667	0.249	0.0830	144020.2981	920.4245
29	0.25	0.0833	0.125	0.0417	289895.1761	1845.2907
30	0.375	0.1250	0.187	0.0623	192439.0813	1228.2217
31	0.375	0.1250	0.187	0.0623	192439.0813	1228.2217
32	3.072	1.0240	2.094	0.6980	37420.6759	174.7230
33	3.072	1.0240	2.094	0.6980	37420.6759	174.7230
34	199.636	66.5453	128.034	42.6780	529.0072	2.6252
35	149.727	49.9090	96.026	32.0087	705.3481	3.5003
36	199.636	66.5453	128.034	42.6780	529.0072	2.6252
37	199.636	66.5453	128.034	42.6780	529.0072	2.6252
38	199.636	66.5453	128.034	42.6780	529.0072	2.6252

A.1.4 Source data

Source 132kV 50Hz

MVA Base 100

A.1.5 Transformer Delta-Wye

30 MVA

132/11kV

$R^+ = 0.01040$ p.u.

$X^+ = 0.09940$ p.u.

Ground Resistance 4Ω

APPENDIX B. Test results of fault at midpoint section

B.1 Shortest Distance technique

B.1.1 Test results of single line to ground fault (phase A to ground fault)

Section	Rank number of the actual faulty section					
	45 ohm	55 ohm	65 ohm	75 ohm	85 ohm	95 ohm
1	1	1	1	1	1	1
2	1	1	1	1	1	1
3	3	5	2	2	2	2
4	1	2	2	4	4	3
5	1	1	1	1	2	2
6	4	3	3	1	1	1
7	1	1	1	2	2	2
8	2	4	5	5	4	2
9	2	3	2	2	3	3
10	2	2	3	3	3	5
11	2	2	4	1	2	2
12	1	1	2	1	1	1
13	5	5	1	3	5	5
14	5	3	4	3	4	4
15	4	4	5	4	1	1
16	1	1	2	1	1	2
17	1	1	1	1	1	1
18	2	2	2	2	2	2
19	1	1	1	1	1	1
20	1	1	1	1	1	2
21	1	2	2	3	3	3
22	2	2	2	3	4	5
23	1	1	3	3	4	4
24	3	2	2	2	2	2
25	2	2	1	1	1	1
26	1	1	1	1	3	1
27	4	4	2	2	4	4
28	4	2	1	1	1	1
29	2	2	3	3	2	1
30	1	1	1	1	1	1
31	3	2	2	2	2	2
32	2	2	2	2	1	1
33	1	2	2	2	2	2
34	1	3	3	3	3	2

B.1.2 Test results of three phase fault (phase A-B-C fault)

Section	Rank number of the actual faulty section					
	45 ohm	55 ohm	65 ohm	75 ohm	85 ohm	95 ohm
1	1	1	1	1	1	1
2	5	5	4	1	1	2
3	1	1	2	2	2	2
4	2	2	2	2	3	2
5	3	3	3	3	3	3
6	2	2	2	2	2	3
7	3	2	2	1	1	1
8	2	2	3	3	1	1
9	3	3	2	1	1	1
10	2	2	1	1	1	1
11	1	1	1	3	4	4
12	1	2	2	2	2	2
13	1	2	3	5	5	5
14	3	2	2	5	5	5
15	4	3	2	1	1	1
16	1	2	2	1	1	1
17	1	1	1	1	1	1
18	2	2	2	2	1	1
19	1	1	1	1	1	2
20	2	2	1	2	1	1
21	3	3	3	3	3	3
22	2	2	2	2	2	2
23	2	1	1	1	1	1
24	2	1	1	1	1	1
25	1	1	1	1	1	1
26	3	4	4	3	4	4
27	2	2	1	1	2	2
28	1	1	1	1	1	1
29	1	1	2	3	3	3
30	4	3	4	4	4	3
31	3	2	2	1	1	1
32	2	1	2	2	2	2
33	2	2	1	1	1	2
34	4	3	4	3	3	3

B.1.3 Test results of double line to ground fault (phase B-C to ground fault)

Section	Rank number of the actual faulty section					
	45 ohm	55 ohm	65 ohm	75 ohm	85 ohm	95 ohm
1	1	1	1	1	1	1
2	1	1	1	1	1	1
3	1	2	2	2	1	1
4	1	1	1	1	1	1
5	2	1	1	1	1	1
6	2	1	1	1	1	1
7	1	1	1	1	1	1
8	3	3	5	4	3	2
9	3	3	3	3	2	1
10	4	2	2	2	2	2
11	1	1	2	2	2	1
12	2	1	1	1	1	1
13	5	5	3	3	4	3
14	3	3	3	1	1	1
15	1	1	2	2	2	3
16	2	2	1	1	1	1
17	1	1	1	1	1	1
18	1	1	1	1	1	1
19	1	1	1	1	1	1
20	1	1	1	1	1	1
21	2	2	2	2	1	1
22	3	2	2	2	2	2
23	1	1	1	1	1	1
24	1	1	1	1	1	1
25	1	1	1	1	1	1
26	1	1	1	1	1	1
27	4	4	3	2	2	2
28	2	1	1	1	1	1
29	1	1	1	1	1	1
30	1	1	1	1	1	1
31	2	1	1	1	1	1
32	1	1	1	1	1	1
33	2	1	1	1	1	1
34	1	1	1	1	1	1

B.1.4 Test results of line to line fault (phase B-C fault)

Section	Rank number of the actual faulty section					
	45 ohm	55 ohm	65 ohm	75 ohm	85 ohm	95 ohm
1	1	1	1	1	1	1
2	5	5	5	4	3	2
3	4	3	2	1	1	1
4	1	1	1	2	1	1
5	1	1	1	1	2	2
6	1	1	1	1	1	1
7	1	1	1	1	2	1
8	2	2	1	1	1	1
9	3	2	2	2	1	1
10	2	1	3	3	2	1
11	1	1	1	2	4	4
12	1	1	1	1	1	1
13	2	2	2	3	2	1
14	1	1	1	1	1	1
15	1	1	1	1	1	1
16	1	1	1	1	2	2
17	1	1	1	1	1	1
18	3	2	1	1	1	1
19	1	2	1	1	1	1
20	2	2	2	2	2	2
21	2	2	2	2	3	3
22	2	2	1	1	1	1
23	2	2	1	1	1	1
24	2	1	1	1	1	1
25	2	2	2	2	2	2
26	2	2	1	1	1	1
27	2	2	2	2	1	1
28	1	1	1	1	1	1
29	1	1	1	1	1	1
30	4	3	1	1	1	1
31	1	1	1	1	1	1
32	1	1	1	1	1	1
33	1	1	1	2	2	2
34	3	2	2	2	2	2

B.2 Average of Absolute Difference technique

B.2.1 Test results of single line to ground fault (phase A to ground fault)

Section	Rank number of the actual faulty section					
	45 ohm	55 ohm	65 ohm	75 ohm	85 ohm	95 ohm
1	1	1	1	3	3	2
2	1	1	1	1	1	1
3	2	1	1	1	1	1
4	2	1	1	1	1	1
5	1	1	1	1	1	1
6	2	1	1	1	1	1
7	1	1	1	1	1	1
8	1	1	1	1	1	1
9	1	1	1	1	1	1
10	1	1	1	1	1	1
11	1	1	1	1	1	1
12	1	1	1	1	1	1
13	2	2	2	2	1	1
14	2	1	1	1	1	1
15	2	1	2	1	1	1
16	1	1	2	1	2	2
17	2	1	1	1	1	1
18	1	1	1	1	1	1
19	1	1	1	1	1	1
20	2	1	1	1	1	1
21	1	1	1	1	1	1
22	1	1	1	1	1	1
23	1	1	1	1	1	1
24	1	1	1	1	1	1
25	1	1	1	1	1	1
26	1	1	1	1	1	1
27	2	2	1	1	1	1
28	4	1	1	1	1	1
29	2	2	2	2	2	1
30	1	1	1	1	1	1
31	2	2	1	1	1	1
32	1	1	1	1	1	1
33	2	1	1	1	1	1
34	1	1	1	1	1	1

B.2.2 Test results of three phase fault (phase A-B-C fault)

Section	Rank number of the actual faulty section					
	45 ohm	55 ohm	65 ohm	75 ohm	85 ohm	95 ohm
1	1	1	1	3	3	3
2	2	2	2	1	1	1
3	1	1	1	1	1	1
4	1	1	1	1	1	1
5	1	1	1	1	1	1
6	1	1	1	1	1	1
7	1	1	1	1	1	2
8	1	1	1	1	1	1
9	1	1	1	1	1	1
10	1	1	1	1	1	1
11	1	1	1	1	1	1
12	2	3	3	3	3	3
13	2	1	1	1	1	2
14	3	3	2	1	1	1
15	3	2	2	2	2	1
16	2	2	2	2	2	2
17	1	1	1	1	1	1
18	1	1	1	1	1	1
19	3	3	3	2	1	1
20	1	1	1	1	2	2
21	2	2	2	2	1	1
22	1	1	1	1	1	1
23	1	1	1	1	1	1
24	1	1	1	1	1	1
25	1	1	1	1	1	1
26	1	1	1	1	1	1
27	2	2	1	1	1	1
28	1	1	1	1	1	1
29	1	1	1	1	1	1
30	2	1	2	2	2	2
31	2	1	1	1	1	1
32	1	1	1	1	1	1
33	1	1	1	1	1	1
34	2	2	2	2	2	2

B.2.3 Test results of double line to ground fault (phase B-C to ground fault)

Section	Rank number of the actual faulty section					
	45 ohm	55 ohm	65 ohm	75 ohm	85 ohm	95 ohm
1	1	1	1	1	1	1
2	1	1	1	1	1	1
3	2	1	1	1	1	1
4	2	1	1	1	1	1
5	1	1	1	1	1	1
6	2	2	1	1	1	1
7	1	1	1	1	1	1
8	1	1	1	1	1	1
9	1	1	1	1	1	1
10	1	1	1	1	1	1
11	2	1	1	1	1	1
12	1	1	1	1	1	1
13	3	2	2	2	2	2
14	1	1	1	1	1	1
15	2	1	1	1	1	1
16	1	1	1	1	1	1
17	1	1	1	1	1	1
18	1	1	1	1	1	1
19	1	1	1	1	1	1
20	2	1	1	1	1	1
21	1	1	1	1	1	1
22	1	1	1	1	1	1
23	1	1	1	1	1	1
24	1	1	1	1	1	1
25	1	1	1	1	1	1
26	1	1	1	1	1	1
27	2	2	2	1	1	1
28	1	1	1	1	1	1
29	1	1	1	1	1	1
30	1	1	1	1	1	1
31	1	1	1	1	1	1
32	1	1	1	1	1	1
33	1	1	1	1	1	1
34	1	1	1	1	1	1

B.2.4 Test results of line to line fault (phase B-C fault)

Section	Rank Number of the actual faulty section					
	45 ohm	55 ohm	65 ohm	75 ohm	85 ohm	95 ohm
1	1	1	1	1	1	1
2	1	1	1	1	1	1
3	1	1	1	1	1	1
4	1	1	1	1	1	1
5	1	1	1	1	1	1
6	1	1	1	1	1	1
7	1	1	1	1	1	1
8	1	1	1	1	1	1
9	1	1	1	1	1	1
10	1	1	1	1	1	1
11	1	1	1	1	1	1
12	1	1	1	1	1	1
13	2	2	1	1	1	1
14	1	1	1	1	1	1
15	1	1	1	1	1	1
16	1	1	1	1	1	1
17	1	1	1	1	1	1
18	1	1	1	1	1	1
19	3	2	1	1	1	1
20	1	1	1	1	1	1
21	1	1	1	1	1	1
22	1	1	1	1	1	1
23	1	1	1	1	1	1
24	1	1	1	1	1	1
25	1	1	1	1	1	1
26	1	1	1	1	1	1
27	1	1	1	1	1	1
28	1	1	1	1	1	1
29	1	1	1	1	1	1
30	1	1	1	1	1	1
31	1	1	1	1	1	1
32	1	1	1	1	1	1
33	1	1	1	1	1	1
34	1	1	1	1	1	1

BIBLIOGRAPHY

Abdel Aziz, M. S., Hassan, M. A. M., & El-Zahab, E. A. (2012). An Artificial Intelligence Based Approach for High Impedance Faults Analysis in Distribution Networks (pp. 44-59): IGI Global.

Adamiak, M., Wester, C., Thakur, M., & Jensen, C. High Impedance Fault Detection On Distribution Feeders

Adamiak, M., Wester, C., Thakur, M., & Jensen, C. (April 2006). High impedance fault detection on distribution feeders. *Protection and Control Journal*.

Aggarwal, R. K., Aslan, Y., & Johns, A. T. (1997). New concept in fault location for overhead distribution systems using superimposed components. *Generation, Transmission and Distribution, IEE Proceedings-*, *144*(3), 309-316. doi: 10.1049/ip-gtd:19971137

Akorede, M. F., & Katende, J. (2010). Wavelet Transform Based Algorithm for High-Impedance Faults Detection in Distribution Feeders. *European Journal of Scientific Research, 41*(2), pp.238-248.

Ancell, G. B., & Pahalawaththa, N. C. (1994). Maximum likelihood estimation of fault location on transmission lines using travelling waves. *Power Delivery, IEEE Transactions on, 9*(2), 680-689. doi: 10.1109/61.296245

Avdakovic, S., Nuhanovic, A., Kusljugic, M., & Music, M. (2012). Wavelet transform applications in power system dynamics. *Electric Power Systems Research, 83*(1), 237-245. doi: 10.1016/j.epsr.2010.11.031

Bansal, A., & Pillai, G. N. (2007). High impedance fault detection using LVQ neural networks. *International Journal of Computer, Information, and Systems Science, and Engineering, 1*(3), pp. 148–152.

Bernadić, A., & Leonowicz, Z. (2012). Fault location in power networks with mixed feeders using the complex space-phasor and Hilbert–Huang transform. *International Journal of Electrical Power & Energy Systems, 42*(1), 208-219. doi: 10.1016/j.ijepes.2012.04.012

Bhalja, B., & Maheshwari, R. P. (2008). Wavelet-based Fault Classification Scheme for a Transmission Line Using a Support Vector Machine. *Electric Power Components and Systems, 36*(10), 1017-1030. doi: 10.1080/15325000802046496

Bo, Z. Q., Weller, G., & Redfern, M. A. (1999). Accurate fault location technique for distribution system using fault-generated high-frequency transient voltage signals. *Generation, Transmission and Distribution, IEE Proceedings-, 146*(1), 73-79. doi: 10.1049/ip-gtd:19990074

Bretas, A. S., Moreto, M., Salim, R. H., & Pires, L. O. (2006, 15-18 Aug. 2006). *A Novel High Impedance Fault Location for Distribution Systems Considering Distributed Generation.* Paper presented at the Transmission & Distribution Conference and Exposition: Latin America, 2006. TDC '06. IEEE/PES.

Briassouli, A., Matsiki, D., & Kompatsiaris, I. (2010). Continuous wavelet transform for time-varying motion extraction. *Image Processing, IET, 4*(4), 271-282. doi: 10.1049/iet-ipr.2008.0253

Cardoso, G., Jr., Rolim, J. G., & Zurn, H. H. (2004). Application of neural-network modules to electric power system fault section estimation. *Power Delivery, IEEE Transactions on, 19*(3), 1034-1041. doi: 10.1109/tpwrd.2004.829911

Chanda, D., Kishore, N. K., & Sinha, A. K. (2003). A wavelet multiresolution analysis for location of faults on transmission lines. *International Journal of Electrical Power & Energy Systems, 25*(1), 59-69. doi: 10.1016/s0142-0615(02)00021-2

Cnockaert, L., Migeotte, P. F., Daubigny, L., Prisk, G. K., Grenez, F., & Sa, R. C. (2008). A Method for the Analysis of Respiratory Sinus Arrhythmia Using Continuous Wavelet Transforms. *Biomedical Engineering, IEEE Transactions on, 55*(5), 1640-1642. doi: 10.1109/tbme.2008.918576

Dilokratanatrakool, C., Na Ayudhya, P. N., Chayavanich, T., & Prapanavarat, C. (2003, 8-13 Oct. 2003). *Automatic detection-localization of fault point on waveform and classification of power quality disturbance waveshape fault using wavelet and neural network.* Paper presented at the Robotics, Intelligent Systems and Signal Processing, 2003. Proceedings. 2003 IEEE International Conference on.

Dutra, C. A., Matos, R. R., Zimath, S. L., Oliveira, J. P. d., Resende, J. H. M. d., & Moutinho, J. A. P. Fault Location by Traveling Waves: Application in High Impedance Events

Dwivedi, U. D., Singh, S. N., & Srivastava, S. C. (2008, 11-13 Dec. 2008). *A wavelet based approach for classification and location of faults in distribution systems.* Paper presented at the India Conference, 2008. INDICON 2008. Annual IEEE.

El-Hami, M., Lai, L. L., Daruvala, D. J., & Johns, A. T. (1992). A new travelling-wave based scheme for fault detection on overhead power distribution feeders. *Power Delivery, IEEE Transactions on, 7*(4), 1825-1833. doi: 10.1109/61.156985

Elkalashy, N. I., Lehtonen, M., Darwish, H. A., Taalab, A. M. I., & Izzularab, M. A. (2007). DWT-based extraction of residual currents throughout unearthed MV networks for detecting high-impedance faults due to leaning trees. *European Transactions on Electrical Power, 17*(6), 597-614.

Elkalashy, N. I., Lehtonen, M., Darwish, H. A., Taalab, A. M. I., & Izzularab, M. A. (2008a). DWT-Based Detection and Transient Power Direction-Based Location of High-Impedance Faults Due to Leaning Trees in Unearthed MV Networks. *Power Delivery, IEEE Transactions on, 23*(1), 94-101. doi: 10.1109/tpwrd.2007.911168

Elkalashy, N. I., Lehtonen, M., Darwish, H. A., Taalab, A. M. I., & Izzularab, M. A. (2008b). A novel selectivity technique for high impedance arcing fault detection in compensated MV networks. *European Transactions on Electrical Power, 18*(4), 344-363.

Elkalashy, N. I., Lehtonen, M., Darwish, H. A., Taalab, A. M. I., & Izzularab, M. A. (2008c, 17-20 March 2008). *Verification of DWT-Based Detection of High Impedance Faults in MV Networks.* Paper presented at the Developments in Power System Protection, 2008. DPSP 2008. IET 9th International Conference on.

Etemadi, A. H., & Sanaye-Pasand, M. (2008). High-impedance fault detection using multi-resolution signal decomposition and adaptive neural fuzzy inference system. *Generation, Transmission & Distribution, IET, 2*(1), 110-118. doi: 10.1049/iet-gtd:20070120

Filomena, A. D., Resener, M., Salim, R. H., & Bretas, A. S. (2009). Fault location for underground distribution feeders: An extended impedance-based formulation with capacitive current compensation. *International Journal of Electrical Power & Energy Systems, 31*(9), 489-496. doi: 10.1016/j.ijepes.2009.03.026

. "Final report of the CIRED Working Group WG03 Fault Management, 'Fault management in electrical distribution systems',". (pp. www.cired.be/WG03-Final%20Report.pdf).

Gale, P. F., Stokoe, J., & Crossley, P. A. (1997, 25-27 Mar 1997). *Practical experience with travelling wave fault locators on Scottish Power's 275 & 400 kV transmission system.* Paper presented at the Developments in Power System Protection, Sixth International Conference on (Conf. Publ. No. 434).

Gaouda, A. M., Salama, M. M. A., Sultan, M. R., & Chikhani, A. Y. (1999). Power quality detection and classification using wavelet-multiresolution signal decomposition. *Power Delivery, IEEE Transactions on, 14*(4), 1469-1476. doi: 10.1109/61.796242

Garcia-Santander, L., Bastard, P., Petit, M., Gal, I., Lopez, E., & Opazo, H. (2005). Down-conductor fault detection and location via a voltage based method for radial distribution networks. *Generation, Transmission and Distribution, IEE Proceedings-, 152*(2), 180-184. doi: 10.1049/ip-gtd:20041300

Girgis, A. A., Fallon, C. M., & Lubkeman, D. L. (1993). A fault location technique for rural distribution feeders. *Industry Applications, IEEE Transactions on, 29*(6), 1170-1175. doi: 10.1109/28.259729

Girgis, A. A., Hart, D. G., & Peterson, W. L. (1992). A new fault location technique for two- and three-terminal lines. *Power Delivery, IEEE Transactions on, 7*(1), 98-107. doi: 10.1109/61.108895

Glinkowski, M. T., & Wang, N. C. (1995). ANNs pinpoint underground distribution faults. *Computer Applications in Power, IEEE, 8*(4), 31-34. doi: 10.1109/67.468291

Gohokar, V. N., & Khedkar, M. K. (2005). Faults locations in automated distribution system. *Electric Power Systems Research, 75*(1), 51-55. doi: 10.1016/j.epsr.2005.01.003

Haghifam, M. R., Sedighi, A. R., & Malik, O. P. (2006). Development of a fuzzy inference system based on genetic algorithm for high-impedance fault detection. *Generation, Transmission and Distribution, IEE Proceedings-, 153*(3), 359-367. doi: 10.1049/ip-gtd:20045224

Hizman, H., Crossley, P. A., Gale, P. F., & Bryson, G. (2002, 25-25 July 2002). *Fault section identification and location on a distribution feeder using travelling waves.* Paper presented at the Power Engineering Society Summer Meeting, 2002 IEEE.

Hulzink, J., Konijnenburg, M., Ashouei, M., Breeschoten, A., Berset, T., Huisken, J., Stuyt, J., de Groot, H., Barat, F., David, J., & Van Ginderdeuren, J. (2011). An Ultra Low Energy Biomedical Signal Processing System Operating at Near-Threshold. *Biomedical Circuits and Systems, IEEE Transactions on, 5*(6), 546-554. doi: 10.1109/tbcas.2011.2176726

Ibe, A. O., & Cory, B. J. (1986). A Travelling Wave-Based Fault Locator for Two- and Three-Terminal Networks. *Power Delivery, IEEE Transactions on, 1*(2), 283-288. doi: 10.1109/tpwrd.1986.4307961

IEEE Guide for Determining Fault Location on AC Transmission and Distribution Lines. (2005). *IEEE Std C37.114-2004*, 0_1-36. doi: 10.1109/ieeestd.2005.96207

Jarventausta, P., Verho, P., & Partanen, J. (1994). Using fuzzy sets to model the uncertainty in the fault location process of distribution networks. *Power Delivery, IEEE Transactions on, 9*(2), 954-960. doi: 10.1109/61.296278

Jensen, K. J., Munk, S. M., & Sorensen, J. A. (1998, 12-15 May 1998). *Feature extraction method for high impedance ground fault localization in radial power distribution networks.* Paper presented at the Acoustics, Speech and Signal Processing, 1998. Proceedings of the 1998 IEEE International Conference on.

John Tengdin, C., Ron Westfall, V. C., & Kevin Stephan, S. (1996). High Impedance Fault Detection Technology *Report of PSRC Working Group D15*.

Johns, A. T., Lai, L. L., El-Hami, M., & Daruvala, D. J. (1991). New approach to directional fault location for overhead power distribution feeders. *Generation, Transmission and Distribution, IEE Proceedings C, 138*(4), 351-357.

Jung, C. K., Kim, K. H., Lee, J. B., & Klöckl, B. (2007). Wavelet and neuro-fuzzy based fault location for combined transmission systems. *International Journal of Electrical Power & Energy Systems, 29*(6), 445-454. doi: 10.1016/j.ijepes.2006.11.003

Kejun, M., Rovnyak, S. M., & Chee-Mun, O. (2006, 0-0 0). *Dynamic event detection using wavelet analysis.* Paper presented at the Power Engineering Society General Meeting, 2006. IEEE.

Krajnak, D. J. (2000, 2000). *Faulted circuit indicators and system reliability.* Paper presented at the Rural Electric Power Conference, 2000.

Kumano, S., Ito, N., Goda, T., Uekubo, Y., Kyomoto, S., Kourogi, H., & Ariura, Y. (1993). Development of expert system for operation at substation. *Power Delivery, IEEE Transactions on, 8*(1), 56-65. doi: 10.1109/61.180319

Lai, T. M., Snider, L. A., Lo, E., & Sutanto, D. (2005). High-impedance fault detection using discrete wavelet transform and frequency range and RMS conversion. *Power Delivery, IEEE Transactions on, 20*(1), 397-407. doi: 10.1109/tpwrd.2004.837836(410) 2

Lee, H., & Mousa, A. M. (1996). GPS travelling wave fault locator systems: investigation into the anomalous measurements related to lightning strikes. *Power Delivery, IEEE Transactions on, 11*(3), 1214-1223. doi: 10.1109/61.517474

Li, H., Mokhar, A. S., & Jenkins, N. (2005). Automatic fault location on distribution network using voltage sags measurements. *IEE Conference Publications, 2005*(CP504), v3-98-v93-98.

Magnago, F. H., & Abur, A. (1999, 18-22 Jul 1999). *A new fault location technique for radial distribution systems based on high frequency signals.* Paper presented at the Power Engineering Society Summer Meeting, 1999. IEEE.

Mahmoud, G., Doaa khalil, I., & El Sayed Tag, E. (2007). Traveling-Wave-Based Fault-Location Scheme for Multiend-Aged Underground Cable System. *Power Delivery, IEEE Transactions on, 22*(1), 82-89. doi: 10.1109/tpwrd.2006.881439

Martin, F., & Aguado, J. A. (2003). Wavelet-based ANN approach for transmission line protection. *Power Delivery, IEEE Transactions on, 18*(4), 1572-1574. doi: 10.1109/tpwrd.2003.817523

Martinez, E. M., & Richards, E. F. (1991, 28-30 Apr 1991). *An expert system to assist distribution dispatchers in the location of system outages.* Paper presented at the Rural Electric Power Conference, 1991. Papers Presented at the 35th Annual Conference.

Michalik, M., Lukowicz, M., Rebizant, W., Seung-Jae, L., & Sang-Hee, K. (2007). Verification of the Wavelet-Based HIF Detecting Algorithm Performance in Solidly Grounded MV Networks. *Power Delivery, IEEE Transactions on, 22*(4), 2057-2064. doi: 10.1109/tpwrd.2007.905283

Michalik, M., Rebizant, W., Lukowicz, M., Seung-Jae, L., & Sang-Hee, K. (2006). High-impedance fault detection in distribution networks with use of wavelet-based algorithm. *Power Delivery, IEEE Transactions on, 21*(4), 1793-1802. doi: 10.1109/tpwrd.2006.874581

Mohamed, S. S., El-Saadany, E. F., Abdel-Galil, T. K., & Salama, M. M. A. (2003, 27-30 Dec. 2003). *ANN-based technique for fault location estimation using TLS-ESPRIT.* Paper presented at the Circuits and Systems, 2003 IEEE 46th Midwest Symposium on.

Mokhlis, H., Li, H. Y., & Khalid, A. R. (2010). The application of voltage sags pattern to locate a faulted section in distribution network. *International Review of Electrical Engineering, 5*(1), 173-179.

Mokhlis, H., Li, H. Y., Mohamad, H., & Bakar, A. H. A. (2010). A comprehensive fault location estimation using voltage sag profile for non-homogenous distribution networks. *International Review of Electrical Engineering, 5*(5), 2310-2316.

Mokhlis, H., Mohamad, H., Bakar, A. H. A., & Li, H. Y. (2011). Evaluation of fault location based on voltage sags profiles: A study on the influence of voltage sags patterns. *International Review of Electrical Engineering, 6*(2), 874-880.

Mokhlis, H., Mohamad, H., Li, H., & Bakar, A. H. A. (2011). Voltage Sags Matching to Locate Faults for Underground Distribution Networks. *Advances in Electrical and Computer Engineering, 11*(2), pp. 43-48. doi: 10.4316/AECE.2011.02007

Nath, S., Sinha, P., & Goswami, S. K. (2012). A wavelet based novel method for the detection of harmonic sources in power systems. *International Journal of Electrical Power & Energy Systems, 40*(1), 54-61. doi: 10.1016/j.ijepes.2012.02.005

Novosel, D., Hart, D. G., Udren, E., & Garitty, J. (1996). Unsynchronized two-terminal fault location estimation. *Power Delivery, IEEE Transactions on, 11*(1), 130-138. doi: 10.1109/61.484009

Pinnegar, C. R., & Mansinha, L. (2003). A method of time–time analysis: The TT-transform. *Digital Signal Processing, 13*(4), 588-603. doi: 10.1016/s1051-2004(03)00022-8

Poisson, O., Rioual, P., & Meunier, M. (2000). Detection and measurement of power quality disturbances using wavelet transform. *Power Delivery, IEEE Transactions on, 15*(3), 1039-1044. doi: 10.1109/61.871372

S. Nath, A. D., A. Chakrabarti. (2009). Detection of power quality disturbances using wavelet transform. *World Academy of Science Engineering and Technology, 49*, pp. 869-873.

Samantaray, S. R., Panigrahi, B. K., & Dash, P. K. (2008). High impedance fault detection in power distribution networks using time-frequency transform and probabilistic neural network. *Generation, Transmission & Distribution, IET, 2*(2), 261-270. doi: 10.1049/iet-gtd:20070319

Santoso, S., Dugan, R. C., Lamoree, J., & Sundaram, A. (2000, 2000). *Distance estimation technique for single line-to-ground faults in a radial distribution system.* Paper presented at the Power Engineering Society Winter Meeting, 2000. IEEE.

Sarlak, M., & Shahrtash, S. M. (2011). High impedance fault detection using combination of multi-layer perceptron neural networks based on multi-resolution morphological gradient features of current waveform. *Generation, Transmission & Distribution, IET, 5*(5), 588-595. doi: 10.1049/iet-gtd.2010.0702

Sidhu, T. S., & Zhihan, X. (2010). Detection of Incipient Faults in Distribution Underground Cables. *Power Delivery, IEEE Transactions on, 25*(3), 1363-1371. doi: 10.1109/tpwrd.2010.2041373

Spoor, D., & Jian Guo, Z. (2006). Improved single-ended traveling-wave fault-location algorithm based on experience with conventional substation transducers. *Power Delivery, IEEE Transactions on, 21*(3), 1714-1720. doi: 10.1109/tpwrd.2006.878091

Stockwell, R. G., Mansinha, L., & Lowe, R. P. (1996). Localization of the complex spectrum: the S transform. *Signal Processing, IEEE Transactions on, 44*(4), 998-1001. doi: 10.1109/78.492555

Takagi, T., Yamakoshi, Y., Yamaura, M., Kondow, R., & Matsushima, T. (1982). Development of a New Type Fault Locator Using the One-Terminal Voltage and Current Data. *Power Apparatus and Systems, IEEE Transactions on, PAS-101*(8), 2892-2898. doi: 10.1109/tpas.1982.317615

Tria, M., Ovarlez, J. P., Vignaud, L., Castelli, J. C., & Benidir, M. (2007). Discriminating real objects in radar imaging by exploiting the squared modulus of the continuous wavelet transform. *Radar, Sonar & Navigation, IET, 1*(1), 27-37. doi: 10.1049/iet-rsn:20050124

Uriarte, F. M., & Centeno, V. (2005, 23-25 Oct. 2005). *High-impedance fault detection and localization in distribution feeders with microprocessor based devices.* Paper presented at the Power Symposium, 2005. Proceedings of the 37th Annual North American.

Vazquez, E., Castruita, J., Chacon, O. L., & Conde, A. (2007). A New Approach Traveling-Wave Distance Protection—Part I: Algorithm. *Power Delivery, IEEE Transactions on, 22*(2), 795-800. doi: 10.1109/tpwrd.2007.893376

Wavelet guide. Available at http://www.polyvalens.com/blog/?page_id=15 [assessed on 13-09-2012].

Wavelet Transform. Available at: MATLAB Toolbox.

Wen-Hui, C., Chih-Wen, L., & Men-Shen, T. (2000). On-line fault diagnosis of distribution substations using hybrid cause-effect network and fuzzy rule-based method. *Power Delivery, IEEE Transactions on, 15*(2), 710-717. doi: 10.1109/61.853009

Wen, F., & Han, Z. (1995). Fault section estimation in power systems using a genetic algorithm. *Electric Power Systems Research, 34*(3), 165-172. doi: 10.1016/0378-7796(95)00974-6

Wenzhong, G., & Jiaxin, N. (2011). Wavelet-Based Disturbance Analysis for Power System Wide-Area Monitoring. *Smart Grid, IEEE Transactions on, 2*(1), 121-130. doi: 10.1109/tsg.2011.2106521

Ying-Hong, L., Chih-Wen, L., & Chi-Shan, Y. (2002). A new fault locator for three-terminal transmission lines using two-terminal synchronized voltage and current phasors. *Power Delivery, IEEE Transactions on, 17*(2), 452-459. doi: 10.1109/61.997917

Yuan-Yih, H., Lu, F. C., Chien, Y., Liu, J. P., Lin, J. T., Yu, P. H. S., & Kuo, R. R. T. (1991). An expert system for locating distribution system faults. *Power Delivery, IEEE Transactions on, 6*(1), 366-372. doi: 10.1109/61.103760

Zadeh, H. K. (2005). An ANN-Based High Impedance Fault Detection Scheme: Design and Implementation. *International Journal of Emerging Electric Power Systems, 4*(2). doi: http://dx.doi.org/10.2202/1553-779X.1046

Zeng, X., Li, K. K., Liu, Z., & Yin, X. (2004, 3-7 Oct. 2004). *Fault location using traveling wave for power networks.* Paper presented at the Industry Applications Conference, 2004. 39th IAS Annual Meeting. Conference Record of the 2004 IEEE.